

**Towards understanding the benefits, establishment and
maintenance of host-microbe homeostasis in *Hydra***

Dissertation

Zur Erlangung des Doktorgrades
der Mathematisch-Naturwissenschaftlichen Fakultät
der Christian-Albrechts-Universität zu Kiel

vorgelegt von

Sören Franzenburg

Kiel, im Januar 2013

Erster Gutachter: Prof. Dr. Dr. h.c. Thomas Bosch

Zweiter Gutachter: Prof. Dr. John Baines

Tag der mündlichen Prüfung: 25.03.2013

Zum Druck genehmigt: 25.03.2013

Meinen Eltern

<u>I.</u>	<u>Summary</u>	<u>V</u>
<u>II.</u>	<u>Zusammenfassung</u>	<u>VI</u>
<u>III.</u>	<u>Abbreviations</u>	<u>VII</u>
<u>1</u>	<u>Introduction</u>	<u>1</u>
1.1	The Holobiont – Microbes as Partners	1
1.2	Microbial colonization- Who controls the crowd?	2
1.3	<i>Hydra</i> – a model for host-microbe interactions	4
1.3.1	Phylogeny – at the base of animal evolution	4
1.3.2	Morphology and Histology	5
1.3.3	Biology – life in a freshwater habitat	6
1.3.4	<i>Hydra</i> 's innate immune system	7
1.4	Host-microbe interactions in <i>Hydra</i>	14
1.5	Aims of the thesis	15
<u>2</u>	<u>Results</u>	<u>16</u>
2.1	<i>Hydra</i> polyps are associated with host-specific, stable bacterial communities	16
2.2	Commensal bacteria protect <i>Hydra</i> from a fungal pathogen	19
2.3	The ontogenetic establishment of the microbiota in <i>Hydra</i>	20
2.3.1	Bacterial population profiles in newly hatched <i>Hydra</i> polyps	21
2.3.2	Computing the microbial assembly pattern	26
2.4	The role of TLR-sensing in host-microbe homeostasis	28
2.4.1	Generation of MyD88-deficient (MyD88 ⁻) <i>Hydra vulgaris</i> (AEP)	30
2.4.2	Absence of bacteria as well as MyD88 deficiency influence central parts of the TLR-signaling cascade	31
2.4.3	Gene-expression-profiling of MyD88-knockdown and germfree polyps	32
2.4.4	A subset of MyD88 downstream genes is regulated by JNK	35
2.4.5	MyD88 deficient <i>Hydra</i> display delayed bacterial recolonization upon antibiotic treatment	36
2.4.6	TLR-signaling in pathogen defense in <i>Hydra</i>	38
2.5	Host-specific antimicrobial peptides shape bacterial communities	40
2.5.1	AMPs of the arminin family show species-specific composition in different species of <i>Hydra</i>	40
2.5.2	Knockdown of arminin decreases the antibacterial activity of <i>Hydra</i> tissue	42
2.5.3	Species-specific arminins select for co-evolved bacterial partners	44
<u>3</u>	<u>Discussion</u>	<u>50</u>
3.1	The host determines the composition of its bacterial microbiota	50
3.2	Commensal bacteria produce antifungal substances	51

3.3	How does <i>Hydra</i> assemble its specific set of microbes?	53
3.4	Bacterial sensing is an ancient function of TLR-signaling	55
3.5	TLR-signaling promotes re-establishment of bacterial homeostasis	56
3.6	MyD88 target genes include taxonomically restricted and conserved genes	57
3.7	<i>Hydra</i> species express distinct sets of antimicrobial peptides	57
3.8	Species-specific AMPs select for suitable bacterial partners	58
3.9	Conclusions	60
3.10	Perspective: Host-bacterial interactions and their role in speciation	61
<u>4</u>	<u>Material</u>	<u>63</u>
4.1	Organisms	63
4.2	Chemicals	63
4.3	Media	65
4.4	Buffer and Solutions	65
4.5	Kits	66
4.6	Enzymes	66
4.7	Antibodies	67
4.8	Vectors	67
4.9	DNA size standards	67
4.10	Oligonucleotides (Primer)	67
4.11	Devices	69
4.11.1	PCR- Thermocyclers	69
4.11.2	Gel electrophoresis chambers	69
4.11.3	Incubators / Shakers	70
4.11.4	Electroporation devices	70
4.11.5	Centrifuges	70
4.11.6	Microscopy	70
4.11.7	UV-devices	70
4.11.8	Photometer	70
4.11.9	Microinjection	71
4.11.10	Sequencers	71
4.11.11	Other devices	71
4.12	URLs	71
4.13	Software	71
<u>5</u>	<u>Methods</u>	<u>73</u>
5.1	Cultivation of Organisms	73

5.1.1	Cultivation of <i>Hydra</i>	73
5.1.2	Cultivation of <i>Artemia salina</i>	73
5.1.3	Cultivation of <i>Hydra</i> -associated bacteria	74
5.1.4	Generation of germ-free <i>Hydra</i>	74
5.1.5	Generation of mono-associated <i>Hydra</i>	74
5.2	Standard laboratory methods	75
5.2.1	RNA Isolation	75
5.2.2	First strand cDNA synthesis	75
5.2.3	Polymerase chain reaction	75
5.2.4	Electrophoretic separation of DNA samples	77
5.2.5	Extraction of DNA fragments from agarose gels	77
5.2.6	Restriction Digestion of DNA	77
5.2.7	Ligation of DNA fragments	77
5.2.8	Transformation of <i>E. coli</i>	78
5.2.9	Preparation of plasmids	79
5.2.10	Sanger DNA sequencing	79
5.3	Whole mount in situ hybridization	80
5.3.1	Riboprobe generation	80
5.3.2	Preparation of polyps	80
5.3.3	Probe hybridization and staining	80
5.4	Generation of transgenic <i>Hydra vulgaris</i> (AEP)	82
5.4.1	Construct for downregulation of MyD88	82
5.4.2	Construct for downregulation of arminins	82
5.4.3	Embryo- microinjection	83
5.5	<i>Hydra</i> infection experiments	83
5.5.1	Infection with <i>Fusarium sp.</i>	83
5.5.2	Infection with <i>Pseudomonas aeruginosa</i> (PA14)	83
5.6	DNA Extraction and Sequencing of 16S rRNA Genes	84
5.6.1	16S rRNA 454 analysis	85
5.7	Mathematical Modeling	85
5.8	Custom made <i>Hydra vulgaris</i> (AEP) microarray	86
5.8.1	RNA isolation and microarray gene expression experiments	86
5.8.2	Microarray data extraction, filtering and analysis	87
5.9	SP600125 JNK inhibitor treatment	87
5.10	Phylogenetic Analysis	88

5.11	Peptide extraction from <i>Hydra</i> tissue	88
5.11.1	Test for antimicrobial activity of <i>Hydra</i> tissue extracts	88
<u>6</u>	<u>References</u>	<u>90</u>
<u>7</u>	<u>List of Publications</u>	<u>98</u>
<u>8</u>	<u>Acknowledgements</u>	<u>99</u>
<u>9</u>	<u>Appendices</u>	<u>100</u>
<u>10</u>	<u>Erklärung</u>	<u>102</u>

I. Summary

Animals evolved in a biotic environment dominated by microbes. Thus, all animals, ranging from simple invertebrates to primates, are host to complex microbial communities, which are essential for the host's health. However, the mechanisms determining the community composition and homeostasis within this microbiota are not fully understood. The present thesis includes a detailed analysis of the microbiota in the cnidarian host *Hydra*, including its beneficial function, establishment, regulation and maintenance.

First, the bacterial community composition was profiled in polyps of seven distinct species of hydras. Although laboratory reared under identical conditions for three decades, this survey revealed host-species specific bacterial communities, partially resembling host phylogeny. This finding indicated distinct selective pressures in different host species.

Germfree *Hydra* polyps turned out to be prone to fungal infection. Controlled *in vivo* infections experiments identified several members of the microbiota to significantly inhibited fungal growth. Thus, bacterial symbionts seem to be an integral part of *Hydra's* antifungal immunity.

To identify regulatory principles of the microbiota assembly, the ontogenetic establishment of the bacterial community was investigated in *Hydra*. The community assembly turned out to follow a robust, temporal progression comprising conserved key features as the animal approaches adulthood. Mathematical modeling identified interbacterial interactions as well as host modulation to mediate this colonization process.

How does the host sense its bacterial colonizers? To answer this question, transgenic *Hydra* polyps with an interfered Toll-like-receptor (TLR) signaling pathway were generated. TLR-signaling serves different functions in a variety of model organisms. The data of the present thesis clearly indicated a role of TLR-signaling in *Hydra's* bacterial perception, being involved in the mediation of bacterial colonization and pathogen defense.

Antimicrobial peptides (AMPs) of the arminin peptide family show highly species-specific expression profiles in four species of *Hydra*. Their potential roles in shaping the observed host-species specific bacterial communities were analyzed using arminin loss-of-function polyps. The specific, differential recolonization of arminin deficient polyps strongly indicated a role of these peptides in the selection of co-evolved bacterial associates.

Taken together, the present study elucidates the active mediation of bacterial colonization by innate immune mechanisms of the host.

II. Zusammenfassung

Die Evolution der Tiere fand in einer von Bakterien dominierten Umwelt statt. Daher beherbergen alle Tiere komplexe bakterielle Gemeinschaften, welche essentiell für die Gesundheit des Wirtes sind. Die Mechanismen, welche die Zusammensetzung und Homöostase in dieser Mikrobiota regulieren, sind nicht vollkommen verstanden. Diese Arbeit enthält detaillierte Analysen der Mikrobiota des Süßwasserpolyphen *Hydra*, einschließlich ihrer biologischen Funktion, Etablierung, Regulation und Aufrechterhaltung.

Zunächst wurde die Mikrobiota in Polypen von sieben verschiedenen Spezies untersucht. Obwohl diese seit 30 Jahren unter identischen Laborbedingungen kultiviert wurden, deckte diese Untersuchung Wirts-spezifische bakterielle Besiedlung auf, wobei die Mikrobiota Zusammensetzung teilweise den evolutionären Verwandtschaftsverhältnissen der *Hydra*-Arten entsprach.

Bakterienfreie Tiere zeigten sich anfällig für Pilz-Infektionen. Kontrollierte *in vivo* Versuche zeigten, dass einige Mitglieder der Mikrobiota das Pilz-Wachstum hemmten. Bakterielle Symbionten sind somit wesentlicher Bestandteil der antifungalen Immunabwehr in *Hydra*.

Um regulatorische Prinzipien zur Assemblierung der Mikrobiota zu identifizieren, wurde die ontogenetische Etablierung der bakteriellen Gemeinschaft in *Hydra* untersucht. Die Etablierung der Mikrobiota folgte einer definierten robusten, temporären Abfolge. Mathematische Modellierung identifizierte sowohl interbakterielle Wechselwirkungen, als auch Wirts-Regulation als essentielle Modulatoren des Kolonisierungsprozesses.

Wie erkennt der Wirt seine bakteriellen Besiedler? Um diese Frage zu beantworten wurden transgene *Hydra* Polypen mit einem gestörten Toll-like-receptor (TLR) Signalweg hergestellt. TLR-Signalwege führen in verschiedenen Organismen diverse Funktionen durch. Die Ergebnisse dieser Arbeit legen eine Rolle des TLR-Signalweges in *Hydra's* bakterieller Erkennung nahe, welche die Besiedelung sowie die Abwehr von Krankheitserregern beeinflusst.

Antimikrobielle Peptide (AMPs) der Arminin-Familie zeigen hoch artspezifische Expressions-profile in vier Arten von *Hydra*. Mittels Polypen mit experimentell reduzierter Arminin-Expression wurde untersucht, ob diese AMPs für die beobachtete artspezifische bakterielle Besiedelung verantwortlich sind. Die spezifische, differentielle Wiederbesiedelung dieser Polypen legt eine Rolle dieser Peptide in der Selektion ko-evolvierter bakterieller Partner nahe.

Zusammenfassend beleuchtet diese Arbeit die aktive Regulation der bakteriellen Besiedelung durch Mechanismen des angeborenen Immunsystems des Wirtes.

III. Abbreviations

% (v/v)	Volume concentration (volume/volume)
% (w/v)	Mass concentration (weight/volume)
A	Adenine
Aa	Amino acids
AEP	<i>Hydra vulgaris</i> (AEP)
Amp	Ampicillin
ANOVA	Analysis of variance
AP	Alkaline phosphatase
Bcl-2	B-cell lymphoma 2
BLAST	Basic Local Alignment Search Tool
bp	Basepairs
BSA	Bovine serum albumin
C	Cytosine
cDNA	Complementary DNA
CFU	Colony forming units
cm	Centimeter
ddATP	Dideoxyadenosine triphosphat
ddCTP	Dideoxycytosine triphosphat
ddGTP	Dideoxyguanosine triphosphat
ddNTP	Dideoxynucleotide triphosphat
ddTTP	Dideoxythymidine triphosphat
DNA	Deoxyribonucleic acid
DNase	Deoxyribonuclease
dNTP	Deoxynucleotide triphosphat
ds	Doublestranded
<i>E. coli</i>	<i>Escherichia coli</i>
<i>e.g.</i>	Lat.: exempli gratia, engl.: for example
EGF	Epidermal growth factor
eGFP	Enhanced green fluorescent protein
G	Guanine
g	Gram or g-force
GAL-lectin	Galactosamine inhibitable lectin
GFP	Green fluorescent protein
H.	<i>Hydra</i>
hF	Hectofarad
H. vul (AEP)	<i>Hydra vulgaris</i> (AEP)
H. mag	<i>Hydra magnipapillata</i>

H. oli	<i>Hydra oligactis</i>
H. vir	<i>Hydra viridissima</i>
<i>i.e.</i>	Lat.: id est, engl.: that is
IKK	Inhibitor of kappa B kinase
i kappa B	Inhibitor of kappa B
IL-1R	Interleukin-1 receptor
IL-6	Interleukin 6
ITS	Internal transcribed spacer
JNK	c-Jun N-terminal kinase
JSP-1	JNK stimulatory phosphatase 1
K ⁺	Potassium cation
kV	Kilovolt
l	Liter
LB	Lauria Bertani (bacterial growth broth)
LBP	Lipopolysaccharide-binding protein
LPS	Lipopolysaccharide
M	Molar
mA	Milliampère
MAP	Mitogen-activated protein
mg	Milligram
min	Minute(s)
ml	Milliliter
mM	millimolar
mRNA	Messenger-RNA
µg	Microgram
µl	Microliter
µM	Micromolar
n	Number of replicates
NCBI	„National Center for Biotechnology Information“
neg.	Negative
NFκB	Nuclear factor kappa-light-chain-enhancer of activated B cells
ng	Nanogram
NOD	Nucleotide binding oligomerization domain
ORF	Open reading frame
p38	P38 mitogen-activated protein kinases
PBS	Phosphat buffered saline
PCR	Polymerase-chain-reaction
RNA	Ribonucleic acid
RNAi	RNA interference
RNase	Ribonuclease
rp	Repeat

rpm	Rounds per minute
rRNA	Ribosomal RNA
RT	Room temperature or reverse transcription
RT-PCR	Reverse Transcriptions-PCR
SD	Standard deviation
SDS	Sodiumdodecylsulfate
Secr.	Secreted
SEM	Standard error of the mean
sp.	Species
ss	Singlestranded
T	Thymine
TAE	Tris-Acetate-EDTA-buffer
Taq	<i>Thermophilus aquaticus</i>
TBE	Tris-Boric acid-EDTA-buffer
TEMED	N,N,N',N'- Tetraethylendiamin
TGF β	Transforming growth factor beta
T _m	Melting temperatur
TNF α	Tumor necrosis factor-alpha
TNFR	Tumor necrosis factor receptor
TRAM	TRIF-related adaptor molecule
TRIF	TIR-domain-containing adaptor protein-inducing IFN- β
Tris	Tris-(Hydroxymethyl)-Aminomethane
TRR	Toll-receptor related
U	Units or Uracil
UV	Ultraviolette Light
V	Volt
wt	Wild type

1 Introduction

1.1 The Holobiont – Microbes as Partners

The first bacterial cells developed approximately 3.25 billion years ago, whereas the first multi-cellular eukaryotes are estimated to be 1.2 billion years old (Ley *et al*, 2008b). The evolution of metazoans, therefore, took place in a “bacterial suspension”. This omnipresence of bacteria caused strong interactions and co-evolution between hosts and microbes. Thus, all animals, ranging from simple invertebrates to primates, are host to complex microbial communities, the so called microbiota (Fraune and Bosch, 2007, Ley *et al*, 2008b, Ochman *et al*, 2010). The commensal microbiota became an essential factor for the host’s health, as germfree animals, experimentally deprived of their bacterial associates, display severe fitness disadvantages. Thus, instead of single animal organism, an ecological consortium of the host and its associated microbes, *i.e.* the holobiont, interacts with its environment (**Figure 1.1**).

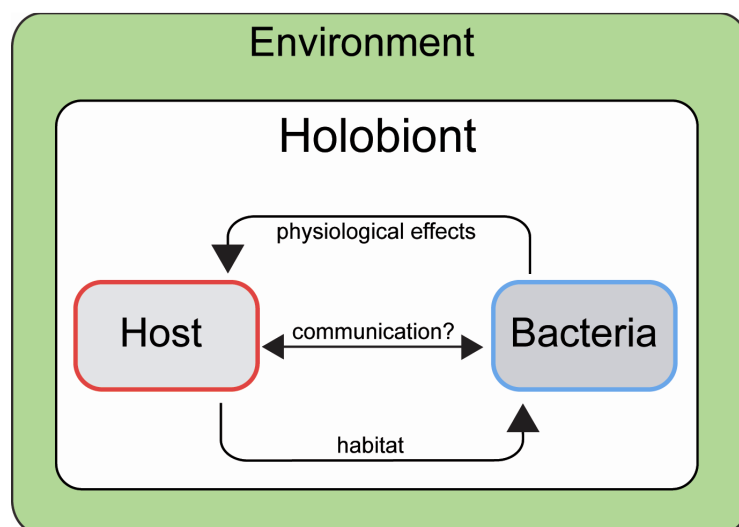


Figure 1.1: Schematic model of the holobiont.

The host organism and its associated bacteria form the holobiont, which interacts with its environment and thus is considered to be the unit of selection.

In many cases, the bacterial community acts as a metabolic organ, enabling the host to utilize otherwise unfavorable nutrient sources. A prominent example is the obligate symbiosis between aphids and their intracellular bacteria of the genus *Buchnera*. Aphids feed on nutrient-poor plant phloem sap, lacking a variety of essential amino acids, which instead are synthesized by the endosymbiont (Douglas *et al*, 2001, Sandstrom *et al*, 2000). In vertebrates,

certain gut bacteria enhance the nutrient extraction of ingested food and regulate fat storage, thus likely affecting obesity (Backhed *et al*, 2004). Despite these metabolic influences, commensal bacteria affect the development of intestinal epithelia (Bates *et al*, 2006, Rawls *et al*, 2004) and strongly interact with the host's immune system, which relies on microbial stimuli for its maturation (Dobber *et al*, 1992, Mazmanian *et al*, 2005). Further, the permanent recognition of the commensal microbiota by Toll-like Receptors (TLRs) is implicated in intestinal homeostasis (Rakoff-Nahoum *et al*, 2004). By occupying potential niches and competing for nutrients, commensal bacteria directly act against opportunistic pathogens, a mechanism known as colonization resistance (Stecher and Hardt, 2008).

The genetic information provided by the host organism, united with the genomes of its associated microbes, forms the hologenome, which is several fold more complex than the genomes of the single organisms (Backhed *et al*, 2004). The hologenome contains a high potential for fast adaptation to changing environmental parameters by changes in the abundance of associated bacteria or uptake of new bacterial symbionts (Reshef *et al*, 2006). Mutualistic associations between animals and microbes can evolve by distinct selective forces. Since association with a beneficial microbiota increases the host's fitness, selective pressures should act on host-mechanisms, e.g. immune effectors, ensuring suitable bacterial colonization. Additionally, vertically transmitted bacteria are selected for being beneficial to the host, since the increase in the host's fitness ensures the future availability of the habitat (Ley *et al*, 2006a). This interlinked dependencies between the host and its associated microbes (*i.e.* the holobiont, **Figure 1.1**) led to the hypothesis of the "hologenome theory of evolution", considering the holobiont as unit of natural selection (Rosenberg *et al*, 2009).

1.2 Microbial colonization- Who controls the crowd?

Microbial colonization appears to be an essential step in vertebrate ontogeny, contributing to the maturation of the immune system and gut development (Kelly *et al*, 2007, Mazmanian *et al*, 2005, Rawls *et al*, 2004). Neonatal recolonization of germ-free mice with microbes prevents enhanced colitis and asthma sensitivity while inoculation of adult mice is not effective (Olszak *et al*, 2012). In invertebrates, germfree *Drosophila* larvae show drastically increased mortality compared to conventional larvae when reared on a nutrient poor diet (Shin *et al*, 2011). Thus, vertebrates and invertebrates appear not only to tolerate, but to require colonization by beneficial microorganisms for metabolism, immune defense, development,

behavior and most likely many other not yet identified functions (Chow *et al*, 2010, Mazmanian *et al*, 2005, Nyholm and McFall-Ngai, 2004, Rawls *et al*, 2004, Sandstrom *et al*, 2000, Xu *et al*, 2003).

In this sense, humans develop into ecological communities after being born with a sterile gastrointestinal tract that is successively colonized with microbial populations until adult-like communities stabilize (Koenig *et al*, 2011, Walter and Ley, 2011). Despite its importance, the processes which control community membership in the neonatal gut and influence the colonization pattern during infancy and childhood are poorly understood. A vitally important question to ask, therefore, is what are the factors and rules in a particular host which influence community assembly, composition and diversity?

Because a dysregulation of host-microbe homeostasis can have severe impact on the host's health (French and Pettersson, 2000, Mao-Jones *et al*, 2010, Ott *et al*, 2004), controlling and mediating "correct" bacterial colonization in early life would confer fitness advantages to the host. This view has encouraged discussions as to what extent the microbiota is controlled by the host through top-down mechanisms involving the immune system, relative to microbiota intrinsic bottom-up mechanisms (Ley *et al*, 2006a). A compelling evidence for host-control over commensal bacteria comes from reciprocal microbiota transplantations from zebrafish and mice into germfree recipients (Rawls *et al*, 2006). In this study, Rawls *et al*. demonstrated, that the recipient hosts shape the community structure of the transferred, foreign microbiota to resemble their native bacterial communities (Rawls *et al*, 2006). Similarly, host-phylogenetic relationship was identified as determining factor of the intestinal microbiota in termites (Hongoh *et al*, 2005), parasitoid wasps (Brucker and Bordenstein, 2011), and seven species of hominids (Ochman *et al*, 2010). However, these studies did not elucidate the factors responsible for host-mediated community control. Several host-factors are suggested to have influence on the microbiota composition, ranging from oxygen conditions in the gut, nutrient intake (diet), mucus barriers and immunity (reviewed in (Bevins and Salzman, 2011a)).

Despite the importance of understanding the factors that control bacterial colonization in man, the inaccessibility of the microbial niches of the human gut and the restriction to collection of fecal samples in studies with infants (Cilieborg *et al*, 2012) make it desirable to use animal models for understanding basic principles of colonization processes in detail.

1.3 *Hydra* – a model for host-microbe interactions

In recent years, the fresh water polyp *Hydra* became an important model organism for studying host-microbe interactions. The 0.5 cm sized polyps are easily cultured and can be genetically manipulated by transgenesis (Wittlieb *et al*, 2006), offering opportunities to directly interfere with the host-bacterial crosstalk. The genome sequence of *Hydra magnipapillata* (Chapman *et al*, 2010) as well as transcriptomes of *Hydra vulgaris* (AEP) (Hemrich *et al*, 2012), *Hydra viridissima* and *Hydra oligactis* (unpublished data) are available. The genome of a main bacterial colonizer, *Curvibacter sp.*, was co-sequenced with the *Hydra magnipapillata* genome (Chapman *et al*, 2010). Major bacterial associates of *Hydra*, including *Curvibacter sp.*, can be cultivated and germfree polyps can be generated by the use of antibiotics (Franzenburg *et al*, 2012). Being an evolutionary basal organism, *Hydra* thus might provide novel insight into the evolution of host-microbe associations and the underlying regulatory mechanisms.

1.3.1 Phylogeny – at the base of animal evolution

The freshwater polyp *Hydra* is a member of the evolutionary basal phylum Cnidaria, which are characterized by their eponymous and phylotypic cell type, the cnidocytes or nematocytes, one of the most complex cell types in the animal kingdom (Tardent, 1995). Belonging to the eumetazoan clade, Cnidaria are phylogenetically distinguished from the Parazoa (Porifera and Placozoa) by the development of true cellular tissues and form a sister clade to the Bilateria (Figure 1.2 A). Besides the class Hydrozoa, the cnidarian phylum includes the classes Anthozoa, Staurozoa, Cubozoa and Scyphozoa.

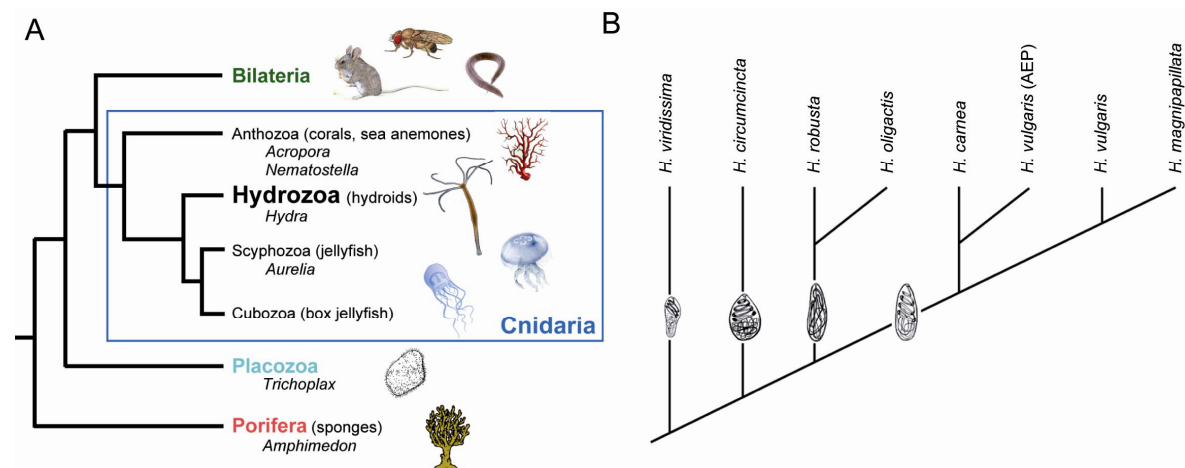


Figure 1.2: Phylogenetic classification of *Hydra*

(A) Schematic phylogenetic tree of Metazoa, highlighting the position of Cnidaria as sister clade to the Bilateria. Figure taken from (Augustin *et al*, 2010). (B) Phylogeny of eight *Hydra* species, resolved by phylogenetic

analysis of two mitochondrial (16S rRNA, COI) and two nuclear genes (18S, 28S rRNA). Species can be distinguished morphological by their depicted holotrichous isorhiza cnidocytes. Figure modified from (Hemrich *et al*, 2007).

Molecular analysis of two mitochondrial and two nuclear marker genes identified *Hydra viridissima* as the most basal representative of the genus *Hydra*. Its basal position is further characterized by harboring symbiotic green algae of the genus *Chlorella*, which no other species of *Hydra* contain. *Hydra magnipapillata* and *Hydra vulgaris* were identified as the most derived species. Surprisingly, *Hydra vulgaris* (AEP), the strain used to generate transgenic polyps (Wittlieb *et al*, 2006), was shown to be closer related to *Hydra carnea* than to the eponymous species *Hydra vulgaris* (**Figure 1.2 B**) (Hemrich *et al*, 2007). The exact systematic classification of *Hydra sp.* is: phylum: Cnidaria; class: Hydrozoa; order: Anthomedusae; family: Hydridae.

1.3.2 Morphology and Histology

The *Hydra* polyp shows radial symmetry with the oral-aboral axis being the only body axis, which can be divided into three structural regions. The head structure at the distal end comprises the hypostome, surrounded by a ring of nematocyte carrying tentacles. The body column includes the gastric region and the budding zone and ends with a foot structure, the basal disk, for adhesion to the substrate (**Figure 1.3 A**). The cnidarian body plan is diploblastic, *i.e.* their bodies are build up by two germ layers, the endoderm and the ectoderm. A mesoderm, which is characteristic for Bilateria, is not present. Both germ layers are separated by an acellular layer, the mesogloea (**Figure 1.3 B**). The *Hydra* polyp is build up by about 20 cell types, which are derived from three stem cell lineages. Besides the epitheliomuscular stem cells, which give rise to endodermal and ectodermal epithelial cells, a population of multipotent interstitial cells (i-cells) resides within the ectoderm throughout the gastric region and gives rise to a variety of specialized somatic cells, *i.e.* nerve cells, nematocytes and gland cells, as well as to germ cells (Bosch, 2007b, David and Murphy, 1977). Therefore, a separation of germ line and somatic line is not present in *Hydra* (Bosch and David, 1987). Epitheliomuscular cells of the ectoderm can differentiate to battery cells, housing 8 to 24 nematocytes (Dubel *et al*, 1987). Endodermal epitheliomuscular cells are interspersed by secretory active gland cells (**Figure 1.3 B**).

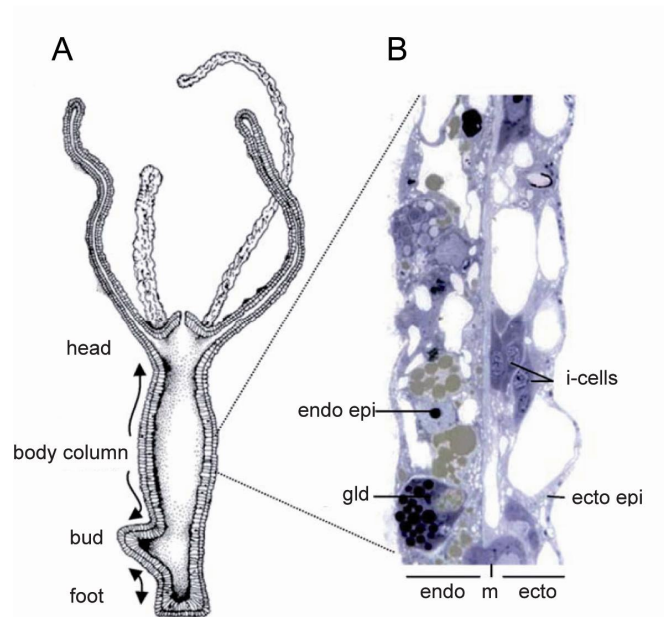


Figure 1.3 The bodyplan of *Hydra*

(A) Schematic longitudinal cross section of a *Hydra* polyp. (B) Cellular composition of the epithelial lining of the body column, showing *Hydra*'s diploblastic organization. endo epi: endodermal epithelial cell, gld: gland cell, i-cells: interstitial cells, ecto epi: ectodermal epithelial cells, endo: endoderm, ecto: ectoderm, m: mesogloea. Figures taken from (Bosch, 2007a).

1.3.3 Biology – life in a freshwater habitat

Unlike most hydrozoans, which reside in marine environments, *Hydra* lives in freshwater ponds or lakes. The polyps are attached to the substratum with their basal disk and feed on small crustaceans like copepodes or daphnia, which are captured using their tentacles, equipped with several types of nematocytes. Reproduction takes place either asexually by budding, leading to a doubling time of three to four days under well fed conditions (Bosch and David, 1984, David and Campbell, 1972), or sexually by the formation of eggs and sperms (Bosch and David, 1987) (**Figure 1.4**). Sexual reproduction is induced by environmental cues, e. g. starvation in *Hydra vulgaris* (AEP) or temperature decline in *Hydra oligactis*. Following fertilization by swarming sperms, *Hydra* oocytes develop by a radial cleavage pattern outside the female polyp (**Figure 1.4, Figure 2.5 A**) (Martin *et al*, 1997). Gastrulation is followed by a cuticle stage which is characterized by a thick protective outer layer (Martin *et al*, 1997). *Hydra* has no specialized larval life stage. Two to four weeks post fertilization, small polyps hatch from the eggs (**Figure 1.4, Figure 2.5 B**) and rapidly grow to adult size.

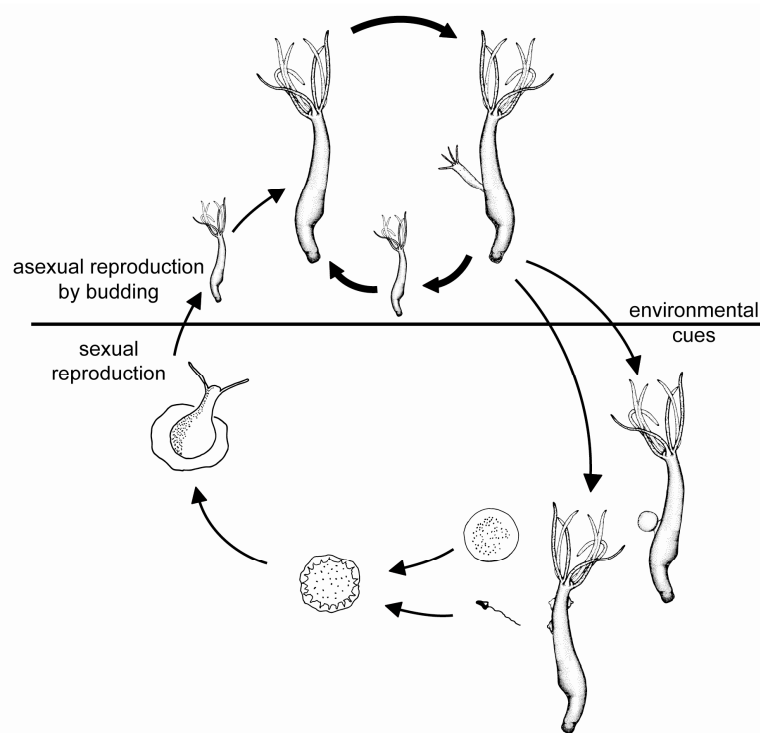


Figure 1.4: Lifecycle of *Hydra*.

Asexual reproduction takes place by budding, leading to a doubling time of three to four days. Sexual reproduction can be induced by environmental cues. The developmental time from fertilization to hatching is two to four weeks. Figure modified from (Bosch, 2012).

1.3.4 *Hydra's* innate immune system

In contrast to vertebrates, which have developed a complex immune system that comprises fast innate immune responses and delayed, adaptive defense mechanisms, invertebrates rely exclusively on their innate immunity to defend themselves against potential pathogens. The innate immune system is well studied in bilaterian invertebrates like *Drosophila* or *Caenorhabditis* and largely relies on receptor-mediated pathogen recognition and the induction of bacteriocidal effector molecules. In contrast to these ecdysozoan model organisms, *Hydra* neither possesses non-permeable barriers like exoskeletal or cuticular structures, nor mobile phagocytes (Bosch *et al*, 2009). Despite its morphological simplicity, *Hydra* has developed complex, epithelial cell based defense mechanisms. Incubation of *Hydra magnipapillata* polyps with virulence factors in culture supernatants of the pathogenic bacterium *Pseudomonas aeruginosa* induces striking changes in ectodermal epithelial cell morphology (Bosch *et al*, 2009). Epithelial cells from immune stimulated polyps round up and form numerous blebs (**Figure 1.5 A, B**). Within the cells, an increased amount of secretory vesicles is formed, likely containing antimicrobial agents or glycocalyx components (**Figure 1.5 C, D**). Thus, similar to immune cells of higher organisms, *Hydra's* epithelial cells

respond to microbial stimuli by cytoskeletal rearrangement and increased secretory activity (Bosch *et al*, 2009).

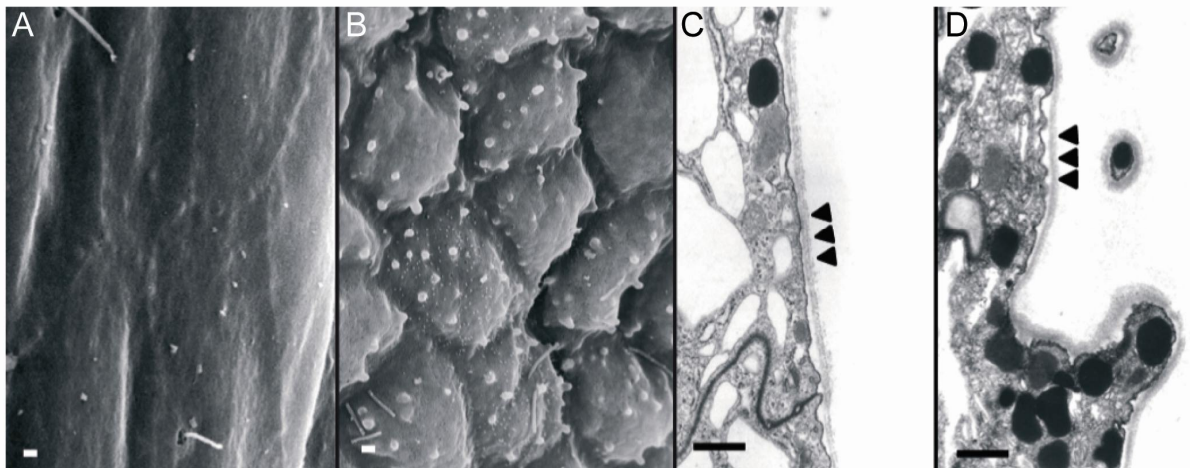


Figure 1.5: Ectodermal epithelial response to pathogen exposure

(A) Scanning electron microscopic (SEM) picture of the ectodermal epithelium of control polyps. (B) SEM picture showing the ectodermal epithelium of polyps exposed to filtrates of adherent grown *Pseudomonas aeruginosa* (*P.a.*). (C) Transmission electron microscopic (TEM) picture of ectodermal epithelial cells of control polyps. Arrowheads indicate the apical cell membrane and the glycocalyx layer. (D) TEM showing ectodermal epithelial cells of *P.a.* filtrate challenged polyps. Note the increased presence of intracellular granules. Arrowheads indicate the apical cell membrane and the glycocalyx layer. Modified from (Bosch *et al*, 2009).

1.3.4.1 Receptors and signal transduction – Toll-like receptor signaling

Hydra is able to respond to microbial stimuli, but the mechanisms of signal perception have not been elucidated. In vertebrates, microbe associated molecular patterns (MAMPs) are recognized by pattern-recognition receptors (PRRs) like Toll-like receptors (TLRs) and NOD-like receptors (NLRs) (Akira *et al*, 2006). TLRs are transmembrane receptors with extracellular leucine-rich repeat (LRR) motifs and an intracellular Toll/interleukin-1 receptor (TIR) domain. Upon stimulation of TLRs, the key adaptor protein myeloid differentiation factor 88 (MyD88) associates with the cytosolic part of the TLR through homophilic interaction of the TIR-domains. In mammals, MyD88 is involved in the signal transduction of all 13 TLRs except TLR-3 (Akira *et al*, 2006). By homophilic binding of the death domains, MyD88 recruits the IL-1R-associated kinase (IRAK), which subsequently associates with the TNFR-associated factor (TRAF). TRAF recruits the TGF- β -activated kinase 1 (TAK1), which induces a phosphorylation cascade finally leading to the nuclear translocation of the transcription-factors NF- κ B via the IKK-signalosome or c-Jun via the JNK / p38-branch of TLR-signaling (Akira *et al*, 2006) (Figure 1.6)

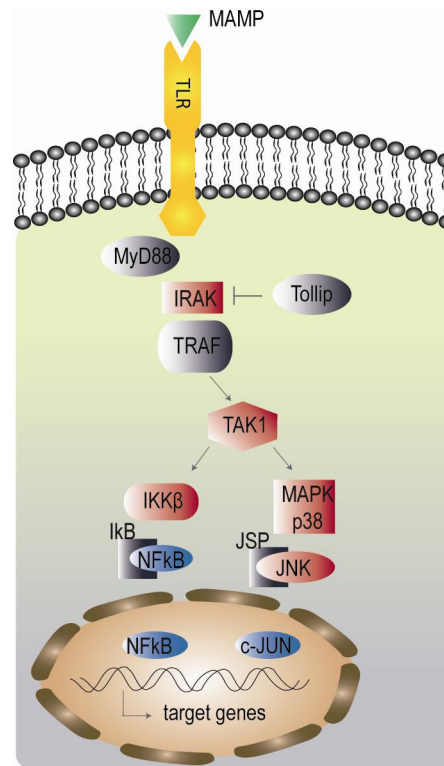


Figure 1.6: Schematic representation of the key elements of TLR signaling

After binding MAMPs, the cytosolic part of TLRs binds to MyD88, which recruits the kinase IRAK. IRAK associates with TRAF. TRAF recruits the kinase TAK1, finally leading to a phosphorylation cascade ending in the release of the transcription factors (TFs) NF κ B or c-Jun from their inhibitors. The TFs translocate into the nucleus and bind to promoters of response genes. Green: ligands; yellow: receptors; gray: adapter proteins and inhibitors; red: kinases; blue: transcription factors. Figure drawn after (Akira *et al*, 2006).

NF- κ B has been shown to induce pro-inflammatory cytokines, like IL-6 and TNF α (Akira *et al*, 2006) and a broad range of antimicrobial peptides (Takeda *et al*, 2003). MAMPs include ubiquitous bacterial components like lipopolysaccharides, flagellin and peptidoglycans (Akira *et al*, 2006, Pasare and Medzhitov, 2005) and are a common feature of pathogenic and commensal bacteria (Otte *et al*, 2004). Thus, vertebrate TLRs are involved in eliminating pathogens and controlling commensal colonization (Akira *et al*, 2006, Round *et al*, 2011, Wen *et al*, 2008). In mice, it was shown that a constant stimulation of TLRs by gut bacteria contributes to the maintenance of intestinal homeostasis (Rakoff-Nahoum *et al*, 2004). A dysregulated interaction between commensal bacteria and TLRs is a factor involved in the occurrence of inflammatory bowel diseases like Crohn's disease and colitis ulcerosa (Mowat, 2009).

Eponymous for TLRs is the *Drosophila* receptor Toll. The Toll pathway was initially identified to be essential in early embryonic development in *Drosophila* (Anderson *et al*, 1985). In addition to its crucial role in the establishment of the dorsal-ventral axis, *Drosophila* Toll-1 was shown to be involved in muscle development (Halfon and Keshishian, 1998) and heart formation (Wang *et al*, 2005). Later on, it was discovered that Toll-1-signaling in

Drosophila also contributes to defense reactions against bacteria as well as to antifungal defense by regulating, among others, the expression of the antifungal peptide drosomycin in adult flies (Lemaitre *et al*, 1996, Rosetto *et al*, 1995). Further immunity functions have been identified for Toll-7 (Nakamoto *et al*, 2012) and Toll-8 (Akhouayri *et al*, 2011). Studies in the mosquito *Aedes aegypti* also identified MyD88-dependant Toll-signaling to mediate immune defenses against Dengue-Viruses (Xi *et al*, 2008). In contrast to *Drosophila* Toll-1, no developmental function could be assigned to any of the 13 mammalian TLRs (Vandewalle, 2008). One other invertebrate model organism, the nematode *Caenorhabditis elegans* lacks central proteins of the canonical TLR-signaling cascade (Pujol *et al*, 2001). Only one Toll-homologue, termed TOL-1, was identified in *C. elegans* (Pujol *et al*, 2001). The fact that TOL-1 mutants show strong developmental defects despite mutants for the putative signaling cascade displaying no developmental abnormalities led to the assumption that TOL-1 in *C. elegans* might function as a cell-cell adhesion protein in neurons instead as pattern-recognition receptor in innate immunity (Pujol *et al*, 2001).

Thus, Toll-like receptors (TLRs) are conserved throughout bilaterian evolution but appear to serve different functions in different model organisms (**Figure 1.7**). Therefore, it was proposed that the immune function of TLR signaling, involving NF- κ B and MyD88, has evolved within the bilaterians and after the divergence of nematodes (Kim and Ausubel, 2005).

This hypothesis was challenged by recent genome sequencing projects. While no TLR-pathway was discovered in the choanoflagellate *Monosiga brevis*, which is considered the closest living unicellular relative of metazoans (King *et al*, 2008), the genomes of the poriferans *Amphimedon queenslandica* (Gauthier *et al*, 2010) and *Suberites domuncula* (Wiens *et al*, 2007) as well as the genomes of the cnidarians *Hydra magnipapillata* (Chapman *et al*, 2010) and *Nematostella vectensis* (Putnam *et al*, 2007) revealed the presence of conserved TLR-signaling cascades including MyD88 and NF- κ B (Bosch *et al*, 2009, Lange *et al*, 2011, Miller *et al*, 2007). Thus, TLR signaling pathways seem to be a common feature of metazoans. Their functions, being it bacterial recognition or developmental regulation, however, remains to be shown (Irazoqui *et al*, 2010).

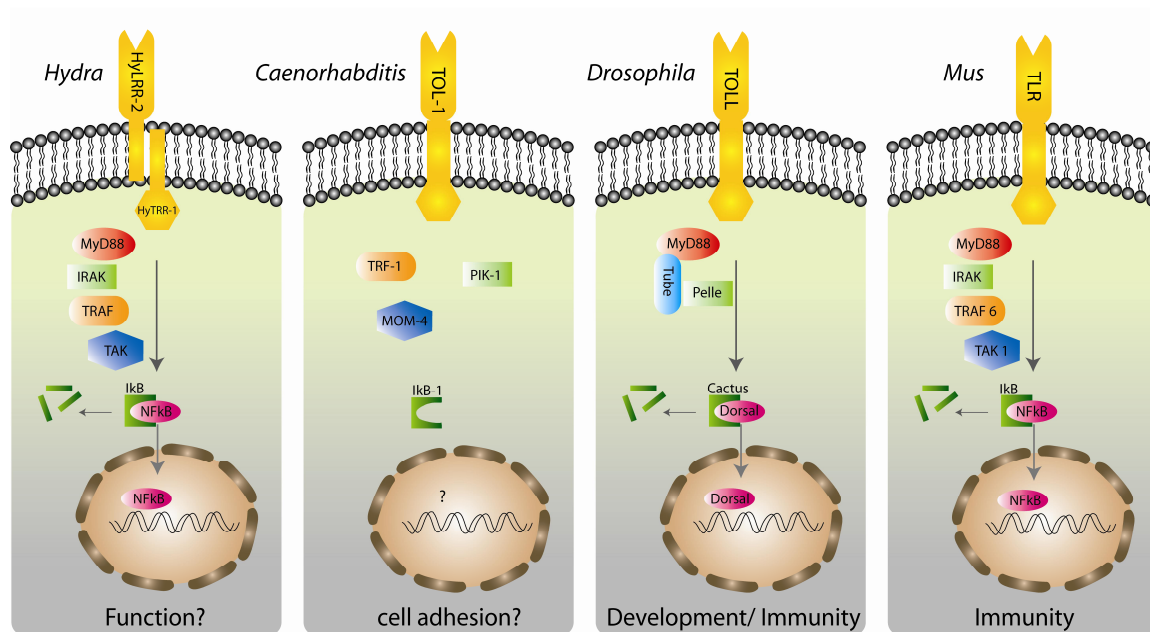


Figure 1.7: TLR-pathway comparison of different model organisms

The genome of the basal metazoan *Hydra* encodes all essential members of the TLR-signaltransduction pathway. Studies in the model organisms *C. elegans*, *D. melanogaster* and the vertebrate *M. musculus* revealed a broad range of biological functions of TLR-signaling. Thus, studies in *Hydra* might reveal the ancient function of TLRs.

The TLR in *Hydra* is not a *bona fide* one, since a functional TLR is assembled by two transmembrane proteins (Bosch *et al*, 2009). A complex of hyLRR-2, carrying an extracellular LRR domain and hyTRR-1, containing an intracellular TIR domain, has been shown to recognize the bacterial MAMP flagellin, leading to an increased nuclear translocation of NF-κB (Bosch *et al*, 2009). However, these assays were performed by transfection of human HEK293 cells and are not necessarily valid in *Hydra in vivo*.

1.3.4.2 Effectors of innate immunity – antimicrobial peptides

Antimicrobial peptides (AMPs) are effector molecules of the innate immune system. Despite AMPs show low sequence homologies and a wide range of secondary structures (Jenssen *et al*, 2006), they share similar characteristic features. Typical AMPs are short (12 to 45 amino acids) and positively charged due to the cationic amino acids lysine and arginine. They form amphiphatic secondary structures (α -helices or β -sheets) and show microbicidal activity against bacteria (Zasloff, 2002), fungi (De Lucca and Walsh, 1999) or viruses (Albiol Matanic and Castilla, 2004) in micromolar concentrations (Jenssen *et al*, 2006, Matsuzaki, 1999). Most eukaryotic AMPs are synthesized as prepropeptides and stored as propeptides after proteolytic removal of the signal peptide (SP). A second proteolytic cleavage releases the mature active AMP, resulting in a N- and C-terminal fragment. Antimicrobial peptides are either expressed

constitutively or are inducible by microbial stimuli. The promoter regions of many AMPs contain binding sites for the transcription factor NF- κ B and thus are prominent effector molecules downstream of TLR- or NLR signaling pathways (Zasloff, 2002). The mode of action is well understood for bacteriocidal AMPs. While the outer cell membranes of multicellular organisms consist of zwitterionic phospholipids like phosphatidylcholine and sphingomyelin, resulting in a neutral charge, bacterial cell membranes contain a high proportion of negatively charged phosphatidylglycerol and cardiolipin. This negative exterior charge of bacterial cell membranes favors the interaction with cationic AMPs (Matsuzaki *et al.*, 1995). Upon binding to the bacterial cell, many AMPs permeabilize the cell membrane by hydrophobic interactions, leading to efflux of intracellular K⁺ ions and collapse of the transmembrane potential (Matsuzaki, 1999). Other AMPs are translocated into the cell and inhibit intracellular processes like nucleic acid synthesis, enzyme activity or cell wall synthesis (Brogden, 2005, Jenssen *et al.*, 2006). Despite their potent function in pathogen defense, AMPs have been proven to additionally affect the commensal microbiota. Elegant studies in mice have shown that the expression level of AMPs of the α -defensin family greatly affects the composition of the commensal community (Salzman *et al.*, 2009).

Until today, three potent AMPs have been identified in *Hydra*. The first AMP, isolated from *Hydra*, was hydramacin-1, a 60 amino acid long, secreted cationic peptide containing eight cysteines. *Hydramacin-1* is expressed in endodermal epithelial cells and upregulated in a concentration dependant manner by the MAMP LPS (Bosch *et al.*, 2009). A second AMP in *Hydra* was identified using suppression subtraction hybridization (SSH), comparing polyps immune stimulated with filtrates of adherent grown *Pseudomonas aeruginosa* with control polyps. Among genes upregulated by *P. a.* virulence factors, the gene *periculin-1* was discovered. Eponymous for this peptide was its inducibility by a variety of “danger” (lat. *pericula*) factors including bacterial flagellin and LPS, viral dsRNA or the endogenous apoptosis signal monosodium urate (MSU) (Bosch *et al.*, 2009). *Periculin-1* is expressed in endodermal epithelial cells and i-cells giving rise to the female germline (Bosch *et al.*, 2009, Fraune *et al.*, 2010) and was proposed to act in maternal protection of the developing embryo (Fraune *et al.*, 2010). *Periculin-1* is synthesized as prepropeptide with a SP, an anionic N-terminal region and a cationic C-terminal fragment, which was shown to proteolytically cleaved, resulting in a bacteriocidal activity against *Bacillus megaterium* in concentrations of 0.2 μ M to 0.4 μ M (Bosch *et al.*, 2009).

The same SSH library, leading to the identification of *periculin-1*, resulted in the isolation of a third AMP called arminin 1a. Like *periculin-1*, arminin 1a is a short (88 aa), secreted peptide.

The pro-peptide consists of an anionic N-terminal region (isoelectric point [pI] = 3.91) and a highly cationic (pI > 12) C-terminal part, which was predicted to be cleaved of to generate the bacteriocidal fragment (Augustin *et al*, 2009a) (Figure 1.8 A). Consistent with that prediction, the synthetically produced C-terminal fragment of arminin 1a showed strong antibacterial activity against *Escherichia coli*, *Bacillus megaterium* and several methicillin-resistant *Staphylococcus aureus* strains in concentrations equal or lower than 0.4 µM. *Arminin 1a* was shown to be expressed in the endoderm (Figure 1.8 B), thus likely being secreted to the gastric cavity.

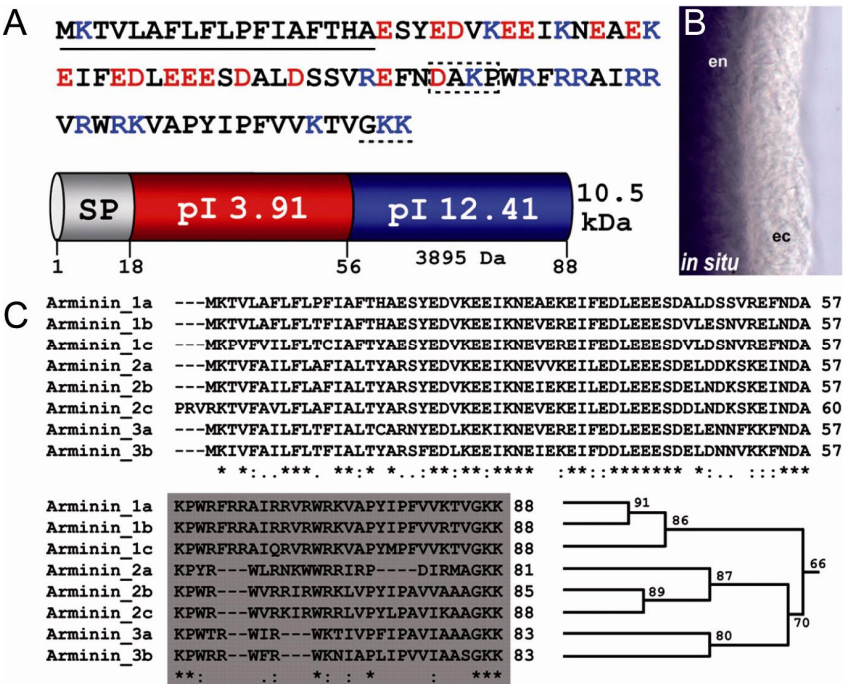


Figure 1.8: The antimicrobial peptide arminin
 (A) Amino acid sequence and scheme of arminin 1a; underlined: SP, red aa: neg. charged, blue aa: positively charged, dashed box: predicted site for proteolytic cleavage, dashed line: putative amidation signal. (B) In-situ-Hybridization showing arminin 1a mRNA localization in the endoderm; en: endoderm, ec: ectoderm. (C) Amino acid alignment of the arminin peptide family in *Hydra magnipapillata* (Clustal W algorithm), showing the conserved N-terminal region and the variable C-terminus (highlighted in gray). The homology tree illustrates how arminin family members group together according to their sequence identity (the numbers given at the nodes of the tree are the percentage of identical amino acid residues). Modified from (Augustin *et al*, 2009a). Analysis of the *Hydra magnipapillata* genome (Chapman *et al*, 2010) and expressed sequence tags (ESTs) identified an arminin peptide family, consisting of eight closely related members (Augustin *et al*, 2009a). Interestingly, sequence alignment of these eight arminins revealed a high degree of conservation in the negatively charged N-terminal part and a high variability within the active, cationic C-terminal part (Augustin *et al*, 2009a) (Figure 1.8 C), likely resulting in differential bacteriocidal activity.

1.4 Host-microbe interactions in *Hydra*

In 2007, *Hydra* polyps were shown to be stably associated with distinct bacterial communities (Fraune and Bosch, 2007). The bacterial microbiota of two species, *Hydra vulgaris* and *Hydra oligactis*, was compared in laboratory cultures and animals freshly isolated from the wild (**Figure 1.9 A**). Intriguingly, the microbiota of the two species was clearly distinguishable and displayed similar characteristics comparing polyps from the wild with polyps from cultures, laboratory maintained for more than 30 years (**Figure 1.9 B**). This long-term maintenance of specific host-bacterial associations implied a strong host-specific selective pressure imposed on the bacterial community (Fraune and Bosch, 2007).

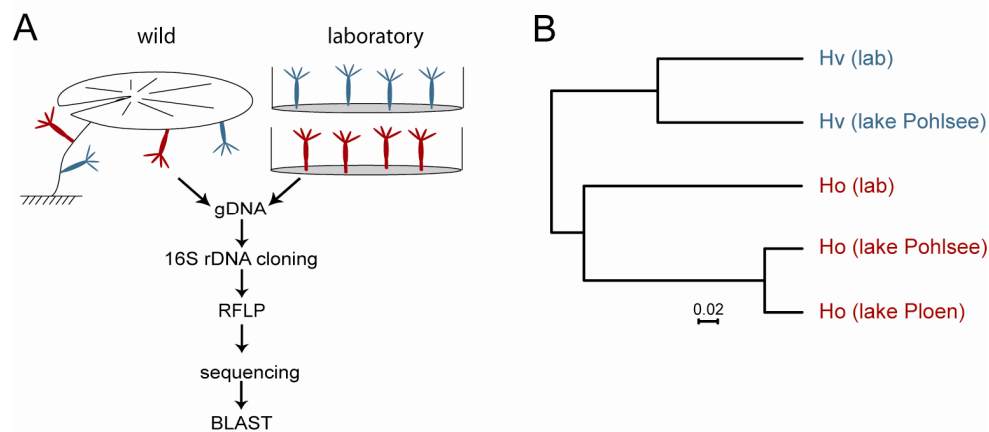


Figure 1.9: Long-term maintenance of species-specific bacterial associations in *Hydra*.

(A) Schematic representation of the experimental approach. Bacterial microbiota were compared between *H. vulgaris* (blue) and *H. oligactis* (red) from laboratory culture (Right; drawn in plastic dishes) and the wild (Left; attached to water lily). (B) Jackknife environment cluster tree (weighted UniFrac metric) of the analyzed bacterial communities. One hundred jackknife replicates were calculated, and each node was recovered with 99.9%. (Scale bar: distance between the environments in UniFrac units.) Hv, *H. vulgaris*; Ho, *H. oligactis*; lab, animals from laboratory culture; lake Pohlsee, animals taken from Lake Pohlsee; lake Ploen, animals taken from Lake Ploen. Figures modified from (Fraune and Bosch, 2007).

This finding was validated by a strong link between epithelial tissue homeostasis and bacterial community composition (Fraune *et al*, 2009a), since elimination of derivatives of the interstitial stem cell lineage caused significant alterations in the microbiota (Fraune *et al*, 2009a). Thus, an intimate interplay exists between the *Hydra* tissue and its associated bacteria, shaping the microbiota in a host-species specific manner. It was shown previously (Fraune *et al*, 2010) that early embryonic stages prior to the cuticle stage are colonized by a limited number of microbes, which are clearly distinct from later developmental stages. Interestingly, the sequential colonization is reflected in differential expression of AMPs from the periculin peptide family, inferring a role of these peptides in mediating the colonization process (Fraune *et al*, 2010).

1.5 Aims of the thesis

Using highly informative molecular techniques like 454 pyrosequencing, microarray gene expression profiling, transgenesis and the generation of germfree *Hydra* polyps, the following questions were addressed in this thesis:

1. How do bacterial associations differ between various *Hydra* species?
2. How does *Hydra* benefit from its associated bacterial microbiota?
3. How do host-bacterial associations establish during host development?
4. Is the host actively sensing its commensal bacteria using Toll-like receptor signaling?
5. Do host-specific antimicrobial peptides shape species-specific bacterial communities?

2 Results

2.1 *Hydra* polyps are associated with host-specific, stable bacterial communities

In 2007, Fraune *et al.* uncovered that two species of the cnidarian *Hydra* are colonized by remarkable different bacterial communities, although being cultured under identical laboratory conditions for three decades (Fraune and Bosch, 2007). These analyses were done using restriction fragment length polymorphism (RFLP), limiting the sampling depths to approximately 50 analyzed bacterial clones per sample (Fraune and Bosch, 2007). In the present thesis, this approach was extended by conducting a multi-species comparison using modern deep sequencing technologies. Therefore, the associated bacterial communities of seven *Hydra* species, laboratory-reared under identical conditions including diet, medium and temperature for more than three decades, were characterized by 454 pyrosequencing the variable regions 1 and 2 (V1V2) of the bacterial 16S rRNA gene, amplified from total DNA extracted from single *Hydra* polyps (**Figure 2.1**). Pyrosequencing resulted in 79,130 high quality reads ranging from 1410 to 10130 reads per sample. For inter-sample comparisons, sequences were rarified to 1300 reads per sample, grouped into operational taxonomic units (OTUs) at a $\geq 99\%$ sequence identity threshold and classified by RDP classifier.

The microbiota of all seven *Hydra* species was dominated by gram-negative bacteria. Betaproteobacteria of the family Comamonadaceae or Burkholderiaceae dominated in the closely related species *Hydra magnipapillata*, *Hydra carnea*, *Hydra vulgaris* (AEP), and *Hydra vulgaris*. The most basal species, *Hydra viridissima*, was colonized by species-specific bacterium of the Alcaligenaceae family. The general primers, used to amplify the bacterial 16S rRNA gene sequence, also target the ribosomal DNA of chloroplasts from the symbiotic algae *Chlorella sp.* Note that these chloroplast sequences were removed from *H. viridissima* samples.

Hydra oligactis and *Hydra circumcincta* were characterized by the dominance of Alphaproteobacteria or Spirochaetes, respectively (**Figure 2.1**).

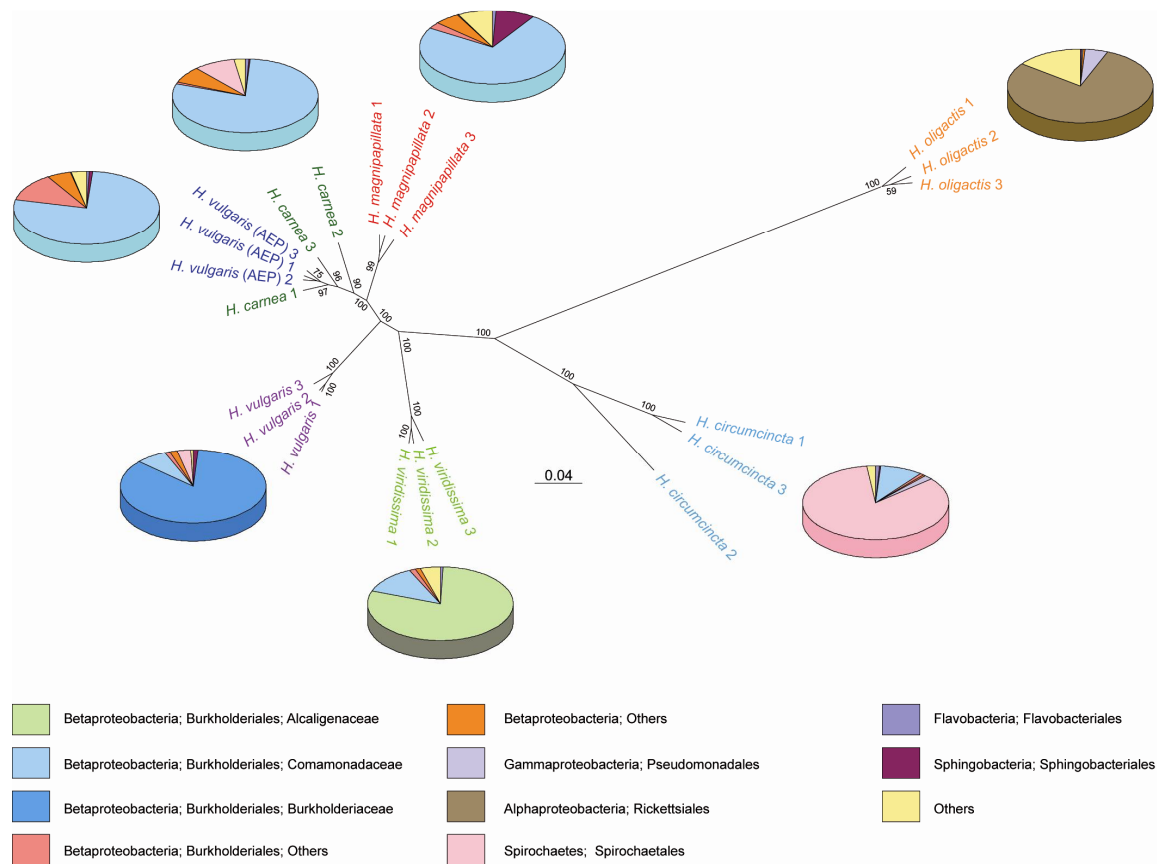


Figure 2.1 Different species of the cnidarian *Hydra* are colonized by distinct bacterial communities.

Jackknife environment cluster tree (weighted UniFrac metric, rarified to 1300 sequences/sample) of 21 bacterial communities from seven different *Hydra* species. 1000 replicates were calculated, nodes are marked with Jackknife support values. The branch length indicator displays distance between samples in Unifrac units. Pie charts represent relative abundance of bacterial orders (pooled data of n=3). The highly variable Burkholderiales order was separated into different families. Note that the proportion of *Chlorella sp.* sequences in *H. viridissima* was removed *in silico*.

Interestingly, the microbiota of *Hydra vulgaris* (AEP), the strain used to generate transgenic *Hydra*, clustered together with *Hydra carnea*. This is noteworthy, since molecular phylogenetics in *Hydra* revealed that *Hydra vulgaris* (AEP) is more closely related to *Hydra carnea* than to its eponym *Hydra vulgaris* (Hemrich *et al.*, 2007).

Although unlikely due to the observed correlation between microbiota and host phylogenetic relationship, the observed species-specificity of host-bacterial associations could result from long-term separate cultivation and accidental exposure to different bacteria. To exclude that, pairwise co-cultivation of the morphologically distinguishable species *Hydra vulgaris* (AEP), *Hydra oligactis* and *Hydra viridis* were conducted. To facilitate transfer of bacteria, co-cultivation of two individual polyps was conducted in a relatively small volume of 1.5 ml Hydra-Medium. Following five weeks of co-cultivation, single polyps were subjected to 454 pyrosequencing of the microbiota. Chimeric sequences were identified and removed using Chimera Slayer (Haas *et al.*, 2011). After removal of chimeric sequences and reads assigned to

Chlorella sp. chloroplasts in *H. viridissima*, pyrosequencing resulted in 1394 to 6790 reads per sample and were subsequently rarified to 1350 reads per sample.

As shown in **Figure 2.2**, all three *Hydra* species maintain their specific bacterial profiles even under co-cultivating conditions, leading to three distinct clusters in a principle coordinate analysis of the weighted Unifrac distance matrix. These results clearly validate the host tissue as determinant for bacterial community composition.

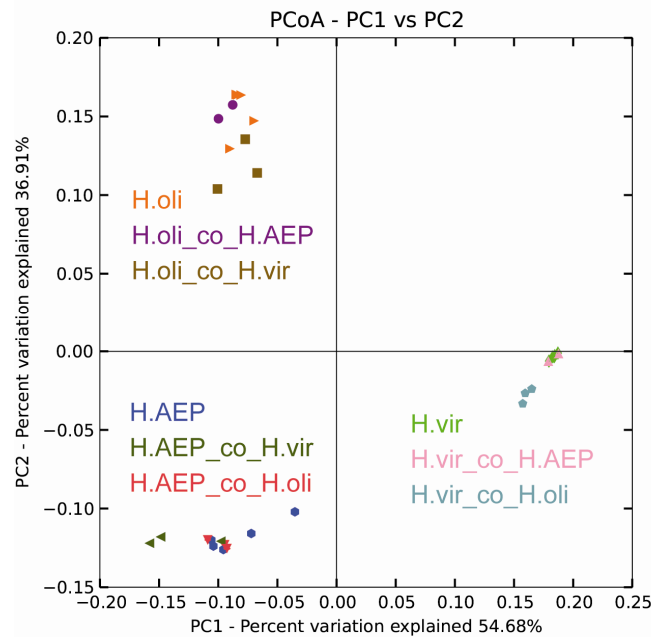


Figure 2.2: Host-species specific bacterial communities remain stable in coculture.

Bacterial communities clustered using principle coordinate analysis of the weighted Unifrac distance matrix. The percent variation explained by the principle coordinates is indicated at the axes. Reads were rarified to 1350 reads/sample. *H.oli* = *Hydra oligactis*; *H.AEP* = *Hydra vulgaris* (AEP); *H.vir* = *Hydra viridissima*; co = co-cultured. For co-cultivation samples, colored symbols refer to the first species named. Co-cultivations were conducted in biological triplicates (n=3); n=5 for non-co-cultivated polyps (*H.oli*, *H.AEP*, *H.vir*). Certain samples cluster strongly together such that single symbols may be overlaid. Note that cocultivation with other *Hydra*-species does not influence the microbiota.

Taken together, these data uncover strong host-specificity of the associated bacterial communities, which partially reflect phylogenetic relationship of the hosts. Since environmental conditions were identical for all investigated species for decades, the host evidently seems to sculpture and maintain its microbiota.

2.2 Commensal bacteria protect *Hydra* from a fungal pathogen

Effects of the host-associated microbiota can be tested by generation of germfree animals, followed by a phenotypical readout. Once an effect on host-fitness was discovered, mono-associations studies using single bacterial species can be used to determine the specific bacteria responsible for the observed effect. Germfree *Hydra vulgaris* (AEP) polyps were generated by the use of antibiotics. In contrast to control cultures, growth of fungal hyphae was observed regularly in germfree cultures (**Figure 2.3 A, B**), finally leading to the death of polyps. Sequencing of the internal transcribed spacer (ITS1 and ITS2) ribosomal DNA identified the fungi as *Fusarium sp.* (GU982311.1, also known as *Gibberella sp.*). *Fusarium* is a large genus of filamentous fungi. Most members are harmless saprobes but some species are described as pathogens, producing mycotoxins like fumonisins or trichothecenes (Dean *et al.*, 2012, Scott, 2012, Ueno *et al.*, 1972).

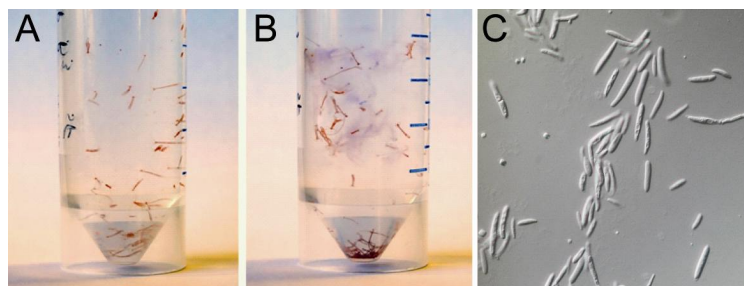


Figure 2.3: Germfree *Hydra* cultures are prone to fungal infection by *Fusarium sp.*

(A) Control culture showing no fungal growth, (B) germfree *Hydra* culture, infected by *Fusarium sp.*, contrast was increased for better visualization of fungal hyphae. (C) Phase contrast microscopic image of fungal spores present in the culture supernatant.

To analyze fungal infection under controlled conditions and to elucidate which bacteria inhibit growth of *Fusarium sp.*, ex-germfree polyps, mono-associated with single bacterial species, as well as germfree, control and conventionalized (*i.e.* ex-germfree polyps reinfected with a complex, native microbiota) polyps were incubated with spores of *Fusarium sp.* (**Figure 2.3 C**). Seven days post infection, polyps were screened for the presence or absence of fungal hyphae in a single-blind trial. As shown in **Figure 2.4 A**, germfree polyps were susceptible to fungal outgrowth in all replicates, while control polyps largely inhibited fungal germination. The re-introduced complex microbiota (conventionalized), as well as four bacterial monoassociations, *Acidovorax sp.*, *Curvibacter sp.*, *Pelomonas sp.* as well as an Oxalobacteraceae species, effectively protected the host against fungal infection *in vivo*.

All bacterial types were additionally tested in an *in vitro* assay. Bacterial cultivars were locally spotted on Reasoner's 2A agar (R2A) plates. After two days of bacterial growth, fungal spores were added to the center of the bacterial plaque and fungal growth was quantified after five days by measuring the diameter of visible hyphae. Only one bacterial cultivar, *Pelomonas sp.*, showed strong antifungal activity by almost complete inhibition of fungal growth (**Figure 2.4 B**). Surprisingly, this bacterium showed only weak antifungal activity *in vivo*, while *Acidovorax sp.*, which showed the strongest antifungal activity *in vivo*, had no effect *in vitro* (**Figure 2.4 B**).

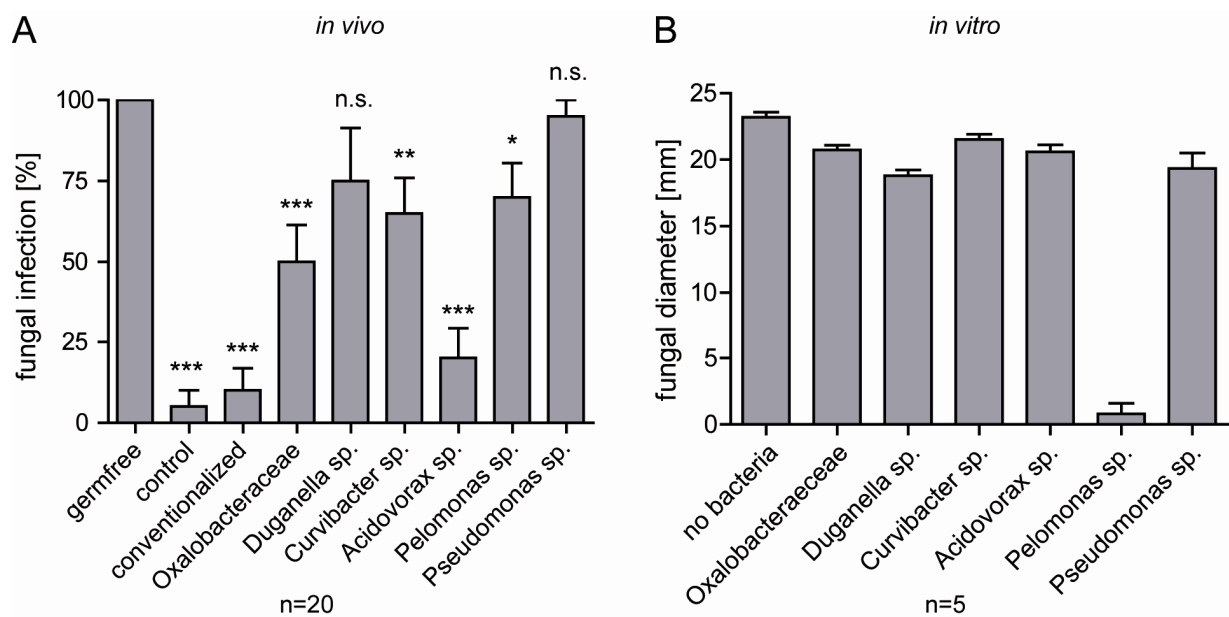


Figure 2.4: The microbiota is protective against fungal infection

(A) *In vivo* infection with *Fusarium* spores. Germfree polyps are prone to fungal infection, while the native microbiota is protective. Certain bacterial mono-associations decrease the susceptibility to fungal infection significantly compared to germfree conditions. Statistical analysis was conducted by Fisher's exact test ($p < 0.05 = *$, $p < 0.01 = **$, $p > 0.001 = ***$, $n = 20$). (B) *In vitro* plate test for fungal inhibition by bacteria isolated from *Hydra* tissue. *Pelomonas sp.* inhibits fungal outgrowth almost completely ($n = 5$).

2.3 The ontogenetic establishment of the microbiota in *Hydra*

In the model organism *Hydra*, unlike most animal systems, it is possible to examine temporal bacterial profiles of genotypes without being limited to fecal samples, since *Hydra* can be proliferated clonally under constant laboratory conditions.

Following fertilization, *Hydra* oocytes develop by a radial cleavage pattern outside the female polyp (**Figure 2.5 A**) Young *Hydra* polyps directly hatch from the cuticle stage (**Figure 2.5**

B) and start to proliferate asexually within one week under well-fed conditions. To elucidate how bacterial communities assemble in newly hatched *Hydra* polyps, the composition of the microbiota in polyps was profiled over the first 15 weeks after hatching (**Figure 2.5 C**) using culture independent pyrosequencing of bacterial DNA.

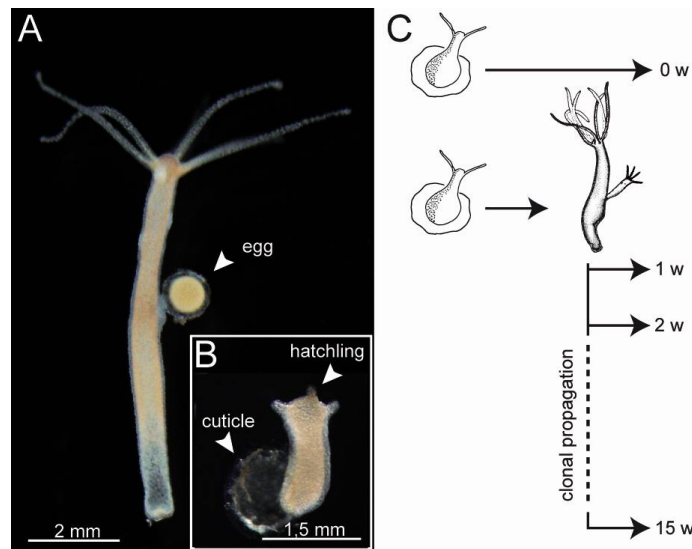


Figure 2.5 *Hydra* morphology and experimental design.

(A) Female polyp of *Hydra vulgaris* (AEP) with a developing embryo. (B) *Hydra* hatchling eclosing from the cuticle. (C) Experimental design: First batch of hatchlings was used for immediate DNA extraction. Second batch of hatchlings was used for the establishment of clonal cultures, from which one polyp was removed for DNA-extraction every week until week 15. Subsequently, the bacterial communities of these samples were determined by 454 sequencing.

2.3.1 Bacterial population profiles in newly hatched *Hydra* polyps

To follow the assembly of the microbiota in newly hatched polyps, four clonal cultures (*i.e.*, four replicates) of single hatchlings were established and examined for up to 15 weeks (**Figure 2.5 C**). Four additional hatchlings were used for immediate DNA extraction. The composition of the microbiota was determined by pyrosequencing of the variable regions 1 and 2 (V1V2) of the bacterial 16S rRNA gene, amplified from total DNA extractions of single polyps. Pyrosequencing resulted in 177,862 high quality reads ranging from 2110 to 9845 reads per sample. For inter-sample comparisons, the number of reads was normalized to 2000 reads per sample. In all four replicates, comprising bacterial profiles of a total of 36 polyps, bacterial species estimation using the Chao1 metric showed the highest bacterial diversity immediately after hatching (black line, **Figure 2.6**). About 350 different operational taxonomic units (OTUs) (97% sequence similarity) were estimated in polyps just emerging from the cuticle stage. In all four replicates, bacterial diversity decreased in the following two to three weeks to about 150 OTUs. Four weeks post hatching, a transient but distinct increase

in bacterial diversity to 200-300 OTUs per polyp was observed (**Figure 2.6**), followed by a decrease in bacterial diversity in all four replicates to ~100 OTUs per polyp 15 weeks post hatching. Thus, the diversity of the bacterial community in *Hydra* polyps at various time points after hatching was negatively correlated with developmental age (**Figure 2.9 A**).

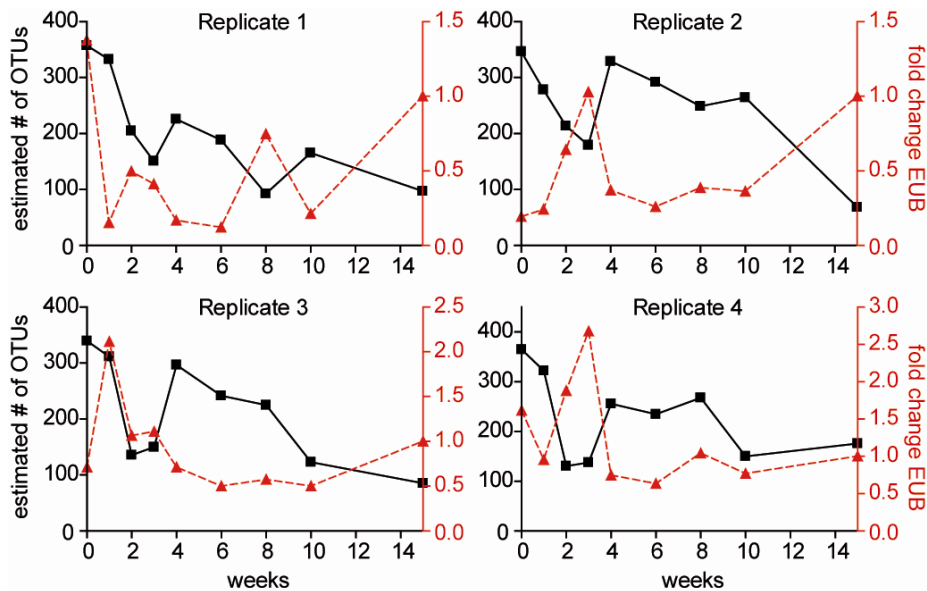


Figure 2.6: Dynamics of bacterial diversity and bacterial load.

Estimated number of OTUs (97% sequence identity, Chao1 metric, black line) was plotted against time post hatching. Red lines indicate the relative bacterial (EUB) abundance per host cell as analyzed by qRT-PCR for the bacterial 16S gene (equilibration to *Hydra actin*, reference value 15 weeks post hatching).

To examine whether the changes in bacterial diversity are accompanied by changes in the overall density of bacteria, bacterial abundance was quantified using a broad-range bacterial primer pair. As shown in **Figure 2.6** (red line), fluctuations in bacterial load across replicates and between time points were observed. For example, in replicate 1, bacterial abundance per host cell was highest immediately after hatching whereas in replicate 2 hatchlings had a rather low bacterial abundance. Thus, bacterial abundance is not correlated with bacterial diversity or with developmental age.

The next question addressed was, which bacterial species are members of the microbiota and whether membership changes during development. Sequence analysis uncovered remarkable differences between the bacterial communities in newly hatched polyps compared with adult (*i.e.* 15 weeks post hatching) animals (**Figure 2.7 A**).

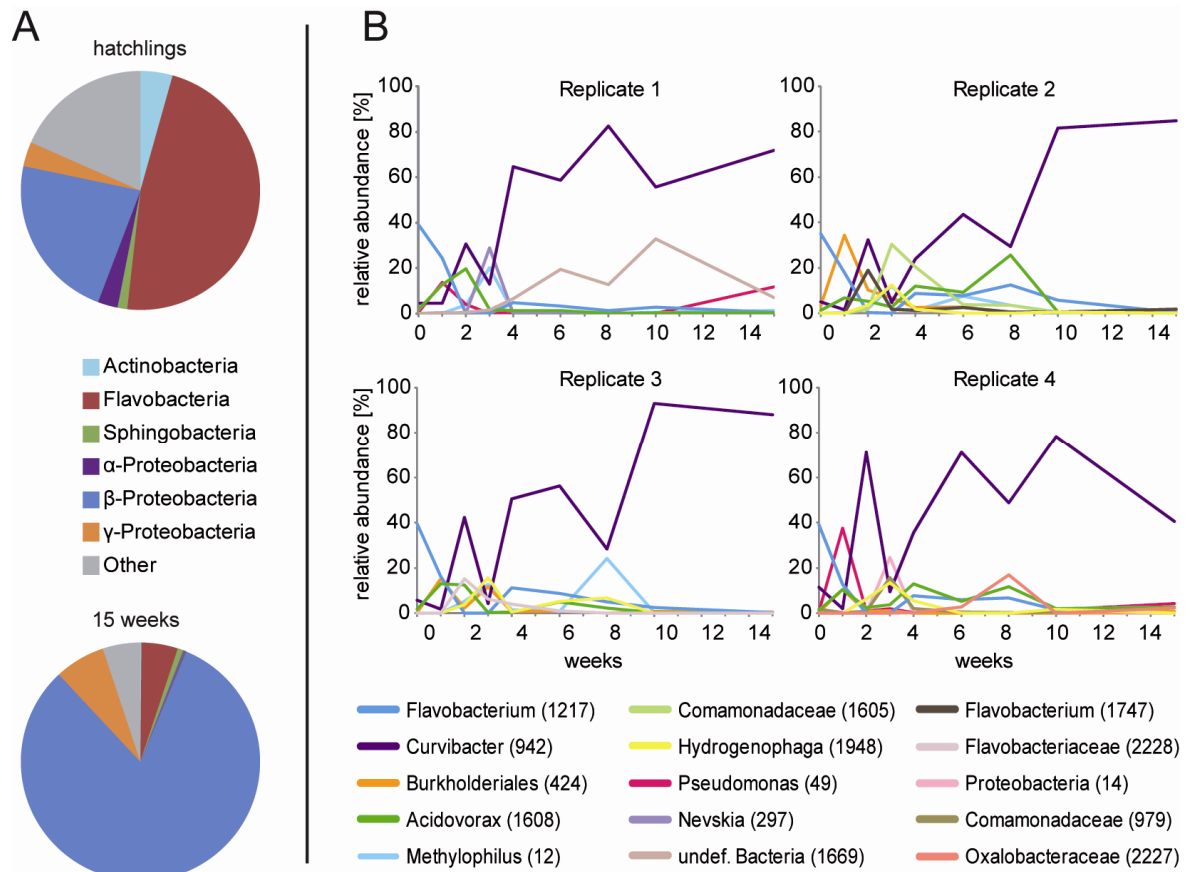


Figure 2.7: Dynamics in the microbiota composition.

(A) Pie diagrams representing the bacterial community of *Hydra* polyps directly after hatching and 15 weeks post hatching, respectively. Bacterial OTUs are summarized on class-level. Fraction “other” includes OTUs that could not be assigned to bacterial classes using the ribosomal database project (rdp) classifier at a 60% threshold. (B) Relative abundances of bacterial OTUs (97% similarity) over the first 15 weeks post hatching. Only OTUs exceeding 10% in at least one sample were plotted. Note that OTU 942 (*Curvibacter* sp.) is the most abundant at week 2 in all replicates, declines again and becomes the dominating species in adult polyps.

Hatchlings were characterized by a high abundance of bacteria of the Bacteroidetes (Flavobacteria, Sphingobacteria) group, which represented about 50 % of the total OTUs. In addition, also a large proportion of Betaproteobacteria was identified in hatchlings. Other members of the bacterial community include Actinobacteria, Alphaproteobacteria and Gammaproteobacteria (Figure 2.7 A). In contrast, the bacterial community in polyps 15 weeks post-hatching differed greatly from the composition of the community characteristic for hatchlings (Figure 2.7 A) and resembled the previously described (Fraune *et al*, 2010) bacterial community in clonally growing *Hydra vulgaris* (AEP) polyps.

Figure 2.7 B shows the temporal assembly of the bacterial community (resolved at the OTU level) in four replicates at various time points after hatching. Only OTUs exceeding a relative abundance of 10% in at least one time point are shown. The assembly pattern is characterized by three distinct features. First, the bacterial composition immediately after hatching was similar in all four replicates and was characterized by a large number of *Flavobacterium* sp.

(OTU 1217). Other members of the “young” bacterial community belong to a variety of different bacterial phylotypes and include *Curvibacter sp.* (OTU 942) (**Figure 2.8**). Second, the first three weeks of assembly were characterized by a high degree of fluctuation in community composition with the presence of Burkholderiales (OTU 424) and *Acidovorax sp.* (OTU 1608) bacteria at week one, *Curvibacter sp.* (OTU 942) at week two and *Methylophilus sp.* (OTU 12), Comamonadaceae (OTU 1605) and Hydrogenophaga (OTU 1948) bacteria at week three in all four replicates (**Figure 2.7 B**, **Figure 2.8**). Third, the phase of high variability in the first weeks post-hatching was replaced by the establishment of a robust bacterial composition dominated by *Curvibacter sp.* (OTU 942) (**Figure 2.7 B**).

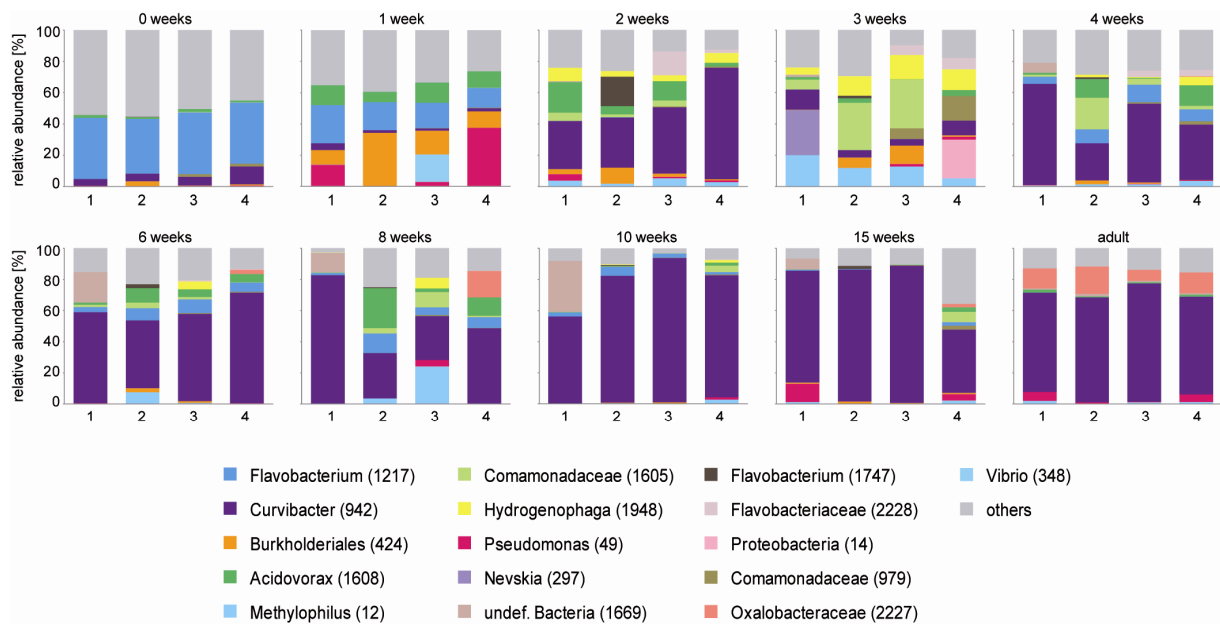


Figure 2.8: Comparison of the microbiota between 4 different replicates.

Only OTUs which exceed 10% in at least one sample are shown. Remaining OTUs were grouped and colored gray, representing the rare microbiota. This portion is highly abundant in the hatching sample and continually decreases with time. Numbers 1 to 4 represent replicate numbers. The sample set “adult” was included from a previous study (Franzenburg *et al*, 2012) and characterizes the bacterial community of a one year old, clonally growing culture.

Interestingly, in all four replicates the occurrence of *Curvibacter sp.* showed a distinct temporal pattern during assembly. While first present at low abundance in newly hatched polyps, *Curvibacter sp.* became the dominant member of the bacterial community for a short period of time two weeks post hatching. Thereafter, abundance of *Curvibacter* decreased markedly again. From week four on, *Curvibacter* became the dominant member of the bacterial community (**Figure 2.7 B**, **Figure 2.8**), which is correlated with a decrease in total bacteria diversity (**Figure 2.9 B**). As there is no general increase in bacterial load over developmental time (**Figure 2.6**), the relative increase of *Curvibacter* is due to relative

interchanges in the community. Therefore, the host seems to offer a certain amount of niches for bacterial colonizers and over time *Curvibacter* is occupying the niches formerly used by other bacteria.

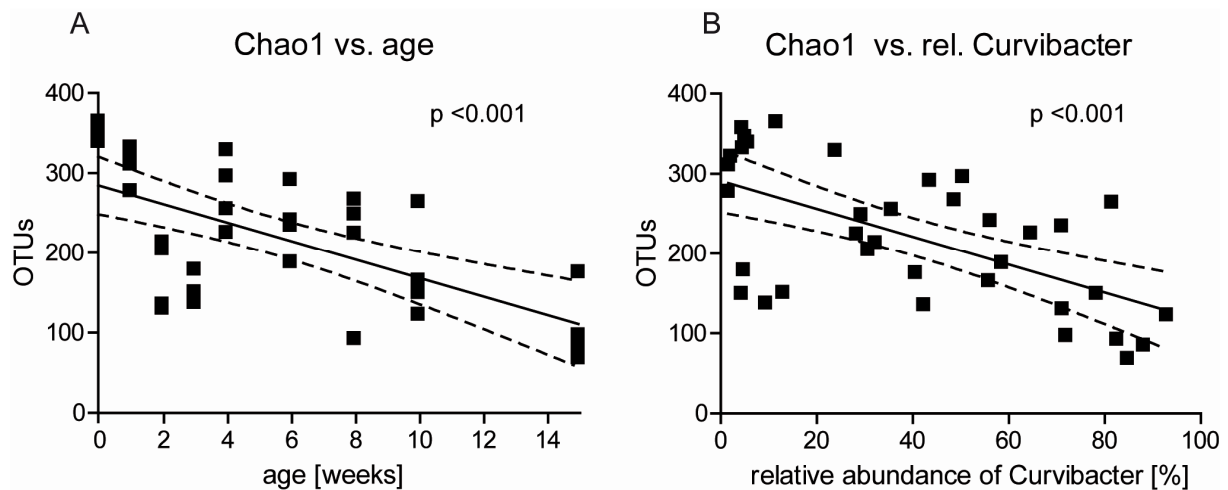


Figure 2.9: Correlating features of the microbiota establishment.

(A) Correlation of Chao1-estimated bacterial diversity with age of the polyps. (B) Correlation of Chao1-estimated bacterial diversity with the relative abundance of *Curvibacter sp.* sequences in the 454 dataset. Dashed line represents 95% confidence interval. Significance was tested by linear regression.

To further analyze the temporal progression of the bacterial community towards an adult like bacterial profile, Principle Coordinate Analysis (PCoA) was conducted (**Figure 2.10 A**) and the average Pearson correlation of each assembly time point was calculated (**Figure 2.10 B**). For comparison bacterial profiles of four long-term cultures of *Hydra vulgaris* (AEP) were used. As shown in **Figure 2.10 A**, the four hatchling samples cluster together, indicating a bacterial composition that substantially differs from all other samples. PCoA analysis also indicates that polyps examined one week after hatching and three weeks after hatching have distinct bacterial communities different from those found in polyps immediately after hatching as well as from adult polyps. According to the PCoA analysis, the microbial community of polyps analyzed 4 to 15 weeks after hatching resembled the adult microbiota found in polyps of long-term cultures (**Figure 2.10 A**). This view is supported by Pearson correlation analysis (**Figure 2.10 B**), which displays a low value immediately after hatching and in one week old polyps, indicating that these bacterial communities differ substantially from adult profiles. Two weeks post-hatching, the correlation was high, indicating striking but transient resemblance to the adult-like microbial pattern. After this transient period the correlation drops to values similar to those found in newly hatched polyps. At four weeks after hatching the correlation increased and remained high in all later time points (**Figure 2.10**

B). These observations indicate that the progressive development of the adult-like microbial profile in *Hydra* encompasses a remarkable transient occurrence of the generic adult-like profile 2 weeks post hatching, leading to a preponderance of *Curvibacter sp.* from four weeks post hatching on.

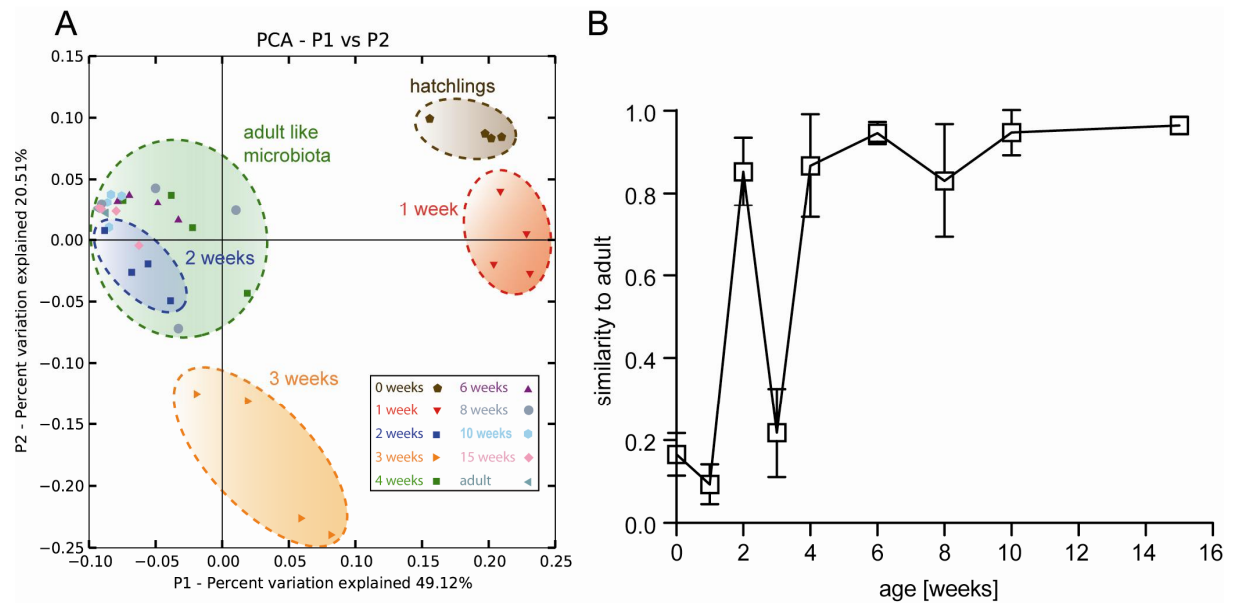


Figure 2.10: Temporal profile of the progression to an adult microbiota.

(A) Principal coordinate analysis of Pearson distances between *Hydra* microbiota at different time points post hatching (OTU level 97%). The percent variation explained by the plotted principal coordinates is indicated at the axes. The microbiota of late time points (10 weeks, 15 weeks, adult) show high similarity such that single symbols may be overlaid. Adult profiles were retrieved from an independent *Hydra* culture, clonally grown for more than one year. (B) Mean Pearson correlation between the microbiota of each time point compared to an adult profile retrieved from 4 independent adult polyps (clonal propagation for one year). Note the peak of the Pearson correlation at the 2 week time point.

2.3.2 Computing the microbial assembly pattern

The surprisingly dynamic, but robust bacterial succession pattern was combined with a mathematical modeling approach to infer organizational principles that may influence community assembly and diversity. Mathematical modeling is a powerful approach to understand the complexity of biological systems (Murray, 2002). To get insights into the principle rules, controlling the microbial assembly process in the *Hydra* holobiont (**Figure 2.11 A**), a cooperation with Dr. Philipp Altrock and Dr. Arne Traulsen from the research group of evolutionary theory at the Max Planck Institute of Plön was established. They tried to find the mathematical model with the lowest degree of complexity, which resembles the observed data. Therefore, a replicator-colonizer approach was applied (Hofbauer and Sigmund, 1998). This models the temporal evolution of an interacting bacterial community in a competitive environment deterministically. This allowed to qualitatively simulate the colonization dynamics based on complex interactions among bacteria and between bacteria

and host. Since microbial communities in *Hydra* contain tens to hundreds of microbial species, this obviously incomprehensible complexity of community member behavior was reduced by assuming that the bacterial community only consists of four distinct members (**Figure 2.11 A**). The main assumption was that the progressive assembly of the bacterial population is restricted to pair-wise interactions. The notations used in the mathematical model are defined in **Figure 2.11 B**.

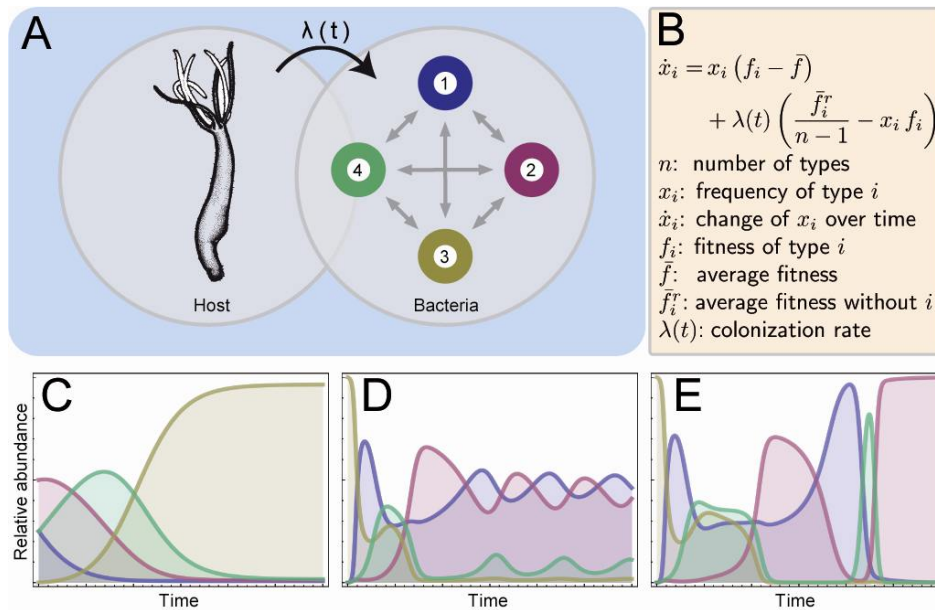


Figure 2.11: Mathematical modelling of the bacterial colonization process in *Hydra*.

(A) Mathematical model of the colonization process with $n=4$ bacterial types, which interact pairwise and grow subject to their fitness and a colonization rate $\lambda(t)$. (B) The basic dynamic equation is the replicator-colonizer equation. (C-E) To gain qualitative understanding of the key factors of the colonization process, we followed three successive steps. (C) First, bacterial interactions are constant, and type specific. The colonization rate is constant $\lambda=0.02$. (D) Second, frequency dependent interactions yield more complex behavior, e.g., cyclic patterns under constant colonization rate ($\lambda=0.02$). (E) Third, adding a time decaying colonization rate, the initially oscillatory / fluctuating behavior is damped by a factor external to the bacterial community, $\lambda(t)=0.02e^{-t/20}$, such that the final distribution with a unique single predominant bacterial type is assumed. Thus, frequency dependent growth rates of the bacteria are not enough to explain the dynamics; an external modulation of the colonization process is additionally required.

The mathematical analysis focused on three possible patterns of interactions within this idealized holobiont. First, constant type specific fitness values (constant growth and colonization rates) were assumed with competition not being dependent on the distribution of relative abundances. Here, the type with the highest growth rate wins the competition if the colonization rate is small enough. As shown in **Figure 2.11 C**, the predicted colonization pattern does not agree with the qualitative pattern of the experimental data (see **Figure 2.7 B**). An intermediate decline in the abundance of the final winner of the competition is not present. Next, fitness of the bacterial members of the microbiota was modeled as abundance dependent. In this case competition can be such that a bacterium has an advantage when it is

rare, but a disadvantage when it is abundant in the community (frequency dependence). This can give rise to more complex patterns over time. The final distribution depends on the initial distribution. This approach was examined by using a constant colonization rate λ (**Figure 2.11 B**). As shown in **Figure 2.11 D**, this can lead to an oscillatory assembly pattern resembling the observed initial colonization dynamics (see **Figure 2.7 B**). However, it does not capture the stable adult bacterial colonization profile of the host, dominated by one bacterial species. In a third modeling step, the colonization rate was assumed to be time dependent, *i.e.* assuming that it decays over time as the organism approaches its adult state, $\lambda(t) = \lambda_0 e^{-t/\tau}$, where τ is an environmentally or host derived specific decay rate. As shown in **Figure 2.11 E**, such an environmental / host controlled colonization rate modulates the abundance dependent competition such that an initially cyclic competition ends up in a final state dominated by a single bacterial type. Following an initial phase of oscillatory behavior, there is a transition period that sensitively depends on initial condition and on the decay rate. According to this model (see **Figure 2.11 B**), the eventual winner of the microbial competition is present transiently at relatively high abundance at an earlier stage, before a stable community with reduced bacterial diversity is reached. This modeling approach qualitatively resembles the experimental data, indicating that both inter-microbial interactions (frequency-dependent fitness) as well as environmental or host-derived factors controlling the bacterial colonization rate (λ) are important in dictating bacterial community assembly in *Hydra* polyps. Note that, instead of fitting parameters to the experimental data, the minimal complexity of a mathematical model that captures crucial dynamical aspects of the colonization process was inferred. In conclusion, this study not only illustrates the feasibility of the combined *in vivo* and mathematical modeling approach to dissect the complexity of host-microbe interactions in the simple metazoan *Hydra*, but also reveals novel steps that modulate the assembly process.

2.4 The role of TLR-sensing in host-microbe homeostasis

Toll-like receptors (TLRs) are conserved throughout animal evolution but appear to serve different functions in different model organisms, ranging from cell adhesion and embryogenesis to immune defense (**Figure 2.12 A**). Cnidaria are a sister group to the Bilateria (Putnam *et al*, 2007) and one of the earliest branches in the animal tree of life. The

recent genome project of the cnidarian *Hydra magnipapillata* identified a conserved TLR-signaling cascade (Bosch *et al*, 2009, Miller *et al*, 2007), (**Figure 2.12 B, Table 2.1**), making *Hydra* a suitable model for addressing questions of the ancestral function of TLR-signaling.

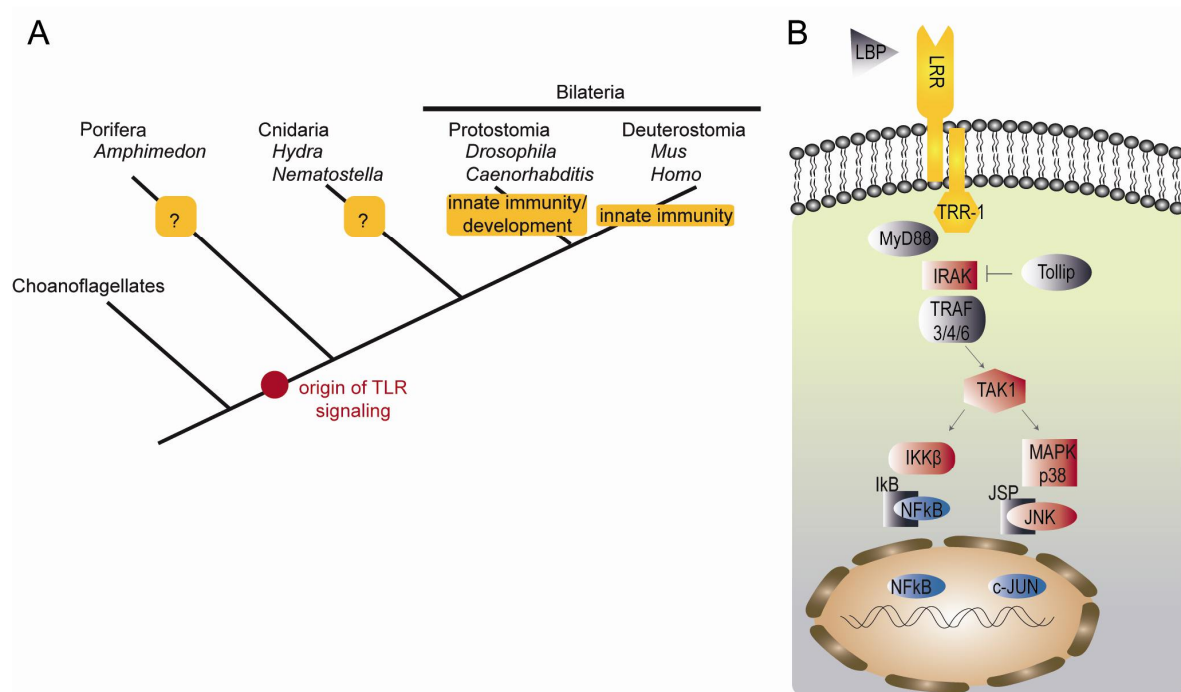


Figure 2.12: The evolution of Toll-like receptor signaling

(A) Emergence and function of TLR-signaling during metazoan evolution. Cnidaria are a sister group to all Bilateria and diverged from a common eumetazoan ancestor ~600-700 million years ago. (B) Schematic representation of TLR-signaling in *Hydra*. Note that the functional *Hydra*-TLR is assembled by two proteins (*HyLRR* and *HyTRR*) (Bosch *et al*, 2009). Yellow: receptors; gray: adapter proteins; red: kinases; blue: transcriptionfactors.

Is the TLR pathway involved in the defense against bacterial pathogens or in maintaining specific host-microbe interactions? Does it affect the mechanisms and routes by which functionally diverse bacteria colonize their host? Is it involved in developmental processes such as axis formation? To gain insight into these questions, MyD88 loss-of-function experiments were performed in *Hydra vulgaris* (AEP). A combination of microarray based gene expression screening and 16S rRNA-gene sequencing was conducted to detect changes in both, the *Hydra* transcriptome and the associated microbiota. Further, the role of TLR-signaling in pathogen defense against *Pseudomonas aeruginosa* was investigated.

2.4.1 Generation of MyD88-deficient (MyD88⁻) *Hydra vulgaris* (AEP)

To analyze the function of TLR-signaling in the basal metazoan *Hydra*, a stable transgenic *Hydra vulgaris* (AEP) line with a drastically reduced expression level of the universal adapter protein MyD88 was generated, using a hairpin cassette containing the *myd88* antisense and sense sequences fused to the reporter gene *egfp* (Figure 2.13 A).

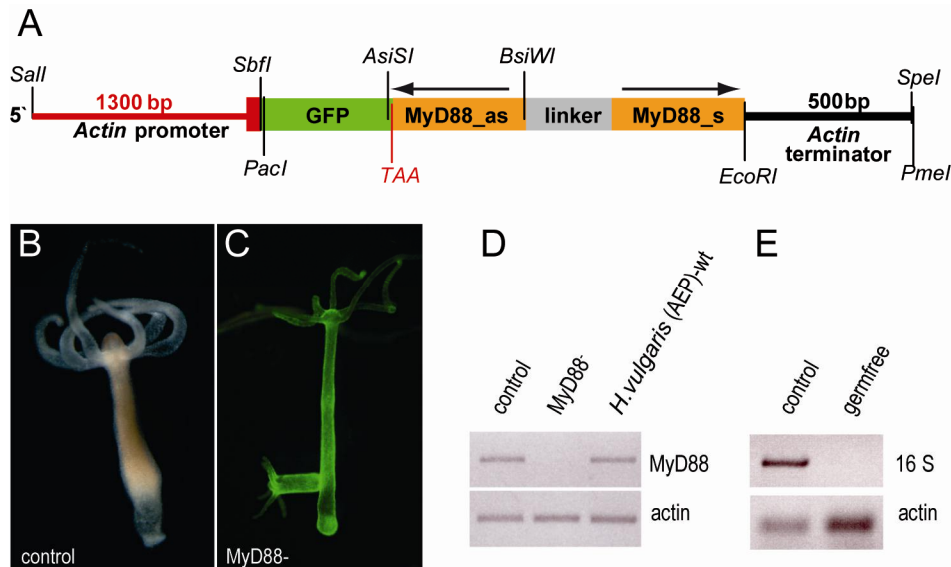


Figure 2.13: Interference with the *Hydra* TLR-signaling pathway by hairpin mediated silencing of MyD88. (A) MyD88-Hairpin construct for generation of transgenic *Hydra* (as: antisense, s: sense, TAA: stop codon). (B) Live image of a MyD88-control polyp (control). (C) Live image of a MyD88-knockdown polyp (MyD88⁻) showing eGFP expression in the endodermal and the ectodermal cell lineage. (D) RT-PCR amplifying *myd88* shows down-regulation in MyD88⁻ polyps compared to control polyps and wild type (wt) *Hydra vulgaris* (AEP). RT-PCR was normalized using the *Hydra actin* gene. (E) Absence of bacteria after antibiotic treatment was confirmed by PCR amplification of the bacterial 16S rRNA gene on genomic DNA normalized to *Hydra actin*.

The transformation of 2-4 cell stage embryos via microinjection resulted in a founder polyp, showing mosaic distribution of GFP-positive endodermal and ectodermal epithelial cells. These positive cells could be enriched or depleted in clones generated by budding, depending on where the bud formed. By several rounds of asexual proliferation, two stable lines were established. They were termed MyD88-control (control) line, which contained no remaining GFP-positive cells (Figure 2.13 B), and the MyD88-knockdown (MyD88⁻) line, which expressed the transgene in the endodermal and ectodermal cell lineage (Figure 2.13 C). The resulting dsRNA triggers the RNAi machinery (Fire *et al.*, 1998, Kennerdell and Carthew, 2000, McManus and Sharp, 2002, Zamore, 2002) which leads to a decrease in the endogenous MyD88-transcript as shown by RT-PCR (Figure 2.13 D). Since both lines were generated from the same founder polyp by asexual reproduction, effects of a drastically decreased MyD88 expression level could be analyzed without the need to account for differences in

genomic background. Neither line displayed any obvious developmental or behavioral abnormalities.

2.4.2 Absence of bacteria as well as MyD88 deficiency influence central parts of the TLR-signaling cascade

To assess the transcriptional consequences of a MyD88 knockdown and identify potential downstream effector genes of the TLR-signaling cascade, microarray analyses were performed. Expression levels of both, MyD88⁻ polyps as well as germfree polyps (**Figure 2.13 E**) were compared to control polyps. The MyD88⁻ polyps combined with the germfree polyps provided novel resources that allowed to directly investigate the connection between TLR-signaling and the regulation of associated bacterial diversity. Statistical analysis was carried out by ANOVA with Student-Newman-Keuls (SNK) post-hoc tests and false discovery rate (FDR) correction. The microarray data independently validate the successful MyD88 knockdown. Contig 11552, encoding for *myd88*, shows a 4.29 fold downregulation ($p < 0.001$) in MyD88⁻ polyps and was not differentially expressed in germfree polyps (fold change 1.09, n.s.) (**Table 2.1**). To check for transcriptional changes of other putative members of the TLR-cascade, the *Hydra vulgaris* (AEP) transcriptome (Hemmrich *et al*, 2012) was screened for homologues of previously described members of the TLR pathway. The majority of central cascade members are present in *Hydra vulgaris* (AEP) (**Figure 2.12 B**, **Table 2.1**). Various central components of the putative TLR cascade including members of the TRAF-family of ubiquitin protein ligases, the kinase TAK1, MAP-kinase p38 and the cJun-terminal kinase (JNK) inhibitor JSP-1 showed significantly decreased expression in germfree and/or MyD88-deficient conditions (**Table 2.1**).

Table 2.1: Putative TLR-cascade members show differential expression in germfree and / or MyD88-deficient conditions in *Hydra*

Annotation	Contig*	Blastp**	MyD88 ⁻		germfree	
			fold change	p value	fold change	p value
LBP	9861	7,00E-40	1,01	0,723	0,74	0,026
LRR1	47938		1,15	0,032	1,13	0,022
LRR2	46369		1,08	0,049	1,17	0,033
TRR1	708		1,06	0,268	0,82	0,045
TRR2	10818		0,97	0,532	0,88	0,032
MyD88	11552	3,00E-34	0,23	0,000	0,91	0,115
IRAK	7139	1,00E-20	0,88	0,261	0,88	0,261
Tollip	46616	1,00E-65	0,98	0,590	0,87	0,017
TRAF4	12390	2,00E-26	1,01	0,963	0,64	0,010
	13328	2,00E-40	1,02	0,946	0,61	0,010
	44978	1,00E-13	0,89	0,100	0,65	0,004
TRAF3	45514	7,00E-31	0,85	0,021	0,68	0,003
	45513		0,80	0,020	0,57	0,003
	12389		0,78	0,006	0,56	0,002
TRAF6	46773	3,00E-92	0,95	0,479	1,19	0,069
TAK1	474	1,00E-95	0,84	0,020	0,79	0,000
IKK β	47555	3,00E-88	0,92	0,623	1,05	0,689
ankyrin_rp	7685		1,34	0,003	1,77	0,000
IkappaB	8355	3,00E-17	1,01	0,857	1,09	0,080
NfkappaB	9522	3,00E-46	0,99	0,714	0,92	0,005
p38 alpha	10926	2,00E-151	0,82	0,003	0,74	0,001
p38 beta	35834	3,00E-18	0,74	0,018	0,60	0,001
JNK	13307	0.0	0,95	0,559	0,90	0,084
JSP-1	12280	3,00E-44	0,79	0,003	0,63	0,005
cJun	43498	2,00E-26	0,89	0,378	1,05	0,038

* Contigs are available at <http://compagen.zoologie.uni-kiel.de/>

** *Hydra vulgaris* (AEP) predicted peptides were blasted (blastp) against human proteins (NCBI). The e-values for the human ortholog are depicted.

Grey marked genes are significantly differentially regulated in both MyD88⁻ and germfree polyps

This indicates the existence of positive feedback loops of the putative effector transcription factors NF- κ B and c-Jun on certain upstream pathway components, pointing towards a functional unity of these proteins in the bacterial sensing process *in vivo*.

2.4.3 Gene-expression-profiling of MyD88-knockdown and germfree polyps

After identifying the conserved components of the TLR-pathway in *Hydra*, downstream target genes were identified in an analysis not based on gene homologies. Therefore, only contigs

exceeding a significant ($p \leq 0.05$) fold-change threshold of 1.5 in at least one of the comparisons were considered for further analyses. This resulted in 183 differentially regulated (122 downregulated, 61 upregulated) contigs in MyD88⁻ polyps (0.5 % of total contigs) and in 741 differentially regulated contigs (320 downregulated, 421 upregulated) in germfree polyps (2.0 % of total contigs) (**Figure 2.14 A**).

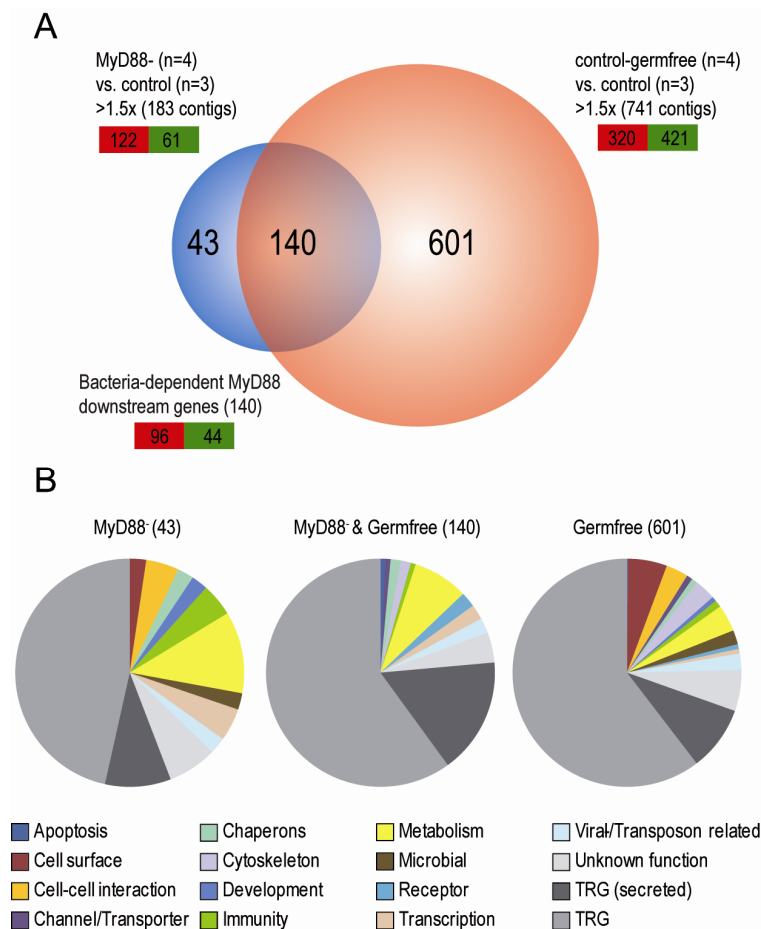


Figure 2.14: Microarray analysis reveals differential gene expression due to MyD88 down-regulation and the absence of the associated microbiota.

(A) Graphic representation of differentially regulated (≥ 1.5 fold change, $p \leq 0.05$) contigs in MyD88⁻ and germfree- compared to control polyps. Note the overlap between both experiments. All 140 shared contigs were differentially regulated in the same direction in both treatments. Down-regulated contigs are highlighted in red, up-regulated contigs in green. (B) Categorization of differential contigs. Pie charts were separated in MyD88⁻ but not bacterial regulated contigs (left), MyD88⁻ as well as bacterial-regulated contigs (middle) and MyD88⁻ independent bacterial regulated contigs (right). Contigs were assigned into self chosen categories.

Interestingly, the signature of MyD88⁻ polyps overlapped substantially (76.5%) with the germfree signature (**Figure 2.14 A**). The overlapping signature of 140 contigs included a large proportion (> 75 %) of taxonomical restricted genes (TRGs), *i.e.* contigs of unknown function with no homologue detected in other species (**Figure 2.14 B**). 21% of these TRGs lack a transmembrane domain but have a predicted signal peptide. This is notable because

such secreted peptides might directly interact with associated bacteria. Annotated transcripts included metabolic genes such as carbonic anhydrases, protein modifying enzymes like kinases and ubiquitinases, receptors, chaperons, viral-/transposon related genes such as transposases and reverse transcriptases as well as transcription factors. In **Table 2.2**, the fold changes of six representative genes are shown. Additionally, three significantly ($p < 0.05$) differentially regulated genes of the germfree vs. control comparison that had a significant fold change below the 1.5x threshold in the MyD88⁻ samples were included (**Table 2.2**). These genes include previously described TLR-downstream genes such as a lectin, bcl-2 and alkaline phosphatase (Bates *et al*, 2007, Catz and Johnson, 2001, Hsu *et al*, 1996).

Table 2.2: Differential expression of representative genes in MyD88- and germfree polyps

Annotation	Contig*	MyD88 ⁻		germfree	
		fold change	p value	fold change	p value
secr. peptide	732	0,66	0,002	0,44	0,001
secr. EGF	12837	0,57	0,006	0,50	0,005
	24241	0,57	0,004	0,49	0,007
secr. protein	16151	0,63	0,000	0,54	0,004
T-Box	19777	0,64	0,000	0,45	0,001
cadherin	34924	0,54	0,001	0,30	0,001
	14903	0,59	0,009	0,33	0,002
secr. protein	43476	0,62	0,026	0,40	0,002
Gal-lectin	1372	0,73	0,005	0,39	0,004
bcl2	7659	0,72	0,015	0,56	0,005
alkaline phosphatase	45829	0,70	0,000	0,49	0,002

* Contigs are available at <http://compagen.zoologie.uni-kiel.de/>

The differential expression of these representative target genes was validated by qRT-PCR (**Figure 2.15**). All analyzed contigs showed a higher fold change in the absence of bacteria than in MyD88-deficient conditions (**Table 2.2**).

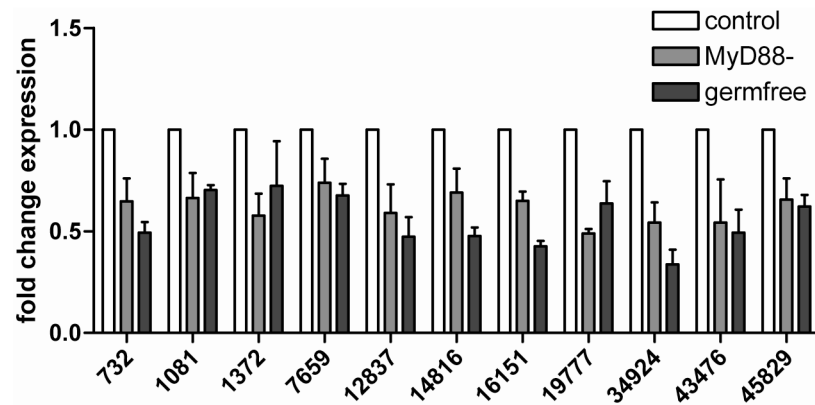


Figure 2.15: Differential gene expression between control-, MyD88-knockdown-, and germfree polyps. Expression changes of MyD88 candidates were validated by qRT-PCR. The cDNA amounts were equilibrated by elongation factor 1 alpha (EF1 α), the graphic shows means + SD (n= 3). Genes are named according to their contig-number in the *Hydra vulgaris* (AEP) transcriptome, an annotation is shown in **Table 2.2**.

The fact that expression of more than 75% of the MyD88-responsive transcripts is also altered in germfree polyps (**Figure 2.14 A**) suggests that these MyD88 downstream genes are bacteria-responsive in *Hydra*.

Notably, MyD88 dependent transcripts were not enriched for genes with known developmental functions (**Figure 2.14 B**). However, a developmental role of certain TRGs cannot be excluded. In comparison, the 601 transcripts that are regulated by the presence of the bacterial microbiota in a MyD88 independent way include a noticeable proportion of genes involved in cell-surface components and cell-cell interaction like mucins, lectins and cadherins. Since the glycocalyx of epithelial cells is a habitat for *Hydra* associated bacteria (S. Fraune, personal communication), it is possible that these colonizers induce changes in their own *Hydra*-cell associated environment.

2.4.4 A subset of MyD88 downstream genes is regulated by JNK

Upon stimulation by microbial associated molecular patterns (MAMPs), the TLR-signaling cascade in vertebrates can regulate the expression of target genes via two major downstream branches, leading to the nuclear translocation of the transcription factors NF- κ B or c-Jun (**Figure 1.6**) (Akira *et al*, 2006). In *Hydra*, the expression levels of putative members of the JNK / p38 branch of TLR-signaling leading to c-Jun translocation (TAK1, p38 α , p38 β and JSP-1) were significantly affected by both the absence of bacteria as well as by silencing of MyD88 expression (**Table 2.1**). To directly analyze the role of JNK in TLR-signaling, the expression of the nine representative contigs (see **Table 2.2**) was examined after treatment with the JNK-specific inhibitor SP600125 (Bennett *et al*, 2001, Philipp *et al*, 2009), which was shown to act specifically in the cnidarian *Hydra* (Philipp *et al*, 2009). As shown in

Figure 2.16 A, four of nine candidate genes were negatively regulated by SP600125 in a concentration dependent manner. This included *bcl2* (contig 7659), a known NF- κ B target genes in vertebrates (Catz and Johnson, 2001). Thus, *bcl-2* might be transcriptionally regulated by both, NF- κ B and c-Jun transcription factors. To exclude an unspecific, broad effect of the inhibitor SP600125, qRT-PCRs with a set of nine random genes was conducted. None of them was affected by SP600125 treatment (**Figure 2.16 B**). These results point towards a key role of MAP-kinase signaling in the MyD88-mediated perception of bacterial signals via TLRs in *Hydra*.

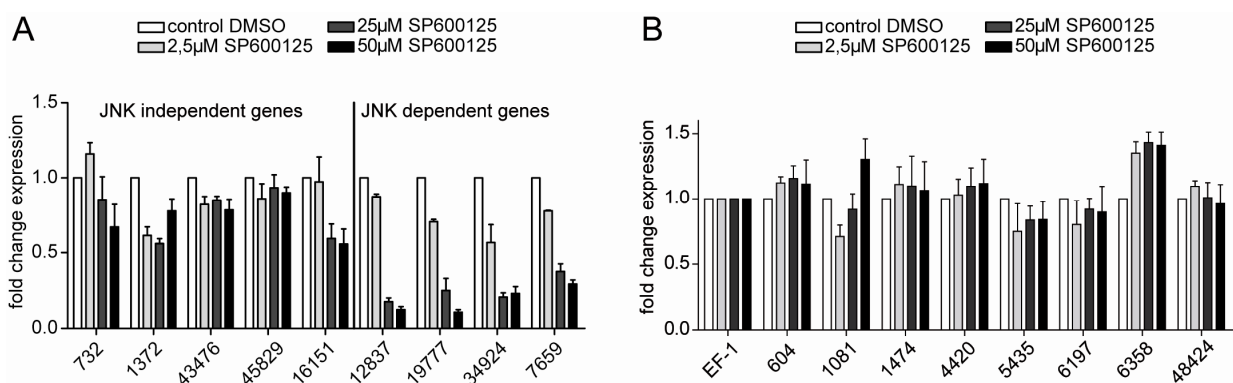


Figure 2.16: JNK phosphorylation is mediating the expression of several MyD88-downstream genes.

(A) Relative expression level of the candidate genes upon administration of the JNK inhibitor SP600125 (Philipp *et al*, 2009), determined by qRT-PCR. Note that the expression of *12837*, *19777*, *34924* and *7659* is influenced by SP600125 in a concentration dependant manner. cDNA amounts were equilibrated by *elongation factor 1 alpha*, the graphic shows means + SD (n=3). (B) The effect of SP600125 was tested by qRT for 9 randomly chosen genes to exclude broad and unspecific transcriptome changes after inhibitor administration. cDNA amounts were equilibrated by *elongation factor 1 alpha*, the graphic shows means + SD (n=3)

2.4.5 MyD88 deficient *Hydra* display delayed bacterial recolonization upon antibiotic treatment

After validating that TLR-signaling in *Hydra* senses host-associated bacteria, it was examined whether a MyD88 knockdown affects the community composition of the colonizing microbiota. 454 pyrosequencing was performed using the variable regions 1 and 2 (V1V2) of the bacterial 16S rRNA gene, amplified from total DNA of control and MyD88⁻ polyps after a four week period of co-cultivation. Chimeric sequences were identified and removed using Chimera Slayer (Haas *et al*, 2011). Resulting high quality reads ranged from 2739 to 7394 per sample. Sequences were normalized to 2700 sequences per sample, grouped into operational taxonomic units (OTUs) at a $\geq 99\%$ sequence identity threshold and classified by RDP classifier.

The microbiota of both, control and MyD88⁻ polyps, was found to be dominated by Betaproteobacteria (**Figure 2.17 A**), mainly of the genus *Curvibacter*. On average,

Curvibacter sp. accounted for 94% of the microbiota in control polyps and 92% in MyD88⁻ polyps (**Figure 2.17 A**). This bacterium was previously co-sequenced with the genome of *Hydra magnipapillata* (Chapman *et al*, 2010). Rare fractions of the *Hydra*-associated bacterial community include Alphaproteobacteria, Gammaproteobacteria and Flavobacteria (**Figure 2.17 A**).

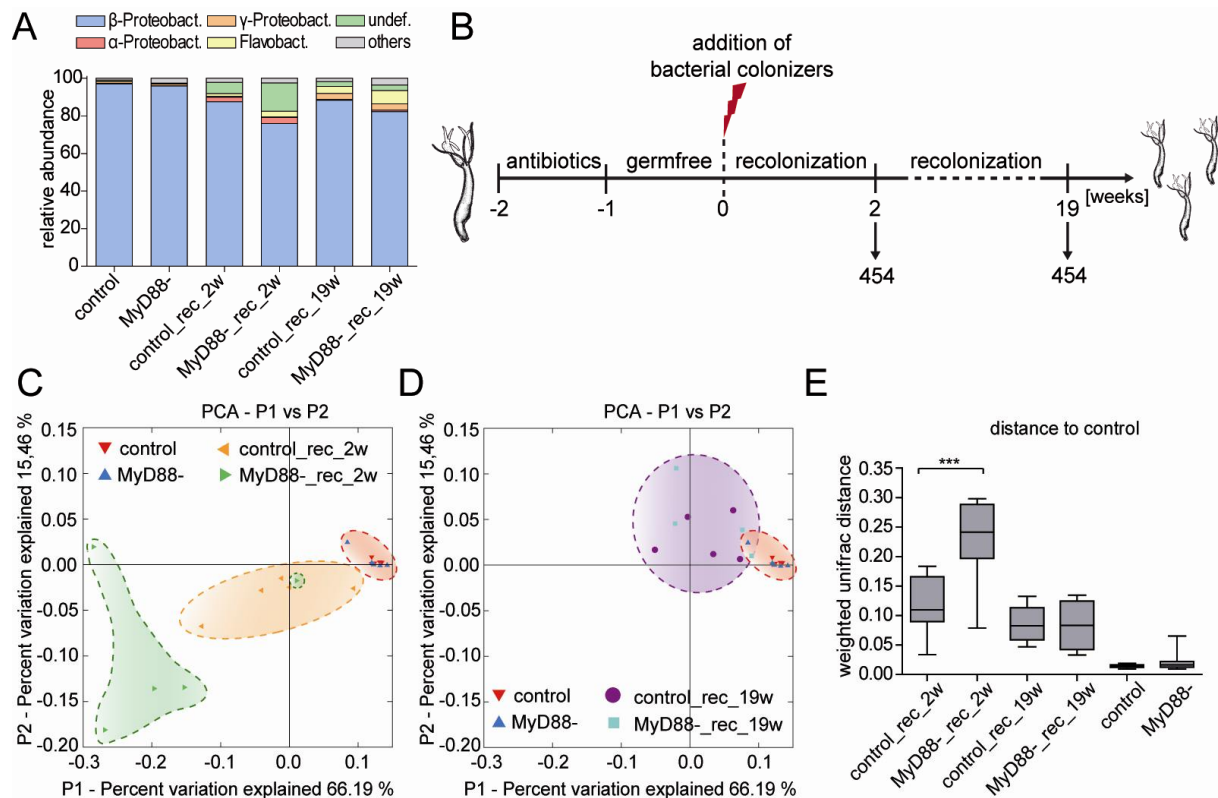


Figure 2.17: 454 sequencing of bacterial 16S rDNA reveals minor impact of MyD88 in bacterial colonization.

(A) Bar charts representing bacterial communities of *Hydra* polyps on class level (means of 5 replicates). Rare bacterial taxa (<1% relative abundance) were grouped to the fraction “others”. (B) Experimental design. Germfree MyD88⁻ and control polyps were inoculated with potential bacterial colonizers derived from pond water, *Hydra*-culture supernatant and *Hydra* tissue homogenates. Single polyps were removed from clonally growing cultures 2 weeks and 19 weeks post inoculation and subjected to 454 sequencing of the microbiota. (C, D) Bacterial communities clustered using principle coordinate analysis of the weighted Unifrac distance matrix. The percent variation explained by the principle coordinates is indicated in the axes. (E) Weighted unifrac differences calculated by pairwise comparisons of the bacterial profile to control polyps. Statistical analysis was carried out using two-tailed t-test (* $p \leq 0.05$; ** $p \leq 0.01$; *** $p \leq 0.001$).

To investigate whether TLR-signaling plays a role in the microbiota assembly process, germfree control- and germfree MyD88⁻ polyps were generated by antibiotic treatment and reinfected with a complex pool of potential colonizing bacteria, retrieved from the supernatant of a non-germfree culture, pond water and *Hydra* tissue homogenates (**Figure 2.17 B**). Individual polyps were examined for their microbiota by 454 pyrosequencing 2 weeks and 19

weeks post bacterial inoculation. Principle coordinate analysis (PCoA) of the weighted unifrac metric revealed a relatively high separation of bacterial communities of MyD88⁻ polyps (MyD88⁻_rec_2w) from the pre-antibiotic control-state, whereas control samples (control_rec_2w) cluster in close proximity to the pre-antibiotic state (red cloud) (**Figure 2.17 C, E**). After 19 weeks of recolonization (**Figure 2.17 D, E**), this initial difference between the bacterial communities of control and MyD88⁻ polyps was equalized. Taken together, these results demonstrate a role of MyD88-mediated TLR-signaling in the re-establishment of *Hydra*-associated bacterial communities by promoting bacterial recolonization. However, MyD88 does not appear to be essential for maintaining bacterial homeostasis in adult polyps of *Hydra vulgaris* (AEP).

2.4.6 TLR-signaling in pathogen defense in *Hydra*

Pseudomonas aeruginosa is a pathogenic bacteria which can infect a broad range of host organisms including plants, nematodes, insects and mice (Rahme *et al*, 2000). To examine whether silencing of MyD88 affects pathogen defense in *Hydra*, *P. aeruginosa*, strain UCBPP-PA14 (PA14) (Rahme *et al*, 1995), was used to infect MyD88⁻ and control polyps. Single polyps (n= 24 each) were cultured in medium containing 1.8×10^8 PA14 cells/ml. Polyps were screened daily and the impact of the pathogenic bacterium was scored according to the disease phenotypes presented in **Figure 2.18 A**. 24 hours post infection, MyD88⁻ as well as control polyps suffered from severe tentacle shortening (mean score ~ 2) (**Figure 2.18 B**). 48 hours post infection, the disease state was characterized by a complete loss of tentacles in a subset of polyps both in control (7/24 polyps with score 3) and MyD88⁻ (10/24). Whereas the control polyps started to recover, disease severity increased in MyD88⁻ polyps in the following two days (**Figure 2.18 B**), culminating in the complete lysis of three MyD88⁻ polyps after 96 hours (**Figure 2.18 C**). Taken together, the PA14 infection assay showed a significantly higher pathogen susceptibility of MyD88⁻ polyps compared to control polyps.

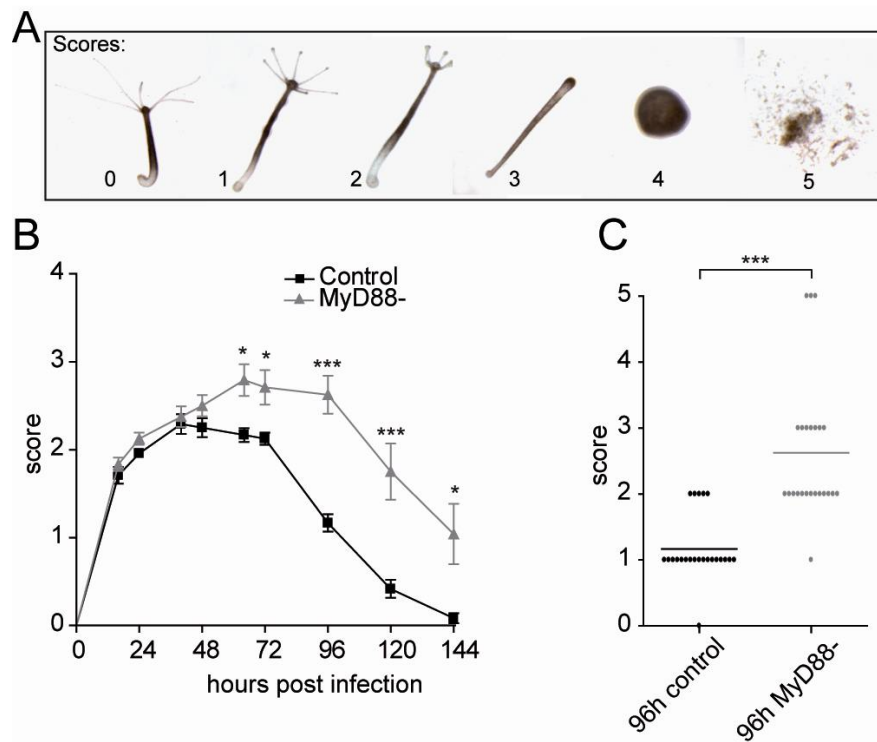


Figure 2.18: MyD88- and control polyps show differential susceptibility to infection by *P. aeruginosa*. (A) Phenotypic scores of the *Hydra* infection model. Disease always starts with swelling of the tentacle tips (score 1), followed by subsequent shortening (score 2) and loss (score 3) of tentacles. Score 4 indicates the loss of body shape with maintenance of an intact epithelium. Score 5 is characterized by tissue lysis. (B) Temporal profile of PA14 infection in *Hydra*. Polyps were incubated in 1 ml Hydra-medium containing $1.8 \cdot 10^8$ CFU P.a.14. Values are plotted as mean + SEM (n=24). (C) Detailed representation of the timepoint 96 hours post infection from (B). Each dot represents one polyp, horizontal line shows the mean. Note that 3 polyps died in the MyD88-knockdown group whereas the maximum score observed in the control group was 2 (tentacle shortening). Statistical significance was tested by two-tailed Mann-Whitney test (* $p \leq 0.05$; ** $p \leq 0.01$; *** $p \leq 0.001$).

2.5 Host-specific antimicrobial peptides shape bacterial communities

The long-term maintenance of host species-specific bacterial communities as well as the modeling approach of the ontogenetic microbiota establishment strongly indicated selective pressures imposed by the host on its associated microbiota. In the present study, the question whether species-specific AMPs sculpture species-specific microbial communities by selecting for co-evolved bacterial partners. In particular, the effects of deficiency in a family of AMPs, the arminins, were investigated in the cnidarian host *Hydra*.

2.5.1 AMPs of the arminin family show species-specific composition in different species of *Hydra*

After assessing the host as one determining factor for the microbiota composition, host factors capable of influencing the bacterial community in a species-specific manner were determined. Since *Hydra* lacks an adaptive immune system, the focus was on the polyp's innate immunity. Tissue homogenates of *Hydra* possess strong bacteriocidal activity (Kasahara and Bosch, 2003), most likely due to the expression of potent antimicrobial peptides (Augustin *et al*, 2009a, Bosch *et al*, 2009, Fraune *et al*, 2010). Arminins (Augustin *et al*, 2009a) are the highest expressed AMPs in *Hydra*. Thus, the transcriptomes of *H. vulgaris* (AEP), *H. oligactis* and *H. viridissima* were screened for orthologs of arminins by comparing the conserved N-terminal region of the previously published *H. magnipapillata* genes (Augustin *et al*, 2009a) through a BLAST search. Compared to ten genes in *H. magnipapillata*, nine orthologs were found in *H. vulgaris* (AEP), six in *H. oligactis* and four in *H. viridissima* (**Figure 2.19 A**). In addition, a cluster of arminin related peptides was discovered. The expression level of the distinct paralogs was determined by comparing microarray signal intensities to the expression level of the highly expressed *beta actin* gene of the corresponding *Hydra* species (**Figure 2.19 B**). The expression of some arminins exceeds the expression of the housekeeping gene *beta actin*, indicating the biological relevance of this gene family in *Hydra*. The expression profile of arminin paralogs differs between *Hydra* species, *e.g.* the highest expressed paralogs of *H. vulgaris* (AEP) are grouped in a different cluster than the dominant arminins in *H. oligactis* (**Figure 2.19**). The closer related species *H. vulgaris* (AEP) and *H. magnipapillata* show a more similar profile of arminin expression. The most basal species, *H. viridissima* expresses the most derived set of arminins. Taken together, this analysis indicates that each *Hydra* species is equipped with its unique composition of AMPs.

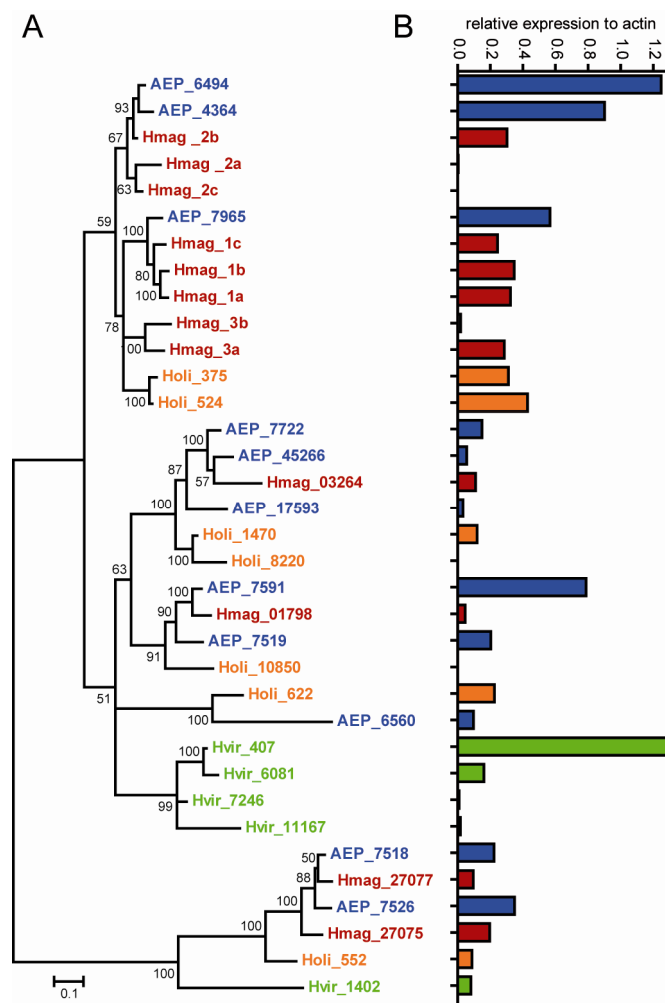


Figure 2.19: The arminin family of antimicrobial peptides.

(A) Phylogenetic analysis of the arminin AMP family from four different *Hydra* species. The tree was built by Bayesian interference of phylogeny. A total of 3 million generations were calculated using the general time reversible model and four chains with a burn-in of 25% and the invgamma rate variation. Posterior probabilities are shown at the corresponding nodes. Genes are colored according to species. Numbers indicate contig numbers in the species transcriptome. AEP= *H. vulgaris* (AEP), Hmag= *H. magnipapillata*, Holi= *H. oligactis*, Hvir= *H. viridissima*. (B) Relative expression of each arminin, compared to the expression of *beta-actin* in the corresponding species. Expression data were retrieved from microarray data.

The expression of arminins in *H. vulgaris* (AEP) was analyzed in more detail. As shown in **Figure 2.20** most arminins are expressed exclusively in endodermal epithelial cells, thus likely being secreted to the gastric cavity, a compartment resembling the mammalian intestine (Fraune *et al*, 2009b). None of the paralogs is expressed in the tentacles or in the hypostome region, restricting the localization to the body column. Paralog 6560 was shown to be expressed in the ectodermal epithelium and thus is the first AMP in *Hydra* identified to be synthesized in ectodermal epithelial cells.

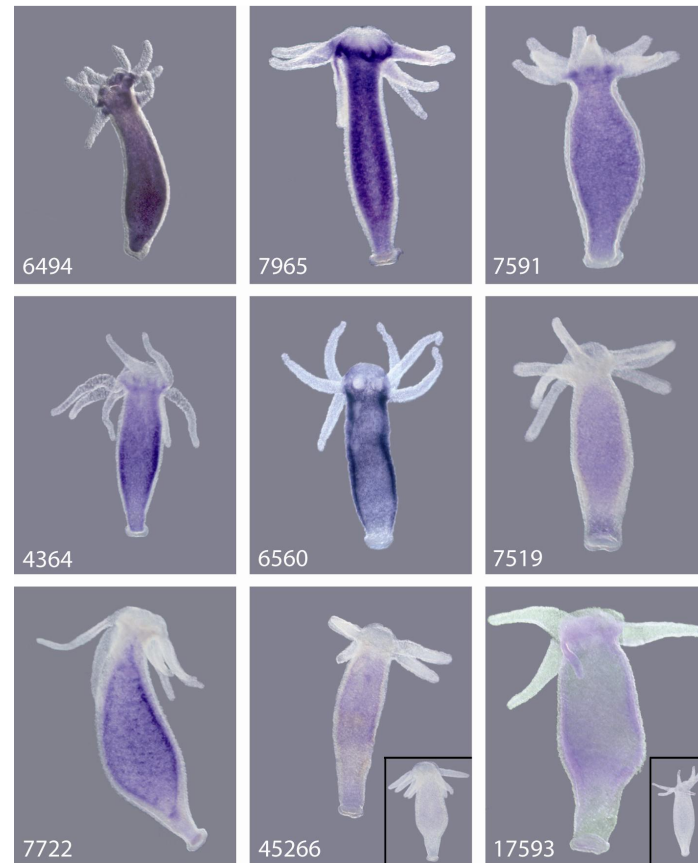


Figure 2.20: *In situ* hybridization localizes most arminins in endodermal epithelial cells.

Expression of nine arminin paralogs in *H. vulgaris* (AEP), localized by whole-mount in situ hybridization. Blue staining indicates endogenous arminin transcripts. Except *arminin 6560*, all candidates are localized in the endoderm. Numbers at the lower left hand corner of each picture indicate the contig number of the arminin candidate gene. For weakly expressed candidates pictures of control staining were included in the lower right hand corner to prove reliability of the staining.

2.5.2 Knockdown of arminin decreases the antibacterial activity of *Hydra* tissue

To broadly interfere with the host's expression of endogenous arminins, transgenic *H. vulgaris* (AEP) polyps, expressing a hairpin cassette containing the *arminin7965* antisense and sense sequences fused to the reporter gene *egfp* (**Figure 2.21 A**), were generated. The transformation of 2-4 cell stage embryos via microinjection resulted in a founder polyp showing mosaic distribution of GFP-positive cells. By several rounds of asexual proliferation, two stable lines were established; the control line, which contained no remaining GFP-positive cells, and the Arminin⁻ line, expressing the hairpin-transgene in the complete endodermal epithelial cell lineage. The resulting dsRNA triggers the RNAi machinery (Fire *et al.*, 1998, Kennerdell and Carthew, 2000, McManus and Sharp, 2002, Zamore, 2002) which leads to a decrease in the endogenous arminin transcript as shown by quantitative real-time PCR (qRT-PCR) (**Figure 2.21 B**). Since the 5-prime sequence of the paralogous arminins is quite conserved (see **Figure 9.1**), the hairpin-mediated RNAi targeted several arminins, leading to a significant decrease in expression of the genes 7965, 6494, 4364, 7722 and

45266. To ensure specificity of used primers, the amplified fragments were cloned and sequenced. This decrease in expression correlates with the sequence identity to the gene 7965, the sequence used to generate the hairpin transgene (**Figure 2.21 C**).

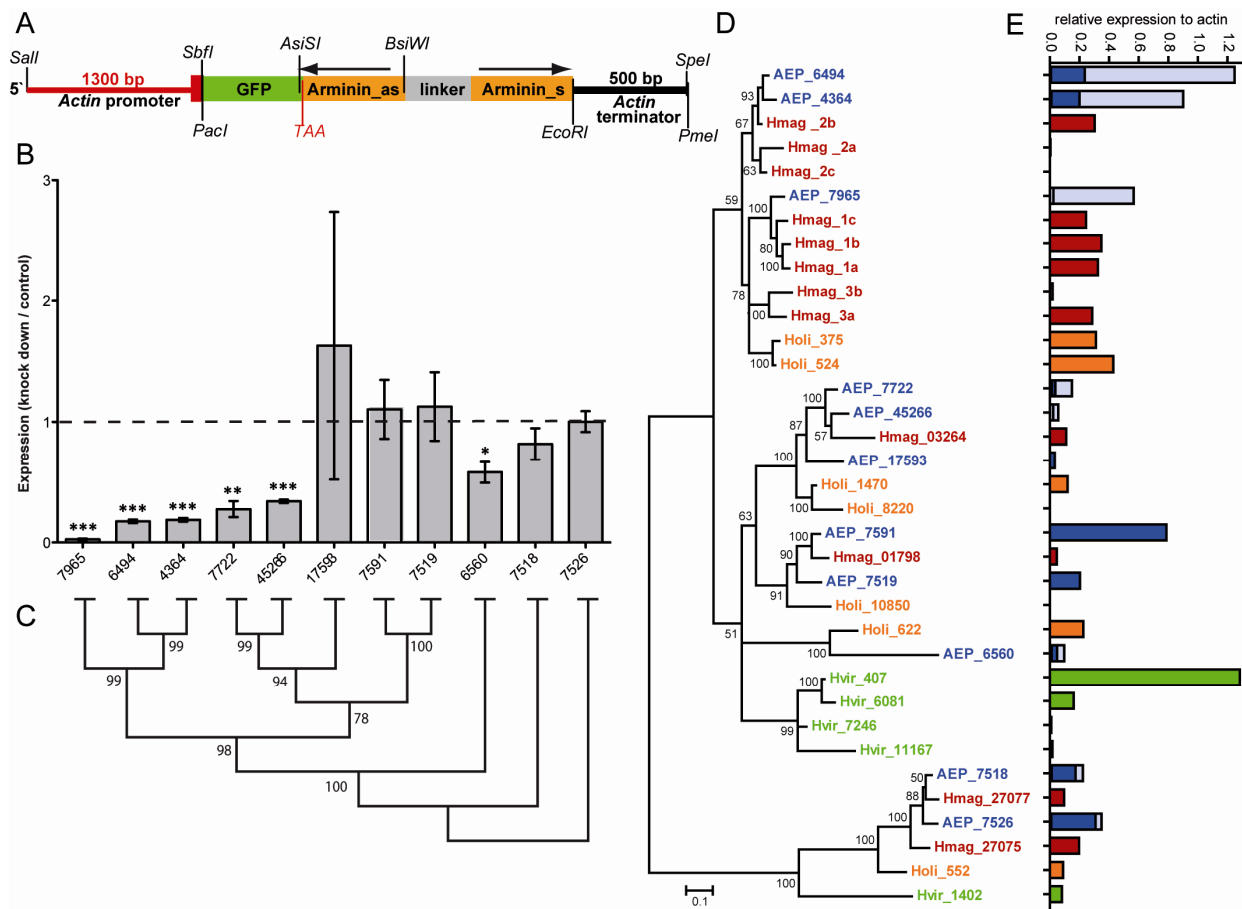


Figure 2.21: Successful knockdown of arminin family members in *Hydra vulgaris* (AEP) by transgenic overexpression of a hairpin-construct targeting gene 7965.



(A) Arminin-Hairpin construct for generation of transgenic *Hydra* (as: antisense, s: sense, TAA: stop codon). (B) Relative expression of arminins quantified by qRT-PCR with specific primers, cDNA amounts were equilibrated by *elongation factor 1 alpha*, the graphic shows means + SEM (n= 3); p < 0.05 *, p < 0.01 **, p < 0.001 ***. (C) Neighbor-Joining tree of arminins from *Hydra vulgaris* (AEP). Bootstrap values are shown at the corresponding nodes (1000 replicates). (D) Phylogenetic analysis of the arminin AMP family from four different *Hydra* species. The tree was built by Bayesian interference of phylogeny. Posterior probabilities are shown at the corresponding nodes. (E) Relative expression of each arminin, compared to the expression of *beta-actin* from the corresponding species. Expression data were retrieved from microarray data. Light blue = original expression (compare Figure 2.19), dark blue = remaining expression after arminin knockdown, calculated with the fold changes retrieved by qRT-PCR.

The decreased expression of several arminins in Arminin⁻polyps drastically changed the AMP composition of the transgenic *H. vulgaris* (AEP) polyps, with the highest expressed paralog switching from 6494 to 7591 (**Figure 2.21 D and E**). Total arminin expression was reduced by ~50%. To assess the impact on protein level, peptide extracts of Arminin⁻polyps and control polyps were tested against *Escherichia coli* DH5 α , which was previously reported to be sensitive to arminin (Augustin *et al*, 2009a). The minimal inhibitory concentration

(MIC) of Arminin⁻ extracts was doubled compared to control extracts (**Table 2.3**). In other words, the bacteriocidal activity of *Hydra* tissue extract was halved in Arminin⁻-polyps. This effect was also clearly visible in radial diffusion assays against *E. coli* DH5 α (**Table 2.3**).

Table 2.3: Tissue of Arminin⁻-Polyps shows a reduced antimicrobial activity against *E. coli* DH5 α .

Small charged peptides were extracted from 1000 polyps each as previously described (Augustin *et al.*). Antimicrobial activity was determined by minimal inhibitory concentration (MIC) assay as well as radial diffusion assay (RDA) against *E. coli* DH5 α . MIC indicated that anti-*E.coli* activity was halved in Arminin⁻-polyps. MIC values are represented as mean of three biological replicates.

Peptide-extract	Mean MIC	RDA
Control (n = 3)	0.91 $\mu\text{g/ml}$	
Arminin ⁻ (n = 3)	1.82 $\mu\text{g/ml}$	

2.5.3 Species-specific arminins select for co-evolved bacterial partners

The expression profile of arminins is specific to different *Hydra* species (**Figure 2.19**) and contributes a major portion to the antibacterial activity of the host's tissue (**Table 2.3**). Therefore, an evident question is, whether host species-specific expression of arminins selects for the observed species-specific bacterial associations (**Figure 2.1**). To answer that question, germfree control and Arminin⁻-polyps (=transgenic *H. vulgaris* (AEP)) were generated by antibiotic treatment. These polyps were separated in single wells and co-cultivated with either *H. vulgaris* (AEP), *H. oligactis* or *H. viridissima* for five weeks. Following that period, the recipients as well as the donor polyps were subjected to 454 sequencing of the bacterial microbiota (**Figure 2.22**). Three biological replicates (=single polyps) were conducted for donor polyps, four biological replicates were conducted for recipient polyps. DNA extraction failed for one sample (control polyps co-cultured with *H. oligactis*), resulting in only three replicates for that treatment. Chimeric sequences were identified and removed using Chimera Slayer (Haas *et al*, 2011). Resulting high quality reads ranged from 2350 to 7499 per sample. Sequences were normalized to 2300 sequences per sample, grouped into operational taxonomic units (OTUs) at a $\geq 97\%$ sequence identity threshold and classified by RDP classifier.

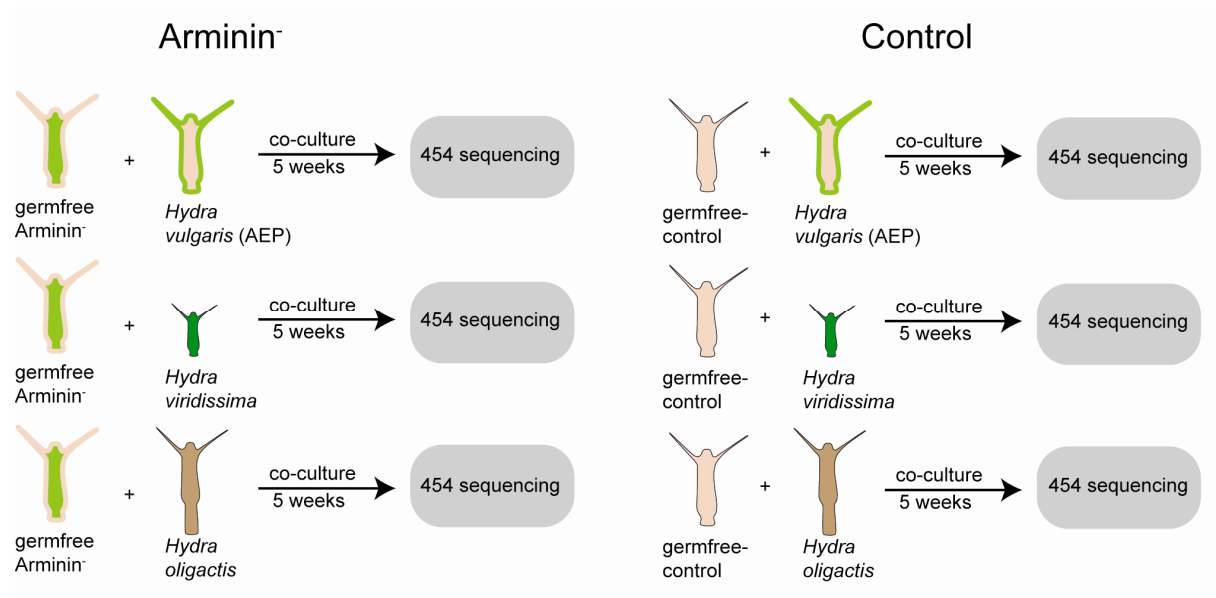


Figure 2.22: Experimental design

Germfree recipient polyps (Arminin⁻ or control) were co-cultivated with either *Hydra vulgaris* (AEP) (strain AL8, expressing eGFP in the ectodermal cell lineage), *Hydra viridissima* or *Hydra oligactis* for a period of five weeks prior to 454 sequencing of the bacterial microbiota.

To transfer native bacterial colonizers, recipient polyps were co-cultured with the transgenic *H. vulgaris* (AEP) strain AL8. This strain expressed eGFP in the ectodermal epithelium, allowing for separation of recipients and donors after the period of co-cultivation. When inoculated with *H. vulgaris* (AEP) specific microbiota, recipient control- and Arminin⁻-polyps displayed no differences in their bacterial recolonization as indicated by their clustering in a principle coordinate analysis (**Figure 2.23 A**). Both, control- and Arminin⁻ polyps opted for major bacterial types of the donor microbiota. *Curvibacter* (Comamonadaceae) and *Legionella* (Gammaproteobacteria) were transferred by co-cultivation and established associations with the recipient polyps (**Figure 2.23 B**). The *H. vulgaris* (AEP) donor polyps (strain AL8) displayed a major fraction of Spirochaetes, which is atypical for *H. vulgaris* (AEP). However, these bacteria were not horizontally transmitted to recipient polyps (**Figure 2.23 B**). To visualize the difference to the generic microbiota of *H. vulgaris* (AEP), five independent profiles of non-transgenic polyps (AEP_wt) were included (**Figure 2.23**).

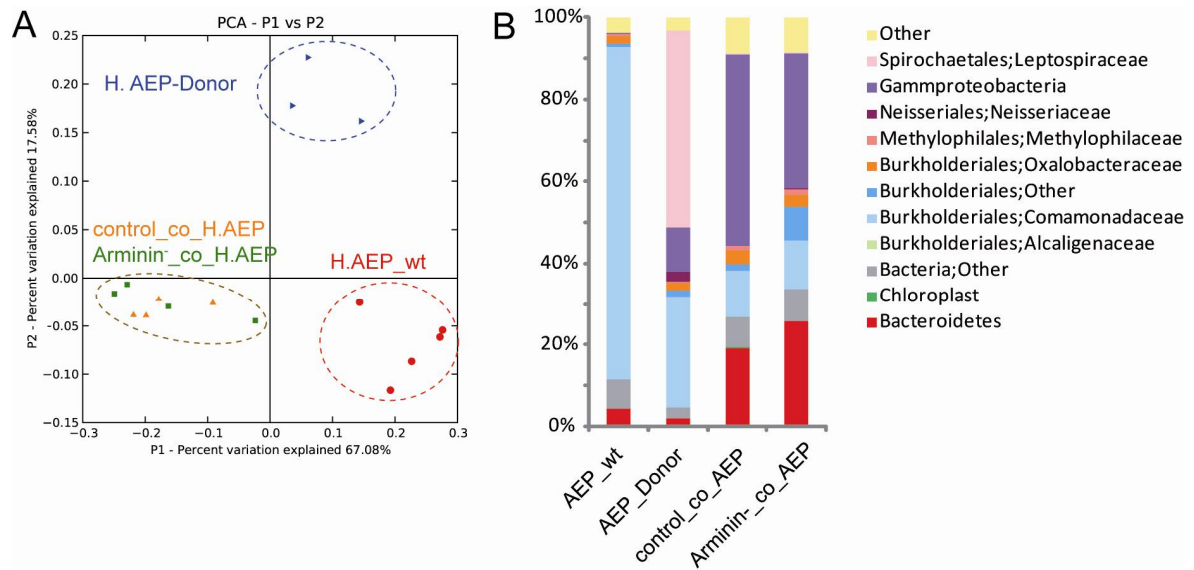


Figure 2.23: *H. vulgaris* (AEP) bacteria colonized control- and Arminin⁻ polyps similarly

(A) Germfree control polyps (orange) as well as germfree Arminin⁻ polyps (green) were co-cultivated with *Hydra vulgaris* (AEP) donor polyps (blue) for five weeks. Bacterial communities were clustered using principle coordinate analysis of the weighted unifrac distance matrix. The percent variation explained by the principle coordinates is indicated at the axes. When infected with a *H. vulgaris* (AEP) microbiota, control- and Arminin⁻ polyps showed no differences in bacterial recolonization. (B) Bar charts representing the microbiota of the different treatments. Bacterial communities are represented at the class level (mean of 3-4 replicates/group). Rare bacterial groups (<1 % relative abundance) were grouped to the fraction “other”. Note that AEP-donors differed from AEP-wt polyps by the occurrence of Spirochates and that major bacterial types including Comamonadaceae and Neisseriaceae were transferred to recipient polyps.

In contrast, inoculation with foreign bacterial communities, provided by *H. oligactis* co-cultivation led to differential recolonization in control- and Arminin⁻ polyps. As indicated by PCoA, microbial profiles of recolonized control and Arminin⁻ polyps clearly clustered separately, with recolonized control polyps clustering in close proximity to *H. vulgaris* (AEP) wild-type polyps (**Figure 2.24 A**). As shown in **Figure 2.24 B**, the microbiota of *H. oligactis* donor polyps was dominated by bacteria from the Rickettsia genus, which were previously described as endosymbionts of *H. oligactis* (Fraune and Bosch, 2007). In contrast, recolonized control- as well as Arminin⁻ polyps were associated with bacterial communities drastically different to the donor microbiota (**Figure 2.24 B**) and thus enriched bacteria from the donor’s rare bacterial associates. Betaproteobacteria (Neisseriales, Methylophilales and Burkholderiales), which are the main colonizers of *H. vulgaris* (AEP) wild-type polyps, made up 64% of the microbiota in recolonized control polyps. In contrast only 39% Betaproteobacteria accounted for the microbiota in recolonized Arminin⁻ polyps (**Figure 2.24 B**). Arminin⁻ polyps showed an increased colonization by Bacteroidetes species and a lower colonization with Burkholderiales and Neisseriales species compared to recolonized control polyps.

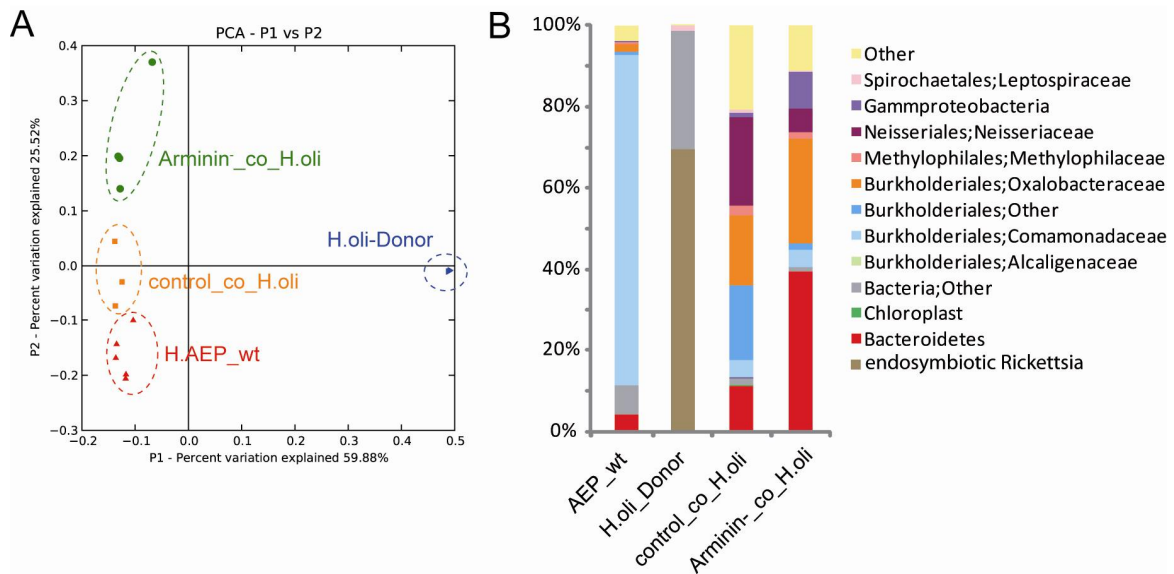


Figure 2.24: *H. oligactis* bacteria colonized control- and Arminin⁻ polyps differently

(A) Germfree control polyps (orange) as well as germfree Arminin⁻ polyps (green) were co-cultivated with *Hydra oligactis* (*H.oli*) polyps (blue) for five weeks. Bacterial communities were clustered using principle coordinate analysis of the weighted unifracs distance matrix. The percent variation explained by the principle coordinates is indicated in the axes. When infected with a *H. oligactis* microbiota, control- and Arminin⁻ polyps cluster separately, with recolonized control polyps clustering next to AEP-wt polyps. (B) Bar charts representing the microbiota of the different treatments. Bacterial communities are represented at the class level (mean of 3-4 replicates/group). Rare bacterial groups (<1% relative abundance) were grouped to the fraction “other”.

Similarly, differential recolonization between control- and Arminin⁻ polyps was observed when recipients were inoculated with microbiota from *H. viridis* (Figure 2.25 A). Recolonized control- as well as Arminin⁻ polyps enriched for bacteria from the donors rare microbiota. Betaproteobacteria (Neisseriales, Methylophilales and Burkholderiales) accounted for 87% of the microbiota of recolonized control polyps in contrast to 36% in recolonized Arminin⁻ polyps. In detail, Arminin⁻ polyps displayed an increased colonization by Bacteroidetes and a decreased prevalence of Neisseriales and Burkholderiales. Neisseriales accounted for 48% of the microbiota in control polyps and were completely absent in Arminin⁻ polyps (Figure 2.25).

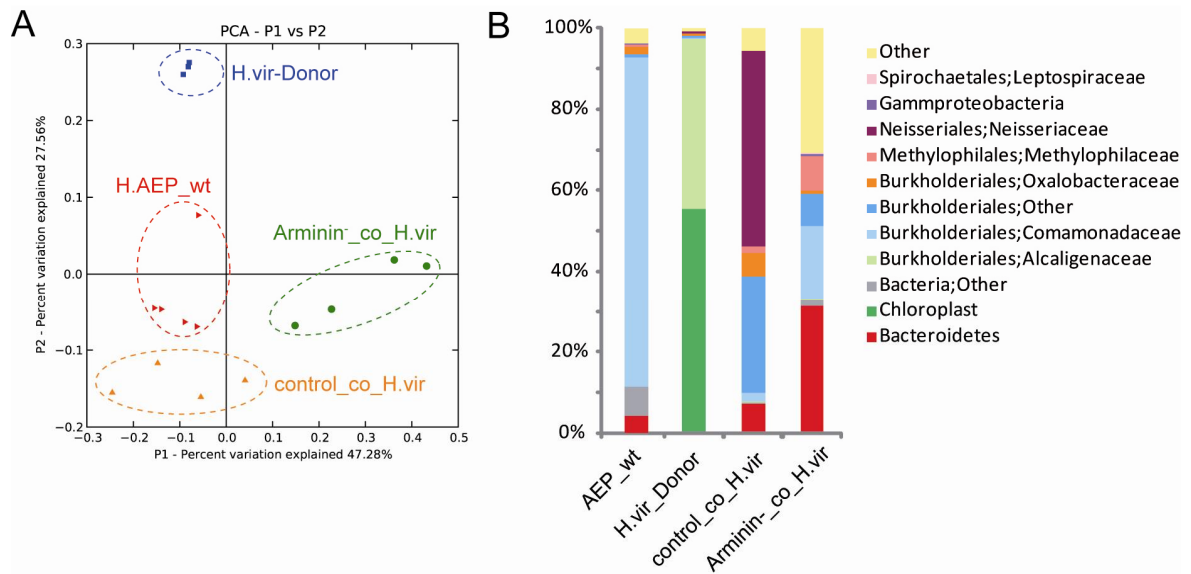


Figure 2.25: *H. viridissima* bacteria colonized control- and Arminin⁻ polyps differently

(A) Germfree control polyps (orange) as well as germfree Arminin⁻ polyps (green) were co-cultivated with *Hydra viridissima* (*H.vir*) polyps (blue) for five weeks. Bacterial communities were clustered using principle coordinate analysis of the weighted unifracs distance matrix. The percent variation explained by the principle coordinates is indicated at the axes. When infected with a *H. viridissima* microbiota, control- and Arminin⁻ polyps clustered separately, with recolonized control polyps clustering next to AEP-wt polyps. (B) Bar charts representing the microbiota of the different treatments. Bacterial communities are represented at the class level (mean of 3-4 replicates/group). Rare bacterial groups (<1% relative abundance) were grouped to the fraction “other”.

When recolonized by foreign bacterial communities, provided by *H. oligactis* or *H. viridissima*, control polyps tend to enrich Betaproteobacteria, a bacterial class characteristic for the native microbiota of *H. vulgaris* (AEP). To quantify the approximation to the native microbiota, weighted unifracs distances were compared between recolonized control polyps, Arminin⁻ polyps and *H. vulgaris* (AEP) wild-type polyps. As shown in **Figure 2.26**, the microbiota of control-polyps recolonized by *H. oligactis* or *H. viridissima* bacterial communities resembled significantly better the microbiota of wild-type *H. vulgaris* (AEP) than the re-established communities in Arminin⁻ polyps, indicating a loss of selective preferences due to disturbed arminin expression.

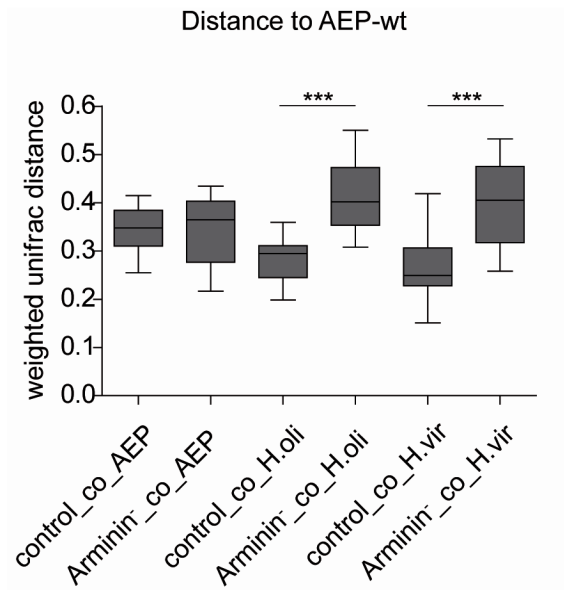


Figure 2.26: Recolonized control polyps select for bacteria resembling their native microbiota

Comparison of the weighted Unifrac distances to a wild-type (wt) *Hydra vulgaris* (AEP) microbiota. Control-polyps inoculated with a *H. oligactis* or *H. viridissima* microbiota show significantly lower unifrac distances to the *bona-fide* wild-type status than Arminin⁻-polyps. These results indicate the potential of *Hydra* polyps to select suitable bacterial partners from a pool of foreign colonizers; a potential that is strongly reduced in Arminin⁻-polyps.

Since antimicrobial activity was reduced to 50% in Arminin⁻-polyps, the absolute abundance of bacteria was quantified for recipient polyps after recolonization. Bacterial load did not differ significantly between treatments. All recipient polyps were colonized by a similar amount of bacteria, regardless of the origin of the inoculated microbiota or the antibacterial status of the tissue (**Figure 2.27**), indicating that all niches, offered by the host, are colonized by bacteria.

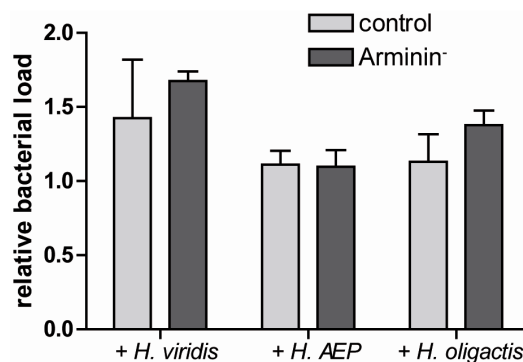


Figure 2.27: Total bacterial load did not differ between control and Arminin⁻-polyps.

qPCR quantification of bacterial load of ex-germfree control and Arminin⁻-polyps after inoculation with bacterial communities by cocultivation with different *Hydra* species. qRT-PCR was conducted with the primers Eub341_F and Eub534_R (Muyzer *et al*, 1993), equilibrated to the *beta actin* gene. Error bars represent standard error of the mean (SEM.). Statistical analysis was conducted by two-tailed t-test, but no significant differences were observed; n=4.

3 Discussion

The aim of this thesis was to obtain a deeper understanding of the associations between the freshwater polyp *Hydra* and its commensal bacteria. Together, host organisms and all associated microbes form a functional unit, called the holobiont. The establishment and maintenance of homeostasis within this consortium is critical for the well-being of the holobiont. Disruptions of the homeostatic balance between the holobiont partners have been associated with obesity (Ley *et al*, 2006b), malnutrition (Kau *et al*, 2011), inflammatory bowel diseases (Dicksved *et al*, 2008, Frank *et al*, 2007), neurological disorders (Gonzalez *et al*, 2011) and cancer (Lupton, 2004) in humans. The first step in understanding this critical homeostasis is to characterize the baseline healthy state of these associations. However, the complexity of the human microbiota and large inter-individual variation complicates the definition of the ideal microbiota. Despite the consistency on phylum level, the relative proportions and species present in the human microbiota vary markedly across individuals, whereas the microbiome, *i.e.* the functional gene profile of the microbiota, is far more conserved (Lozupone *et al*, 2012). These limitations make it desirable to study underlying principles of host-microbe associations in simplified animal models. In the present thesis, specific bacterial communities associated with different species of the basal metazoan *Hydra* were discovered. Under controlled laboratory conditions, the microbiota of *Hydra* polyps shows a comparatively low complexity and a remarkable low inter-individual variation, making *Hydra* a suitable model for investigating host factors which ensure holobiont homeostasis. In the following, I will discuss the benefits of host-bacteria interactions in *Hydra*, their ontogenetic establishment and regulation by the host's innate immune system.

3.1 The host determines the composition of its bacterial microbiota

The analysis of associated bacterial communities of seven species of the cnidarian *Hydra* revealed highly species-specific bacterial associations (**Figure 2.1**), which partially reflected phylogenetic relationships of the hosts. This observation is consistent with similar findings in mammals, including detailed surveys of the microbiota of hominid species (Ley *et al*, 2008b, Ochman *et al*, 2010). The observed associations in *Hydra* are extremely stable, as the analyzed species are cultivated under identical environmental conditions for up to thirty years. These species-specific bacterial signatures are maintained in co-cultivation of different *Hydra*

species. Instead of developing similar bacterial communities, showing intermediate features of both co-cultivated hosts, the microbiota of the investigated *Hydra* species appears to be extremely robust (**Figure 2.2**). Together, these data strongly indicate a role of the host tissue in mediating host-bacterial associations. This is also evident in an elegant study by Rawls *et al.*; reciprocal microbiota transplantations between mice and zebrafish revealed that the recipient host shapes the community structure of the transferred, foreign microbiota to resemble its native bacterial community (Rawls *et al.*, 2006). However, this study did not elucidate the factors responsible for host-mediated community control. Several host-factors are suggested to have influence on the microbiota composition, ranging from oxygen conditions in the gut, nutrient intake, mucus barriers and immunity (reviewed in (Bevins and Salzman, 2011a)). While all these factors are likely to differ drastically between mouse and zebrafish, the species of *Hydra* investigated in the present study share a highly similar physiology. Diet, which has a strong influence on the microbiota (Ley *et al.*, 2008b), was standardized in all *Hydra* experiments. Thus, *Hydra* appears to be a feasible model organism for understanding the underlying principles of host-microbe associations in a controlled environment.

3.2 Commensal bacteria produce antifungal substances

Hydra polyps, artificially deprived of their associated microbiota, are prone to fungal infection by the filamentous fungi *Fusarium sp.* (**Figure 2.3**). Thus, spores of *Fusarium sp.* seem to be part of *Hydra*'s native microbiota, but their germination appears to be inhibited by commensal bacteria. The present data identified several bacterial symbionts, including *Acidovorax sp.*, *Curvibacter sp.*, *Pelomonas sp.* as well as an Oxalobacteraceae species, which significantly inhibit fungal outgrowth *in vivo*. None of these bacteria was previously reported to synthesize antifungal compounds, although *Acidovorax sp.* and *Curvibacter sp.* are reported as symbionts in other organisms (McKenzie *et al.*, 2011, Schramm *et al.*, 2003). Interestingly, the *in vivo* results did not match the results obtained from *in vitro* experiments (**Figure 2.4**), which could be explained by two possible scenarios. First, the bacterial symbionts might produce the antifungal compound only in association with the *Hydra* tissue, likely altering their metabolic state when compared to growth on culture agar. Second, certain associated bacteria might induce the production of host-derived antifungal compounds. Currently, *Acidovorax sp.* and *Pelomonas sp.* are analyzed in cooperation with Dr. Christine

Beemelmann and Prof. John Clardy from the Harvard Medical School to identify antifungal products. Future work will also investigate if the abundance of antifungal bacteria increases when the host is constantly challenged with spores of *Fusarium sp.*

Antifungal effects of commensal bacteria are widely distributed in the animal kingdom. Fungal spores are easily distributed in aquatic habitats and are prominent agents of disease in aquatic systems. A relatively immobile cnidarian polyp might be especially threatened by fungal infection. Likewise, immobile eggs of aquatic organisms are prone to infections by water molds (Gilbert and Epel, 2009).

The emergence of the infectious disease chytridiomycosis, caused by the fungal pathogen *Batrachochytrium dendrobatidis*, is a major factor responsible for the worldwide decline of amphibian species, one-third of which are threatened with extinction (Skerratt *et al*, 2007). In this well studied case, commensal bacteria have been shown to inhibit growth of *B. dendrobatidis* by the production of antifungal molecules like indole-3-carboxaldehyde or violacein (Brucker *et al*, 2008). Susceptibility to *B. dendrobatidis* infection varies among amphibian species and even within species some populations can co-exist with *B. dendrobatidis* whereas others decline to extinction. These differences in disease susceptibility have been correlated with the number of antifungal bacteria associated with a given amphibian population (Woodhams *et al*, 2007) and thus are a valid example for the adaption of the holobiont by changing bacterial partners. Interestingly, a *Curvibacter* species is associated to a variety of amphibian species (McKenzie *et al*, 2011), but was not yet shown to produce antifungal compounds. Another prominent example for fungal defense by symbiotic bacteria is present in fungus-growing ants. These ants grow fungal cultivars for their nutrition, which are prone to infection by the parasitic fungus *Escovopsis sp.* To defend their fungal cultivar against *Escovopsis sp.*, leaf-cutter ants use symbiotic actinobacteria of the genus *Pseudonocardia*, which are housed in specialized cuticular modifications on the ants body (Caldera *et al*, 2009). These symbiotic bacteria produce the cyclic depsipeptide dentigerumycin, which acts highly specific against *Escovopsis sp.*, without harming the fungal cultivar (Oh *et al*, 2009).

Thus, symbiotic bacteria are an integral part of antifungal immunity in a variety of organisms, offering an opportunity to resist fungal infection by a spread of bacterial symbionts.

3.3 How does *Hydra* assemble its specific set of microbes?

Animals from *Hydra* to human are colonized by a complex and species-specific microbiota (Fraune and Bosch, 2007, Ley *et al.*, 2008b). In the same way that microbial communities are expected to change in different parts of a body, they are also dynamic over developmental time. For a first understanding of the processes which control bacterial community membership in newly hatched *Hydra* polyps, the assembly of the microbiota was profiled up to 15 weeks post hatching. The present observations in four independent replicates and profiles of 36 individual polyps indicate that the adult-like microbiota arises in three stages: first (i), the high variability and presence of numerous species in the first three weeks of life, then (ii) the transient preponderance of the bacterial species which later dominate the adult microbiota, and finally (iii) the drastic decrease of diversity and assembly to an adult-like pattern from week four post-hatching on. Due to the complexity of the interactions and large number of components involved, it is almost impossible to intuitively understand processes such as the assembly of the generic adult-like microbiota. Therefore, the *in vivo* profiling was complemented by adding a mathematical model to infer the general principles of the assembly process (cooperation with Philipp M. Altrock and Arne Traulsen, MPI Plön). One of the mathematical models (**Figure 2.11 E**) not only resembles key features of the experimental data, but also makes two interesting predictions for the microbiota establishment in *Hydra*. First, inter-bacterial competition seems to be essential for the observed microbiota establishment profile. Second, external (environmental or host derived) factors given by a decaying colonization rate λ appear to be necessary to restrict oscillatory / strongly fluctuating dynamics in the bacterial population. Because environmental conditions including food, temperature and medium were highly standardized in the experimental setup, external stimuli were reduced to a minimum during the colonization process. This suggests that host factors are responsible for controlling the distinct colonization process by mediating the colonization rate λ . Thus, frequency-dependent bacteria-bacteria interactions and host control through temporal modulation of the colonization rate appear to be key features involved in dictating how the bacterial community is assembled in *Hydra* after hatching.

Interestingly, similar trends were observed in a study of the human infant intestinal microbiota (Palmer *et al.*, 2007). In this study, profiling the postnatal colonization of 14 human infants by fecal analyses showed that the intestinal microbiota is variable in infants and converges to an adult like profile with time (Palmer *et al.*, 2007). Moreover, Pearson correlation shows that progression towards the adult-like microbiota contains a transient state

around day 5 which remarkably resembles the stable communities found in adults (**Figure 3.1 A**). Further, a transient adult-like microbiota seems to be present also in the development of *Drosophila melanogaster* (**Figure 3.1 B**). Early instar larvae, in contrast to third instar larvae and pupa, are colonized by *Lactobacillus fructivorans*, the main bacterial colonizer of adult flies. The transient dominance of *L. fructivorans* remarkably resembles the observations of *Curvibacter sp.* abundance dynamics in *Hydra*. Thus, in hydras, flies and humans the progressive development of the adult-like microbial profile seems to require a transient occurrence of an early generic adult-like profile and it seems likely that the distinct colonization pattern described in this thesis is a common mechanistic process contributing to the composition of animal microbiota.

However, the biological relevance of the fluctuations in community membership during microbiota establishment remains to be uncovered. They could reflect responses to different threats during life history or favor the early adaptive potential of the newborn animal.

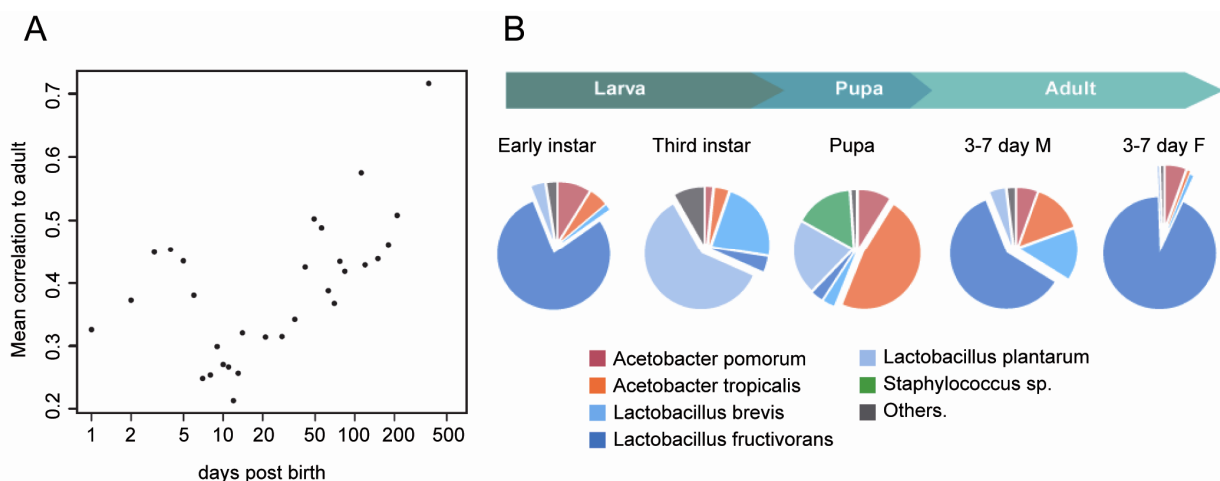


Figure 3.1: The microbiota establishment encompasses an early, adult like pattern.

(A) The fecal microbiota of infants progresses to a generic adult like profile over time, displaying a transient adult-like situation around day 5. Mean Pearson correlation of infant fecal microbiota to an adult microbiota (centroid of 18 adults) was calculated for each timepoint. Modified from (Palmer *et al.*, 2007). (B) Early larvae of *Drosophila melanogaster* are colonized by a transient microbiota remarkable similar to adults. Modified from (Wong *et al.*, 2011).

The factors and processes controlling the bacterial community assembly during ontogeny are not known. In a previous study comparing the microbiota of developing *Hydra* embryos prior to hatching, it was shown that sequential colonization is reflected in differences in antimicrobial activity (Fraune *et al.*, 2010). Thus, antimicrobial peptides are capable of mediating host-microbe homeostasis (Fraune *et al.*, 2010, Login *et al.*, 2011, Salzman *et al.*, 2010, Vaishnava *et al.*, 2008) and therefore are candidates for mediating conserved progressions of certain bacteria during the ontogenetic establishment. Future efforts will be directed towards examining whether a spatially and temporally controlled expression of AMPs contributes to the stepwise microbiota assembly after hatching from the cuticle stage.

To colonize epithelial surfaces, bacteria commonly interact with glycan structures of the host glycocalyx (Hooper and Gordon, 2001). Thus, bacterial colonization of the newly hatched polyp may also be affected by this dynamic mucus layer adherent to epithelial cells, which can serve as both a physicochemical sensor and barrier network across animal species (Moran *et al*, 2011). Interestingly, the genome of *Curvibacter* contains a large number of ABC-transporters for sugar uptake, compared to other Comamonadaceae (Chapman *et al*, 2010). This increased potential of using the host's glycocalyx components as source of sugar for nutrition might explain the high potential of *Curvibacter* to outcompete other bacteria for the colonization of niches offered by the host.

3.4 Bacterial sensing is an ancient function of TLR-signaling

The ability to sense bacterial colonizers is a prerequisite for the host to counteract disturbances of host-microbe homeostasis. Thus, this study elucidated the role of TLR-signaling in bacterial sensing and microbiota modulation.

In vertebrates, most TLRs act as pattern recognition receptors (PRRs) and are involved in the elimination of pathogens and controlling commensal colonization (Akira *et al*, 2006, Round *et al*, 2011, Wen *et al*, 2008). In contrast, the role of *Drosophila* Toll-receptors is less uniform. Their temporal and spatial expression patterns during embryonic development points towards roles in developmental processes by either inducing signaling cascades or acting as cell-adhesion molecules (Kambris *et al*, 2002). However, this is clearly proven only for Toll-1 (Anderson *et al*, 1985). In addition, Toll-1 (Lemaitre *et al*, 1996, Rosetto *et al*, 1995) as well as Toll-7 (Nakamoto *et al*, 2012) and Toll-8 (Akhoyayri *et al*, 2011) act in immune defense against fungi, bacteria or viruses. This functional duality prompted was the reason to search for the ancestral role of TLR-signaling in a more basal metazoan.

The cnidarian *Hydra* possesses a bona fide TLR-signaling cascade (**Figure 1.7, Figure 2.12**) (Miller *et al*, 2007), making it a suitable model for investigating the ancestral function of the TLR-pathway. Together with previous results, showing that the HyLRR-2 receptor in *Hydra* is able to bind flagellin *in vitro* (Bosch *et al*, 2009), the *in vivo* results of this study suggest a role of TLR signaling in bacterial recognition in the cnidarian *Hydra*. Remarkably, MyD88 loss-of-function as well as the absence of commensal bacteria in germfree polyps caused significant and overlapping changes in the transcriptome (**Figure 2.14**). A subset of differential genes is regulated by the JNK / p38 branch of TLR-signaling (**Figure 2.16**). This

shows that TLR-signaling in *Hydra* does not act unidirectionally via the transcription factor NF- κ B but is also linked to MAP-kinases. Notably, a p38 MAPK cascade was identified as a key component of the *C.elegans* immune response and is also present in *Monosiga brevicollis*, a single-cell eukaryote that is most closely related to metazoans (Irazoqui *et al*, 2010). Since JNK and p38 in *Hydra* might be also activated by many other stimuli, including G protein-coupled receptors (Johnson and Lapadat, 2002) and the wnt pathway (Philipp *et al*, 2009), innate immune reactions appear to be controlled by a complex signal transduction network.

3.5 TLR-signaling promotes re-establishment of bacterial homeostasis

Many studies showed that microbes have direct beneficial effects on the host (Douglas *et al*, 2001, Mazmanian *et al*, 2005, Nyholm and McFall-Ngai, 2004, Rawls *et al*, 2004). This is supported by the fact that a dysregulation of host-bacteria homeostasis seems to be involved in the occurrence of disorders, like chronic inflammatory bowel diseases (French and Pettersson, 2000, Ott *et al*, 2004). *Hydra* polyps are colonized by species-specific bacterial communities (Fraune and Bosch, 2007), which are largely determined by the host rather than by the environment (Fraune and Bosch, 2007, Fraune *et al*, 2009a). After verifying that TLR-signaling in *Hydra* is clearly involved in the recognition of bacteria, it was therefore asked if this active crosstalk is involved in the maintenance of host-bacterial homeostasis. The present results show no impact of impaired TLR-signaling on the composition of the bacterial microbiota in healthy animals. However, after active disturbance of the bacterial community by antibiotic treatment or upon bacterial infection with *Pseudomonas aeruginosa*, MyD88-mediated TLR-signaling promotes a reestablishment of bacterial homeostasis. This is concordant with several mechanisms to restrict active immune signaling to disturbance, such as pathogen defense, while being hyporesponsive to the healthy commensal microbiota (Cario and Podolsky, 2005). These mechanisms include (i) a decreased apical surface expression of TLRs, (ii) spatial segregation of host cells and commensal bacteria by mucus layers to limit detection to invasive bacteria that crossed the epithelial barrier and (iii) active bacterial suppression of host immunity, *e.g.* via the induction of the TLR-signaling suppressor Tollip (see **Figure 2.12 B**) by commensal bacteria (Cario and Podolsky, 2005, Otte *et al*, 2004).

3.6 MyD88 target genes include taxonomically restricted and conserved genes

Interestingly, around 75 % of MyD88-, as well as bacteria dependant contigs could not be assigned to functional categories due to the lack of BLAST hits (**Figure 2.14**). This fraction of taxonomically restricted genes (TRGs) (Khalturin *et al*, 2009) is largely overrepresented compared to the overall fraction of TRGs in the whole transcriptome. This high number might indicate that the TLR-dependant response towards commensal bacteria is by and large taxon-specific. Furthermore, 21% of these TRGs possess a predicted signal peptide. Since these secreted peptides may contribute to the properties of *Hydra*'s epithelial environment, they might also affect the colonizing microbiota. It was previously shown (Fraune *et al*, 2011) that antimicrobial peptides, apart from their role in defense against pathogenic bacteria, also have regulatory functions in host-bacterial homeostasis. This adds support to the previously proposed hypothesis (Khalturin *et al*, 2009), that taxonomically-restricted host defense molecules facilitate the disarming of taxon-specific microbial attackers, and at the same time shape the colonizing microbiota. Nevertheless, a small proportion of MyD88 target genes is conserved throughout the animal kingdom. These genes include previously described vertebrate MyD88 dependent NFκB-target genes such as lectins or bcl-2 (Catz and Johnson, 2001, Hsu *et al*, 1996). In addition, alkaline phosphatase in zebrafish also responds to LPS through a mechanism that involves MyD88. It is required to detoxify LPS and prevent intestinal inflammation in response to the resident microbiota (Bates *et al*, 2007). The differentially expressed alkaline phosphatase in *Hydra* (**Table 2.2**) might play a similar role. Based on these results, the TLR/MyD88 pathway in *Hydra* is proposed to be an ancestral immune signaling pathway, predating the evolution of TLR-dependent immune signaling pathways at the origin of metazoan evolution. Recognizing and managing the bacterial communities typically present at epithelial surfaces throughout the animal kingdom likely contributed to its evolution and maintenance.

3.7 *Hydra* species express distinct sets of antimicrobial peptides

In 2009, Fraune *et al*. discovered a direct link between tissue homeostasis and microbiota composition in *Hydra* by investigating a mutant strain with an inducible degradation of nerve cells (Fraune *et al*, 2009a). Interestingly, loss of nerve cells in *Hydra* triggers a drastical

increase in antibacterial tissue activity (Kasahara and Bosch, 2003), most likely due to the upregulation of AMPs. Arminins (Augustin *et al*, 2009a) are highly expressed AMPs in *Hydra magnipapillata*. Therefore, the transcriptomes of *H. vulgaris* (AEP), *H. oligactis* and *H. viridissima* were searched for orthologs of arminins. As indicated in **Figure 2.19**, clusters of arminins were identified, which varied greatly in their expression profiles, likely causing distinct antimicrobial activity in different *Hydra* species as previously observed (diploma thesis Björn Spudy, CAU Kiel). These findings are in line with studies investigating the evolution of insect immunity. The genomic equipment of AMPs varies greatly within insects, with many AMPs being specific only to a few, closely related species (Lazzaro, 2008). Similar to arminins in *Hydra*, AMP variety with independent gene expansions was also found within the genus *Drosophila*, indicating a high evolutionary rate of these peptides (Lazzaro, 2008, Sackton *et al*, 2007). Similar to mammalian α -defensins (Bevins and Salzman, 2011b), arminins seem to be constitutively expressed, since they are not differentially regulated by MyD88 deficiency or the absence of bacteria. This suggests a broader role in mediating the host-microbe interface. Several studies provide compelling evidence that experimental manipulation of AMPs affects the resident microbiota by changing their composition (Fraune *et al*, 2010, Ryu *et al*, 2004, Salzman *et al*, 2010, Vaishnav *et al*, 2008) or behavior (Login *et al*, 2011). However, direct evidence of species-specific AMPs acting as deterrents for host-specific bacterial communities was not proven.

3.8 Species-specific AMPs select for suitable bacterial partners

Similar to a study conducting reciprocal microbiota transplantations between mice and zebrafish (Rawls *et al*, 2006), the role of the *Hydra* host in sculpturing its associated bacterial community was investigated in the present thesis. Instead of a comparison between two different species, this question was investigated within one species, the cnidarian *Hydra vulgaris* (AEP), by comparing control polyps with polyps deficient in a subset of AMPs, called arminins. Bacterial communities (native or foreign) were transferred to germfree control or Arminin⁻ polyps by co-cultivation with different *Hydra* species and the microbiota of the recipient polyps was sequenced five weeks post inoculation. The present data indicate that arminin deficient *Hydra* polyps fail to select suitable bacterial partners from a pool of foreign potential colonizers, as they are colonized significantly different than control polyps, which select for bacterial types partially resembling their native microbiota (**Figure 2.26**).

Interestingly, no differential recolonization between control and Arminin⁻-polyps was observed for transferred native bacterial communities (**Figure 2.23**). The fact that a drastically reduced AMP expression did not affect the recolonization by native bacteria indicates, that the native microbiota might be partially resistant to and thus not influenced by endogenous AMPs, to which they adapted by co-evolution.

Whereas co-cultivation of germfree polyps with *Hydra vulgaris* (AEP) clearly transferred abundant bacteria from donor polyps to the recipients (**Figure 2.23 B**), neither control-, nor Arminin⁻-polyps adapted major fractions of foreign bacterial communities retrieved from *H. viridissima* or *H. oligactis*. Instead, recipient polyps selected bacterial colonizers from the rare microbiota of these donor polyps (**Figure 2.24 B, Figure 2.25 B**). This shows a selective enrichment of rare bacteria and proves the active selection by the host, rather than being a passive substratum. Although native bacteria might not be present, all available niches seem to get occupied by transferred bacteria, as total bacterial load did not differ significantly between treatments, regardless of the AMP deficiency or origin of the transferred bacteria (**Figure 2.27**). This is in line with studies analyzing the effect of changed expression levels of α -defensin AMPs in mice (Salzman *et al*, 2010), which indicated that AMPs are bacterial mediators, rather than unselective bacteriocides.

The microbiota of recolonized recipient polyps did not resemble the microbiota of wild-type polyps in detail, since the right bacteria might just not be present in the donor microbiota, or these bacteria are not horizontally transmitted. However, the weighted unifrac metric indicated an approximation to the wild-type *H. vulgaris* (AEP) microbiota, which was significantly less pronounced in Arminin⁻-polyps (**Figure 2.26**) and was likely caused by a differential colonization with Betaproteobacteria. Unifrac considers phylogenetic relationships within the observed bacteria. Since related bacterial species are more likely performing similar ecological functions, the host might select for certain bacterial divisions by expressing AMPs to which these taxa are less susceptible.

One caveat of our study was the use of transgenic *H. vulgaris* (AEP), which expressed eGFP in ectodermal cells (strain AL8), as donor strain for wild-type *H. vulgaris* (AEP) bacterial communities. This was necessary to separate donor and recipient control polyps after the co-cultivation, since they were not distinguishable by morphology. Unfortunately, the microbiota of these polyps seemed to be disturbed by the occurrence of the spirochaet bacterium *Turneriella parva*. Electron microscopic pictures provide evidence that this bacterium infects the mesogloea of *Hydra* (Stagni and Lucchi, 1969). However, it was never observed before in five independent lines of *Hydra vulgaris* (AEP) (Franzenburg *et al*, 2012, Franzenburg *et al*,

2013). It was not transmittable in our co-cultivation experiments (**Figure 2.23 B**) and is therefore considered as an exceptional condition. Further, some bacteria seem to be able to exploit germfree hosts faster than others. For example, the bacterium *Curvibacter sp.*, which normally dominates the microbiota of *H. vulgaris* (AEP), is outcompeted by a gammaproteobacterium called *Legionella* in recipient hosts at the analyzed timepoint. However, this might be a transient state.

3.9 Conclusions

To conclude, this thesis identified long-term stable, species-specific bacterial communities in different species of the freshwater polyp *Hydra*. These bacterial communities act in the antifungal immune defense of the holobiont and likely perform many other not yet identified functions. The ontogenetic establishment of these communities follows a robust, temporal progression, which is mediated by interactions within the microbiota and host-dependant modulations of the colonization rate. One putative host-factor, regulating the colonization, is the host's innate immune system. TLR-signaling was shown to sense the bacterial microbiota and to affect the routes and kinetics how bacteria recolonize the host. Antimicrobial peptides of the arminin family show highly species-specific expression profiles and act in selecting co-evolved bacterial partners, thus likely contributing to the species-specific bacterial associations observed in different *Hydra* species.

These findings raise some interesting questions for medical application. The curativeness of a healthy microbiota got widely recognized in the last decade, leading to an increased use of probiotics, *i.e.* application of beneficial bacteria. It was previously shown, that the microbiota of patients with inflammatory bowel disease (IBD) displays a decreased diversity and bacterial load, as well as shifts in community composition (Nagalingam and Lynch, 2012). A dysregulation of host-bacteria homeostasis therefore seems to be involved in the occurrence of disorders like Crohn's disease and ulcerative colitis (French and Pettersson, 2000, Ott *et al*, 2004). Probiotics, including *Lactobacillus* and *Bifidobacteria* have been shown to be efficient in treating IBD (Meijer and Dieleman, 2011). The data of the present thesis indicate strong host mediated control over the microbiota, since different host species avoid colonization by foreign microbes, presumably by the use of AMPs. Consistent with that, most probiotics fail to establish permanent associations and only transiently populate the human intestine, questioning their profits (Sartor, 2004, Tannock *et al*, 2000). An alternative to the use of food-

derived probiotics is the use of fecal microbiota therapy (FMT), transplanting the intestinal microbiota of a healthy person to a disease patient. These transplanted bacterial communities were shown to persist for years (Grehan *et al*, 2010) and effectively treated IBDs like Crohn's disease or ulcerative colitis (Damman *et al*, 2012). However, to optimize and personalize probiotic or FMT medications, more knowledge needs to be generated to elucidate the interaction of transferred intestinal bacteria with both, the host's immune system and the endogenous microbiota.

3.10 Perspective: Host-bacterial interactions and their role in speciation

In 1927, the microbiologist Ivan E. Wallin hypothesized in his book, *Symbioticism and the origin of Species*, that the acquisition of bacterial endosymbionts favors the origin of new species. Strong evidence for the validity of this hypothesis comes from studies in aphids. In a comparison between two different strains of the pea aphid (*Acyrtosiphon pisum*), difference in host plant preference was caused by the symbiosis with an endosymbiotic bacterium, which enabled the aphid to utilize white clover (*Trifolium repens*) as food plant (Tsuchida *et al*, 2004). Plant preference could easily lead to reproductive isolation, thus favoring speciation. Further, host-associated bacteria have been shown to cause positive assortative mating in *Drosophila* (Sharon *et al*, 2010). Inoculation with a single bacterial colonizer, *Lactobacillus plantarum*, caused significant sexual isolation, an effect that was reversible by the administration of antibiotics. The authors state bacterial modulation of sex pheromones as cause for the observed mating preferences (Sharon *et al*, 2010). Thus, bacterial symbionts can favor reproductive isolation and therefore accelerate speciation. But how do animals change their bacterial partners? One significant driver of bacterial community composition is diet (Ley *et al*, 2008a, Sharon *et al*, 2010), but also host factors like antimicrobial peptides have been shown to drastically influence the microbiota (Fraune *et al*, 2010, Salzman *et al*, 2010). AMPs evolve fast due to positive selection (Tennessen, 2005) and therefore changes in antimicrobial activity are likely to occur in animals in the wild. The data in this thesis indicate that changes in antimicrobial activity drastically influence the composition of the microbiota and therefore might affect the ecotype of the holobiont. This mechanism would allow adaptation to different niches much quicker than the evolution of metabolic pathways in the host genome. As shown in **Figure 2.1**, different bacterial communities were observed in

various species of the cnidarian *Hydra*. Since these distinct species inhabit different habitats (Bosch *et al*, 1988), differences in the microbiota might be cause or consequence of host speciation.

4 Material

4.1 Organisms

Hydra species:

Hydra vulgaris (AEP) (strain B3)
Hydra viridissima (strain A99)
Hydra oligactis (strain 10/02)
Hydra magnipapillata (strain 105)
Hydra carnea (strain Darmstadt)
Hydra vulgaris (strain Basel)
Hydra circumcincta (strain M7)

Prey organism:

Artemia salina (Silver Star)

Electro-competent bacteria :

Escherichia coli DH5 α
 (invitrogen)

Pathogens:

Pseudomonas aeruginosa (PA14)
Fusarium sp.

Hydra isolated bacteria

Curvibacter sp.
Acidovorax sp.
Duganella sp.
Pelomonas sp.
Pseudomonas sp.
 Unidentified Oxalobacteraceae

4.2 Chemicals

Acetic acid

Roth

Acetic anhydride

Roth

Acetonitrile

Roth

Agar-Agar

Roth

Agarose NEEO Ultra

Roth

Ampicillin

Merck

APS

Roth

Boric acid

Roth

BSA FractionV

Roth

Bromophenol blue	Sigma
Calcium chloride	Roth
Chloroform	Roth
DIG-11-dUTPs	Roche
Dipotassium phosphate (K_2HPO_4)	Merck
dNTPs (100 mM)	Fermentas
EDTA	Sigma
Ethanol	Roth
Ethidium bromide	Roth
Ficoll	Sigma
Formamide	Roth
Formic acid	Merck
Glucose	Merck
Glycerol	Roth
Glycin	Roth
HCl (37 %)	Roth
Isopropanol	Roth
Levamisole	Roth
Magnesium chloride ($MgCl_2$)	Merck
Magnesium sulfate ($MgSO_4$)	Merck
NBT/BCIP	Roche
Neomycin sulfate	Roth
Paraformaldehyde	Roth
Polyvinylpyrrolidone	Sigma
Potassium carbonate	Roth
Potassium chloride (KCl)	Roth
R2A-Agar	Roth
R2A Broth	Lab M
RapidGel-XL-40 % Concentrate	Roth
Rifampicin	Roth
RITC-Dextran	Sigma
Sheep Serum	Sigma
Sea salt (Reef Crystals TM)	Aquarium Systems
Sodium bicarbonate ($NaHCO_3$)	Roth
Sodium chloride (NaCl)	Roth
Sodium citrate ($Na_3(C_6H_5O_7)$)	Roth
Sodium dodecyl sulfate (SDS)	Roth
SP600125	A.G. Scientific
Streptomycin-Sulfate	Roth
TEMED	Merck
Triethanolamine	Sigma
Trifluoroacetic acid (TFA)	Roth
Tris base	Roth
Tris-HCl	Roth

TRIzol®	Invitrogen
tRNA Yeast	Sigma
Trypton	Roth
Tween 20	Roth
Urea	Roth
Urethane	Sigma
Xylene cyanol	Sigma
Yeast extract	Roth

4.3 Media

Artemia-Medium	31.8 g sea salt / 1 l Millipore H ₂ O
Hydra-Medium	0.29 mM CaCl x 2H ₂ O, 0.33 mM MgSO ₄ x 7 H ₂ O, 0.5 mM NaHCO ₃ , 0.08 mM K ₂ CO ₃
LB-Medium	10 g NaCl, 10 g Trypton, 5 g Yeast extract, 1 l Millipore H ₂ O
LB-Amp ⁺ -Medium	LB-Medium + Ampicillin (50 µg/ml)
LB-Amp ⁺ -Plates	1 l LB-Amp ⁺ -Medium, 15 g Agar-Agar
R2A-Medium	3 g R2A Broth / 1 l Millipore H ₂ O
R2A-Plates	18 g R2A-Agar / 1 l Millipore H ₂ O
SOB-Medium	20 g Trypton, 5 g Yeast extrakt, 0.55 g NaCl, 0.19 g KCl, 1 l
SOC-Medium	Millipore H ₂ O, 10 ml MgCl ₂ (1M), 10 ml MgSO ₄ (1 M) 1 l SOB-Medium, 10 ml Glucose (2 M, sterile filtered)

4.4 Buffer and Solutions

APS Stock Solution	10 % in Millipore H ₂ O
Blocking Solution	80 % MAB-T□BSA, 20 % heat□inactivated sheep serum
Denhardt's (50x)	1 % Polyvinylpyrrolidone, 1 % Ficoll, 1 % BSA fraction V in Millipore water (sterile)
DNA-Loading dye	5 ml Glycerol, 200 µl EDTA (0,5 M, pH 8.0), 1 ml 10 % SDS, 10 mg Bromophenol blue, 10 mg Xylene cyanol, 3.8 ml Millipore water
Hybridization Solution	50 % formamide, 5x SSC, 0.1 % Tween20, 0.1 % CHAPS,

	1x Denhardt's, 100 µg/ml Heparin in Millipore H ₂ O
NTM Buffer	100 mM NaCl, 100 mM TRIS□HCl, 50 mM MgCl ₂ , pH 9.5
NTM-T Buffer	NTM, add 0.1% Tween20
MAB Buffer	100 mM maleic acid, 150 mM NaCl, pH 7.5
MAB-T Buffer	MAB, add 0.1 % Tween20
MAB-T-BSA	MAB□T, add 1 % BSA fraction V
PBS Buffer	150 mM NaCl, 80 mM K ₂ HPO ₄ , pH 7.34
PBT Buffer	PBS, add 0.1 % Tween20
Peptide Extraction Solution	8 ml HCl (37 %), 5 ml formic acid, 1 ml trifluoroacetic acid, 1 g NaCl, 86 ml Millipore H ₂ O
SSC buffer (20x)	3 M NaCl, 0.3 M sodium citrate (pH 7.0)
SSC-formamide solution	50 % Formamide, 25 % 20x SSC, 25% Water
TAE-Buffer (50 x)	242 g Tris base, 57.1 ml 100 % acetic acid, 100 ml 0.5M EDTA, Millipore water up to 1l
TBE-Buffer (10 x)	162 g Tris Base, 27.5 g Boric acid, 50 ml 0.5 M EDTA, Millipore water up to 1l
LI-COR Sequencing Gel	10.5 g urea, 14 ml Millipore water, 3.75 ml Rotiphorese® Gel 40, 2.5 ml 10x TBE, 38 µl TEMED, 175 µl 10 % APS

4.5 Kits

DNeasy® Blood & Tissue Kit	Qiagen
DIG RNA Labeling Kit (SP6/T7)	Roche
First Strand cDNA Synthesis Kit	GE Healthcare
GoTaq® qPCR Master Mix	Promega
Micro BCA™ Protein Assay Kit	Pierce
MinElute Gel Extraction Kit	Quiagen
NucleoSpin®Extract II-Kit	Macherey-Nagel
NucleoSpin®Plasmid QuickPure-Kit	Macherey-Nagel
pGEM®-T Vector System	Promega
PureLink® DNase Set	Ambion
PureLink® RNA Mini Kit	Ambion
QIAfilter Plasmid Midi Kit (25)	Qiagen
Qubit® ds BR Kit	Invitrogen
SequiTherm™EXCEL II DNA-Seq. Kit	Epicentre Biotechnologies

4.6 Enzymes

AsiSI	New England Biolabs
BsiWI	New England Biolabs

EcoRI-HF	Fermentas
GoTaq-DNA-Polymerase	Promega
Phusion® HS II High Fidelity Polymerase	Finnzymes
Platinum <i>Taq</i> -DNA-Polymerase	invitrogen
Platinum <i>Taq</i> -DNA-Polymerase High Fidelity	invitrogen
Ribolock™ RNase Inhibitor	Fermentas
T4 DNA-Ligase	New England Biolabs

4.7 Antibodies

Anti-Digoxigenin-AP Fab fragments	Roche
-----------------------------------	-------

4.8 Vectors

LigAF-1	Provided by K. Khalturin
pGEM®-T	Promega

4.9 DNA size standards

GeneRuler™ DNA Ladder Mix	Fermentas
---------------------------	-----------

4.10 Oligonucleotides (Primer)

Table 4.1: Oligonucleotides

Description	Primer ID	Sequence (5' → 3')	Tm [°C]
Standard primers			
Actin promoter	HAP_F(1589)_IRD700	GTTCGTTATTCAGAAGCTTCAG	56.5
Actin terminator	HAT_R(2342)_IRD800	GGACGTCTTTTATATTACAGC	54.0
eGFP	GFP_F (625)_IRD800	CGAAAGATCCCAACGAAAAGA	55.9
	GFP_R (75) IRD700	GTGCCCATTAACATCACCATC	57.9
SP6	SP6	ATTTAGGTGACACTATAGAATAC	53.5
T7	T7	TAATACGACTCACTATAGGG	53.2
Actin	Actin 34	AAGCTCTTCCCTCGAGAAATC	57.9
	Actin 35	CCAAAATAGATCCTCCGATCC	57.9
Eubacteria	Eub_27F	AGRGTGGATCMTGGCTCAG	57.3
	Eub_1492R	GGHTACCTTGTTACGACTT	53.1
M13	M13_F	GTAAAACGACGGCCAGT	52.8
	M13_R	GGAAACAGCTATGACCATG	54.5

Primers for generation of expression constructs

MyD88 Hairpin	SF_MyD88_AEP_F	AAACCAATGGATTGCATTAATAAAG	54.8	
	SF_MyD88_AEP_R	GTTTTAAAATTCTGGGCATTTCAC	55.9	
	SF_MyD88as_F_Asi	TACAAAGCGATCGCGTTTTAAAATTCTG	60.7	
	SF_MyD88as_R_S_E	ACTTAGAATTC AATCGTACGATTAATGAT ACAATTTTATTGAA	63.8	
	MyD88_KOcheck_F	ACTCTGACGTCACCTATG	53.7	
	MyD88_KOcheck_R	GAGTGGTGTTAGGATCTGT	54.5	
	SF_MyD88s_F_SplI	TTAATCGTACGAAACCAATGGATTGCATT AAT	61.8	
	SF_MyD88s_R_EcoR	ATTGTGAATTCGTTTTAAAATTCTGGGCAT TTC	62.0	
	Arminin Hairpin	SF_Arminin_AEP_F	AAAATGAAGACAGTTTTTTGCA	50.1
		SF_Arminin_AEP_R	GAAACGAATTATATCATATGAC	50.9
Arm_as_F_AsisI		CAAAGCGATCGCTTAAGAAACGAATTATA TCATATG	64.9	
Arm_as_R_Bs_Ec		ACTTAGAATTC AATCGTACGAAAATGAAG ACAGTTTTTGC	66.4	
Arm_s_F_BsiWI		ATTTTCGTACGCAAGTGTAGCGGTCAC	65.0	
Arm_s_R_EcoRI		GAATTGTGAATTCGAAACGAATTATATCA TATGAC	62.4	

Primers for qRT-PCR and generation of arminin in-situ hybridization probes

Actin	SF_actin_RT_F	GAATCAGCTGGTATCCATGAAAC	58.9
	SF_actin_RT_R	AACATTGTCTGACCACTGATAG	58.9
Arminin 4364	SF_arm4364_RT_F	G	57.9
	SF_arm4364_RT_R	AGGAACAAGTTTTCTCCATCGTATATC	57.9
Arminin 6494	SF_arm6494_RT_F	GGAAAGTGACGAATTAATGATAAGAG	57.9
	SF_arm6494_RT_R	CAACAACCTGGTATATAAGGAATAAGTTTC	57.9
Arminin 6560	SF_arm6560_RT_F	GAGGATATAAAAGAAGAAATCAAGAACG	57.9
	SF_arm6560_RT_R	ATGAGCCAATTTTTATAACCGCTGGA	57.9
Arminin 7518	SF_arm7518_F	AGGTAATCGAAACCTAAAAGAAGAGA	57.9
	SF_arm7518_R	TAATCTAAGATATTCTTCTATGGGTATTG	57.9
Arminin 7519	SF_arm7519_F	GATGACGAGTTAGATGATAACGC	57.9
	SF_arm7519_R	AAGGCATGTACGGAAGAATCTTC	57.9
Arminin 7526	SF_arm7526_F	GGAAATCGAAACCTAAAAGAAGAGG	57.9
	SF_arm7526_R	TTCGCCACCATAAGAAAGGTTCA	57.9
Arminin 7591	SF_arm7591_F	AGGAAGACGTTAACGAGTTTGAC	57.9
	SF_arm7591_R	CAAGATTCCAAAGTTTAATAGCAGTG	57.9
Arminin 7722	SF_Arm7722_F	GATGACAATGCTCAAGAAGTTAGC	57.9
	SF_Arm7722_R	CCGTTTTGGTAAGCTTTTATTATATG	57.9
Arminin 7965	SF_arm7965_RT_F	GTGACGTGTTAGATAGTAACGTTAG	57.9
	SF_arm7965_RT_R	CTTAACAATAATTGGTACGTAAGGAC	57.9
Arminin 17593	SF_17593_RT_F	AGATTTTGGACGATCTTGAGGAAG	57.9
	SF_17593_RT_R	CTTTTTGCCGACTGGGTAAAAGTC	57.9
Arminin 45266	SF_arm45266_F	GAAAATGATGAGTTAGATGACAACAC	57.9
	SF_arm45266_R	CGGTTTTGGTAAGCTTGATTATACA	57.9
Contig 732	SF_732_RT_F2	CCCCTGGTCTTCCAAAATGAG	59.8
	SF_732_RT_R2	TTGAAGCAAATATTGATGCAGCAGC	59.7
Contig 1372	SF_1372_F	CTTAGTACTAATGGTCTTGGAACAC	59.7
	SF_1372_RT_R	CTGATTTATTCAGGTGATACTGCTTC	60.1
Contig 43476	SF_43476_RT_F	GAGTTTATATACAACAATGTTTTTGTTTTG	57.2
	SF_43476_RT_R	TGCTTTGGTAATAATAAAGTTCGTGC	58.5

Contig 45829	SF_AP_RT_F	AGGGTATCAAAGTCGTGGCAATC	60.6
	SF_AP_RT_R	TGGATCATCAAGATCAGCTTGAG	58.9
Contig 12837	SF_12837_RT_F	GCACAGGAACAAATTCAAAGTCG	58.9
	SF_12837_RT_R	CCAACAACACAAAGTATTCACCTATTC	60.4
Contig 19777	SF_19777_RT_F	CCAATACCGGAAAGACATTGGC	60.3
	SF_19777_RT_R	CTCTGATCCCATGAATTCATAAGG	59.3
Contig 34924	SF_34924_RT_F	TAAATGACAACCTCCCAAAGTTTGAAC	58.9
	SF_34924_RT_R	TGTTCTTCGATCCAATAAAAACAGATG	58.5
Contig 7659	SF_bcl2_RT_F	GAAGAGATCGAGGATTGGTTAAC	58.9
	SF_bcl2_RT_R	CTCAACCCAACCCATAAACTAG	58.4
Contig 1081	SF_1081_F	ATCTCACGTAGTAGCTTTGTGGATTG	59.7
	SF_1081_RT_R	CATACCACCAACCTCCATCATC	60.3
Contig 1474	SF_1474_RT_F	TCATTAATTGGTTTTGGGAACAACG	58.1
	SF_1474_RT_R	TGCTGCAACACAAGCTGACATAC	60.6
Contig 4420	AK_Chordin1qF1	AGATGAATGGTCCCCTGATTC	57.9
	AK_Chordin1qR1	GACGACATCAGTATAGGACATG	58.4
Contig 5435	INSR_F_qRT	CTGGCAATGGTTCATGGACAG	59.8
	INSR_R_qRT	CAGCAAGGCAACAATTACTGCAG	60.6
Contig 6197	SF_paraox_RT_F2	GGCAGTAAGAACTTAACTCTCA	57.1
	SF_paraox_RT_R2	GCGGCAGTAAACCAATGTGTTA	58.4
Contig 6358	AK_BMP2qF1	ATTCGGGATCACGTGTAGGC	59.8
	AK_BMP2qR1	CGTCGAAGATGTAAACGGTCG	59.8
Contig 48424	AK_BMPR3qF3	AGGACACAGGTGCTTGTACG	59.4
	AK_BMPR3qR3	CAGTATGCAAGTGAGCCAACC	59.8
Eubacteria	Eub341_F	CCTACGGGAGGCAGCAG	55.7
	Eub534_R	ATTACCGCGGCTGCTGG	55.7
EF1 α	EF1 alpha F	CACCATCGATATTGCACTATGG	57.9
	EF1 alpha R	GGAGTGGAATGTTATCAAGAGC	59.8

4.11 Devices

4.11.1 PCR- Thermocyclers

Primus 25	MWG-Biotech
Primus 96 <i>advanced</i>	peqLab
Primus 96 <i>plus</i>	MWG-Biotech
Real-Time Cyclers 7300	Applied Biosystems

4.11.2 Gel electrophoresis chambers

Separation system B1A	Owl Separation Systems
Separation system B2	Owl Separation Systems
Separation system D3	peqLab

4.11.3 Incubators / Shakers

Certomat Incubator	B.Braun
KS10 (Rotation-shaker)	Edmund Bühler
Thermo-Incubator	Heraeus Instruments
Thermomixer compact	Eppendorf
ThermoStat plus	Eppendorf
Magnetic Stirrer Heindolph	Eydam

4.11.4 Electroporation devices

Gene Pulser II	Biorad
Pulse Controller II	Biorad

4.11.5 Centrifuges

Centrifuge 5415 D	Eppendorf
Centrifuge 5417 R (Kühlzentrifuge)	Eppendorf
ELMI Centrifuge+Mixer	ELMI Ltd
Mini Spin	Eppendorf
Multifuge 3 S-R	Heraeus Instruments
Multi-Spin MSC-6000	Kisker-Biotech
Sorvall RC 5B	Du Pont Instruments

4.11.6 Microscopy

Axiocam (digital camera)	Zeiss
Axioskop 2	Zeiss
DP71 (digital camera)	Olympus
MS 5 Binocular	Leica
SZX 16 Binocular	Olympus

4.11.7 UV-devices

Gel-Doc™ XR+	Biorad
IMAGO Compact Imaging System	B&L-Systems
UV-table Chroma 43	Vetter GmbH
UV-Stratalinker® 1800	Stratagene

4.11.8 Photometer

BioPhotometer	Eppendorf
Nanodrop ND1000	Eppendorf
Nanodrop ND3300	Eppendorf

4.11.9 Microinjection

CellTram air pump	Eppendorf
CellTram vario pump	Eppendorf
Micromanipulator	Leitz
Micromanipulator 5171	Eppendorf
Vertical Pipette Puller 700 C	Kopf Instruments

4.11.10 Sequencers

4300 DNA Analyzer	LI-COR
454 GS-FLX Titanium	Roche

4.11.11 Other devices

Elektrophoresis Power Suply Consort EL 231	peqLab Kern
Kern 770 Weighing scale	Christ
Lyophilizer Alpha 2-4 LSC	Millipore
Milli-Q Academic System	Hanna Instruments
pH-Meter pH 211	EV H+P Labortechnik GmbH
VARIOKLAV Sterilizer Type 400	LKB Bromma
Varioperpex® II Peristaltic pump	Sartorius
1205 MP Weighing scale	

4.12 URLs

Compagen	http://compagen.zoologie.uni-kiel.de/
NCBI	http://www.ncbi.nlm.nih.gov
MG-RAST	http://metagenomics.anl.gov/
MWG	http://www.eurofinsdna.com/de/home.html
QIIME	http://www.qiime.org
Ribosomal Database Project	http://rdp.cme.msu.edu/
SMART	http://smart.embl-heidelberg.de/
UniProt	http://www.uniprot.org

4.13 Software

Image editing	Adobe Photoshop CS3
---------------	---------------------

Figure preparation	Adobe Illustrator CS3
Microarray analysis	Feature Extraction Software 10.7 (Agilent)
	GeneSpring (Agilent)
	Blast2Go
	Interproscan
Microscopy	Axio Vision 3.1
	CELL*
Sequence analysis	BioEdit
	DNAMAN 4.15
	LICOR eSeq v3.0
	MEGA 5
	QIIME

5 Methods

5.1 Cultivation of Organisms

5.1.1 Cultivation of *Hydra*

Experiments were carried out using *Hydra vulgaris* (AEP) (Hemrich *et al.*, 2007), *Hydra oligactis* (strain 10/02), *Hydra viridissima* (strain A99), *Hydra magnipapillata* (strain 105), *Hydra carnea* (strain Darmstadt), *Hydra vulgaris* (strain Basel) and *Hydra circumcincta* (strain M7). All laboratory cultured strains are available at the University of Kiel. All animals were cultured under constant, identical environmental conditions including culture medium, food (1st instar larvae of *Artemia salina*, fed 3x / week) and temperature according to standard procedures (Lenhoff and Brown, 1970).

For the analysis of the ontogenetic establishment of bacterial communities (**Chapter 2.3**), female polyps of *Hydra vulgaris* (AEP) were induced to sexual reproduction by reduced feeding (Wittlieb *et al.*, 2006). Detached eggs were collected and separated into single wells. Eggs were screened daily for hatched polyps. After 2 weeks, first eclosed polyps were subjected to DNA extraction. Next, clonal cultures were established using four hatchlings eclosed on the same day. Subsequently, one polyp of each clonally aging culture was removed and subjected to DNA extraction every week until 15 weeks post eclosion.

For co-cultivation experiments (**Chapter 2.1**, **Chapter 2.5**), single polyps of two species were cultured in single wells of 12-well plates (Greiner bio-one, Kremsmuenster, Austria) for five weeks with regular feeding. For isolation of DNA, polyps were separated according to morphology or GFP expression.

5.1.2 Cultivation of *Artemia salina*

First instar nauplius larvae of *Artemia salina* served as prey for all used *Hydra* species. Dauer eggs were incubated for 24h at 30 °C in Artemia-Medium under permanent air supply. For feeding of *Hydra* polyps, nauplii were collected, washed with water to remove salts, and re-suspended in Hydra-Medium.

5.1.3 Cultivation of *Hydra*-associated bacteria

Single *Hydra* polyps were placed in a 1.5 ml reaction tube and washed three times with 1 ml sterile filtered Hydra-Medium. After homogenization with a pestle, 100 μ l (equates to $1/10$ of a polyp) were plated on R2A Agar plates. After incubation at 18 °C for five days, single colony forming units (CFUs) were isolated and cultivated in liquid R2A medium. The bacteria were identified by Sanger sequencing of the 16S rRNA gene and stocks were stored in Roti®-Store Cryo Vials at -80 °C

5.1.4 Generation of germ-free *Hydra*

Polyps were incubated for one week in an antibiotic solution containing 50 μ g/ml each of ampicillin, rifampicin, streptomycin and neomycin with daily exchange of the solution. After one week of treatment, the polyps were transferred into sterile-filtered and autoclaved Hydra-Medium and fed with germ-free *Artemia salina* larvae (hatched in 30 ‰ artificial sea water containing the same antibiotics). Following one week of recovery, the absence of bacteria was verified by plating homogenized polyps on R2A-Agar plates. After incubation at 18 °C for five days the CFU were counted. Absence of CFU indicated successful antibiotic treatment. For culture independent analysis, total DNA was extracted from single polyps using the DNeasy Blood & Tissue Kit (Qiagen). 16S rRNA genes were amplified using the universal primers Eub-27F and Eub-1492R (Weisburg *et al.*, 1991) in a 30 cycle PCR. Sterility was verified by the absence of a PCR-product.

5.1.5 Generation of mono-associated *Hydra*

Bacteria isolated from *Hydra* polyps were cultured in liquid R2A medium for 3 days at 18 °C. Following centrifugation with 1380 x g for 10 minutes, the bacterial pellet was resuspended in sterile Hydra-Medium. Using a photometer, the optical density (OD₆₀₀) was adjusted to 0.1. Germfree *Hydra* polyps were incubated in these solutions for 24 hours. Non associated bacteria were removed by washing with sterile Hydra-Medium. Following another 24 hours, the re-association was checked by plating tissue homogenates on R2A Agar plates. Conventionalized polyps were incubated in a mixture of *Hydra vulgaris* (AEP) culture supernatant and *Hydra vulgaris* (AEP) tissue homogenates (one homogenated polyps / ml) instead.

5.2 Standard laboratory methods

5.2.1 RNA Isolation

Total RNA was extracted from 15 sexually undifferentiated polyps using the TRIZOL plus protocol (Invitrogen). Polyps were homogenized in 0.5 ml TRIZOL[®]. After incubation at room temperature (RT) for 5 min, 100 µl of chloroform were added to the homogenate. The tubes were shaken vigorously and incubated at RT for 3 minutes. Phase separation was achieved by centrifugation at 12,000 x g for 10 minutes at 18 °C. The upper aqueous phase, containing the RNA was transferred to a new 1.5 ml tube on ice and mixed with an equivalent volume of 70 % EtOH (ice-cold) by vortexing. The resulting solution was transferred to Invitrogen PureLink Mini Kit columns for RNA purification following the manufacturer's protocol. After binding RNA to the columns membrane by centrifugation at 12,000 x g for 15 seconds, the column was rinsed (15 sec at 12,000 x g) with 700 µl of Washing Buffer (WB) I. An on-column DNase digestion was performed for 30 minutes at RT by adding 8 µl 10x PureLink on-column DNase Buffer, 10 µl PureLink on-column DNase, 2 µl Ribolock[™] RNase inhibitor and 60 µl RNase free water. After DNase treatment, columns were washed twice with 500 µl of WB II. Subsequently, the column was dried for 1 minute at 12,000 x g. Finally, RNA was eluted in 30 µl RNase free H₂O and the concentration of extracted RNA was measured using a NanoDrop Spectrophotometer ND1000. RNA quality was checked by 260/280 and 260/230 ratios and visualization of rRNA bands by agarose-gel electrophoresis.

5.2.2 First strand cDNA synthesis

The synthesis of cDNA was performed using the First Strand cDNA Synthesis Kit (Fermentas) according to the manufacturers protocol using Oligo(dT)₁₈ primer. For subsequent comparative analyses of gene expression by qPCR, equal amounts of RNA were used as templates for the reactions.

5.2.3 Polymerase chain reaction

5.2.3.1 Standard PCR

A standard PCR for amplification of sequences from cDNA or DNA was conducted with the conditions shown in **Table 5.1** and **Table 5.2**.

Table 5.1 Pipetting scheme of a standard PCR

Component	Volume	Final concentration
5x Colorless GoTaq Reaction buffer	2 μ l	1x
dNTP-Mix (10 mM)	0,2 μ l	0,2 mM
Forward-Primer (10 μ M)	1 μ l	1 μ M
Reverse-Primer (10 μ M)	1 μ l	1 μ M
GoTaq DNA-Polymerase (5 U / μ l)	0,05 μ l	0,25 U
DNA template	X μ l	100 ng
Millipore water	5,75 – X μ l	

Table 5.2: Standard PCR program

Step	Temperature [°C]	time [s]
Initial denaturation	94	180
Amplification (up to 40 cycles):		
1. Denaturation	94	30
2. Annealing	T _m - 1	30
3. Elongation	72	t
Terminal Elongation	72	300

T_m= melting temperature of the used primer-pair (see Chapter 4.10)

Elongation time (t) was depending on the length of the amplified PCR fragment. A synthesis rate of the *Taq* polymerase of 1,000 bp per minute was used to estimate the elongation time.

5.2.3.2 Colony Check PCR

Colony Check PCRs serve the amplification of plasmid-inserted sequences, usually carried by transformed bacteria like *E. coli* DH5 α . Therefore, single bacterial CFU were picked from Agar plates and added to a standard PCR reaction mix, serving as DNA template. For the amplification of the inserted sequence, plasmid-specific primers were used. pGEM-T[®]-inserted sequences were amplified using the primer pair SP6 and T7. LigAF-1-inserted sequences were amplified by either using the *actin* promoter specific primer HAP_F and GFP_R (insert was cloned in front of *egfp*) or GFP_F and the *actin* terminator specific primer HAT-R (insert was cloned 5' to *egfp*). Colony check PCRs were run for 40 cycles.

5.2.3.3 Quantitative real-time PCR (qRT-PCR)

Quantitative real-time PCR (qRT-PCR) was conducted using the GoTaq[®] qPCR Master Mix (Promega, Madison, USA) and a 7300 realtime PCR system (ABI, Foster City, USA) according to the manufacturer's protocol. Template cDNA amounts were equilibrated for the reference gene EF1 α gene (EF1 alpha_F and EF1 alpha_R). Template gDNAs for quantification of the bacterial load were equilibrated using the reference gene *beta actin* (SF_actin_RT_F and SF_actin_RT_R). The expression levels, relative to the reference gene,

were calculated using the formula fold change = $2^{-\Delta\Delta C_t}$ (Scheffe *et al*, 2006) with C_t being the PCR threshold cycle. All experiments were conducted with at least three biological replicates.

5.2.4 Electrophoretic separation of DNA samples

Separation of DNA fragments was achieved using horizontal gel electrophoresis. Depending on the fragment size, gels were prepared by dissolving 1 % to 1.5 % agarose (w/v) in 1x TAE buffer. To visualize DNA bands, 5 μ l of ethidiumbromide were added to 100 ml of gel-solution. The electrophoretic separation was conducted with 3-5 V/cm³. After visualization of DNA bands under UV light, the size of fragments was estimated using the the GeneRuler™ DNA Ladder Mix (Fermentas) as size marker.

5.2.5 Extraction of DNA fragments from agarose gels

DNA bands were visualized under UV light. Desired bands were excised and transferred into 1.5 ml reaction tubes. Afterwards DNA was extracted using the NucleoSpin® Extract II Kit (Macherey Nagel) or MinElute Gel-Extraction Kit (Quiagen) according to the manufacturer's protocol.

5.2.6 Restriction Digestion of DNA

DNA was digested with restriction enzymes to generate “sticky end” for ligation of sequence inserts into LigAF-1 vectors. **Table 5.3** shows a typical pipetting scheme for digestion of DNA. The digestion was performed at 37 °C over night and subsequently terminated by incubation at 70 °C for 20 minutes.

Table 5.3: Pipetting scheme for digestion of DNA

Component	Volume	Final concentration
DNA	X	2 μ g
10x Reaction buffer	5 μ l	1x
Restriction enzyme 1	2 μ l	20 U
Restrictions enzyme 2	2 μ l	20 U
Millipore water	43-X μ l	

5.2.7 Ligation of DNA fragments

5.2.7.1 Ligation of PCR-products into pGEM®-T vectors

PCR products were ligated into the pGEM®-T vector (Promega) for subsequent sequencing and expression-construct assembly. Ligation is achieved by TA-cloning. During PCR

amplification, the *Taq*-Polymerase generates adenosine (A) overhangs. These “sticky ends” anneal with thymidin (T) overhangs present in the pGEM®-T vector during ligation. Ligations were carried out over night at 4 °C as described in **Table 5.4** and subsequently terminated by incubation at 70 °C for 20 minutes.

Table 5.4: Pipetting scheme for ligation into pGEM®-T vectors

Component	Volume
Rapid Ligation Buffer (2x)	2,5 µl
PCR-Product	1,5 µl
pGEM®-T Vector (50 ng)	0,5 µl
T4 DNA-Ligase (3 U/µl)	0,5 µl
Total volume	5,0 µl

5.2.7.2 Ligation of DNA fragments into the LigAF-1 vector

Compatible “sticky ends” between vector and insert were generated by restriction digestion. Insert and vector were used for ligation in a molar ratio of 3:1. Ligations were carried out over night at 4 °C as described in **Table 5.5** and subsequently terminated by incubation at 70 °C for 20 minutes.

Table 5.5 Pipetting scheme for ligation into LigAF-1 expression vectors

Component	Volume
10x T4-Ligationbuffer	1 µl
T4-Ligase	0,5 µl
Digested LigAF-1	x µl
Digested insert	x µl
Total volume	10 µl

5.2.8 Transformation of *E. coli*

1.5 µl of ligation product were mixed with 50 µl of *E. coli* ElectroMAX DH5α (invitrogen) cell suspension and electroporated using the devices *Gene Pulser II* and *Pulse Controller II* (Biorad) with the following conditions: 1.8 kV, 25 µF and 200 Ω. Immediately after electroporation, cells were transferred into 1 ml of pre-warmed SOC medium and incubated at 37 °C for 1 hour with continuous shaking at 220 rpm. 100 µl – 400 µl were plated on LB-Amp⁺ agar. Only cells containing the Ampicillin resistance encoding plasmid were able to grow over night at 37 °C.

5.2.9 Preparation of plasmids

5.2.9.1 Mini-preparation

Positive bacterial clones, identified by colony check PCR, were propagated in liquid LB-Amp⁺ medium and subjected to plasmid preparation using the NucleoSpin[®] Plasmid QuickPure Kit (Macherey Nagel) according to the manufacturer's instructions.

5.2.9.2 Midi-preparation

Midi-preparations of LigAF-1 plasmids were conducted using the Plasmid Midi Kit (Qiagen) according to the manufacturer's instructions. Afterwards, an additional precipitation step was performed by the addition of 1/10 volume 3 M Sodium Acetate and 2 volumes of ethanol. After centrifugation for 15 minutes at 20 000 x g at 4 °C, the pellets were washed in 300 µl of 75 % ethanol, the centrifugation step was repeated and the pellet was dried on air and dissolved in 50 µl Millipore water over night at 4 °C.

5.2.10 Sanger DNA sequencing

DNA sequencing was carried out using the SequiTherm EXCEL II DNA Sequencing Kit-LC (Epicentre Technologies) as shown in **Table 5.6**. This technique is based on the Sanger dideoxymediated chain-termination method (Sanger *et al*, 1977). Vector specific primers, IRD-800 or IRD-700 labeled at the 5' end (MWG-Biotech), were used to generate sequence amplicons. Reactions were set up according to the manufacturer's protocol. Sequencing reaction products were separated and detected in a LI-COR Gene ReadIR 4200 (MWG Biotech) automated sequencing machine and analysed with the manufacturer's software.

Table 5.6 Pipetting scheme for Sanger sequencing

Component	Volume
3.5x sequencing buffer	3.6 µl
Plasmid (150 ng) + water	4.1 µl
SequiTherm EXCEL II Polymerase	0.3 µl µl
IRD-Primer (5 µM)	0.5 µl
Total volume	8.5 µl

A total of 2 µl of this mixture was added to 1 µl of nucleotide mix containing the dideoxy nucleodides ddATP, ddCTP, ddGTP or ddTTP, respectively. The samples were subjected to the following PCR program (**Table 5.7**):

Table 5.7: Cycle-Seq program for Sanger sequencing

Step	Temperatur [°C]	Zeit [s]
Initial Denaturation	95	300
Amplification, 30 cycles:		
1. Denaturation	95	30
2. Annealing	T _m - 1	30
3. Elongation	70	60

The reaction was stopped by the addition of 3 µl loading buffer. Prior to loading 0.7 µl of the samples on a 41 cm sequencing gel in the 4300 DNA Analyser (LI-COR Biosciences) they were denaturated for 10 minutes at 95 °C. The results were analysed using the e-Seq 3.0 program.

5.3 Whole mount in situ hybridization

5.3.1 Riboprobe generation

The transcript of interest was amplified from previously generated cDNA. The amplicon was ligated into the pGEM®-T vector, transformed into *E. coli* DH5α and subsequently sequenced to ensure specificity of the primers and orientation of the inserted fragment. Next, a PCR was performed with vector-specific primers (M13_F/M13_R). A total of 0.5 µg purified PCR product was used as template for the DIG RNA Labeling Kit (SP6/T7) according to the manufacturer's protocol.

5.3.2 Preparation of polyps

Polyps were starved for 2 days prior to fixation. Polyps were relaxed by incubation in 2 % Urethane in Hydra-Medium for 2 minutes and subsequently transferred into 4 % paraformaldehyde for tissue fixation. The fixative was removed by washing the animals 3x with PBT for 10 minutes. Finally, polyps were transferred to 100 % methanol for tissue bleaching and stored at -80 °C for at least 2 days.

5.3.3 Probe hybridization and staining

The protocol was modified from previous work (Grens *et al.*, 1999) and conducted in the following steps:

Table 5.8: Protocol for *in situ* hybridization.

Day	Treatment	Temperature	Duration
Day 1	EtOH 100 %	RT	10 min
	EtOH 75 % / PBT 25 %	RT	5 min
	EtOH 50 % / PBT 50 %	RT	5 min
	EtOH 25 % / PBT 75 %	RT	5 min
	wash with PBT	RT	3 x 10 min
	Proteinase K (10 µg/ml) in PBT	RT	20 min
	Glycine (4 mg/ml) in PBT	RT	2 min
	Glycine (4 mg/ml) in PBT	RT	10 min
	wash with PBT	RT	3 x 10 min
	Triethanolamine (0,1 M)	RT	2 x 10 min
	Acetic Anhydrid 2,5 ul/ml in Triethanolamine (0,1 M)	RT	5 min
	Addition of 2,5 ul/ml Acetic Anhydrid	RT	5 min
	wash with PBT	RT	3 x 10 min
	re-fixation with Paraformaldehyde 4 %	4 °C	16 h
Day 2	PBT	RT	3 x 10 min
	SSC 2X	RT	2 x 10 min
	SSC 2X	70 °C	20 min
	Hybridization Solution (HyS) 50 % / SSC 2X 50 %	70 °C	10 min
	HyS 100 %	70 °C	10 min
	tRNA (20 µl/ml) in Hybridization Solution	57 °C	2 h
	Probe (2 µl of 1:15 dilution) in SSC-Formamid solution	57 °C	16-72 h
Day 3	Warm up all solutions!	57 °C	
	HyS 100 %	57 °C	10 min
	HyS 75 % / SSC 2X 25 %	57 °C	10 min
	HyS 50 % / SSC 2X 50 %	57 °C	10 min
	HyS 25 % / SSC 2X 75 %	57 °C	10 min
	0,1 % CHAPS in SSC 2X	57 °C	2 x 30 min
	MAB-T	57 °C	2 x 10 min
	MAB-T-BSA	57 °C	1 h
	Blocking Solution	4 °C	2 h
Anti-DIG-AP fab fragment 1:2000 in Blocking Solution	4 °C	16 h	
Day 4	MAB-T	RT	8 x 15 min
	NTMT	RT	5 min
	Levamisole 1mM in NTMT	RT	5 min
	NBT/BCIP in NTMT- Staining	RT	up to 1 h
	Water	RT	3 x 1 min
	EtOH 50 %	RT	5 min
	EtOH 70 %	RT	5 min
	EtOH 100 %	RT	5 min
embedding in Euparal	RT		

5.4 Generation of transgenic *Hydra vulgaris* (AEP)

5.4.1 Construct for downregulation of MyD88

For generation of *H. vulgaris* (AEP) *egfp:myd88*-hairpin transgenics, a 430 bp antisense (as) fragment of *myd88* was amplified from *H. vulgaris* (AEP) cDNA. The fragment was cloned into the LigAF-1 expression vector using *AsiI* and *BsiWI* restriction sites adjacent to the *egfp*. A stop codon terminating the eGFP was inserted with the forward primer. Next, a 750 bp sense (s) fragment of *myd88* was amplified with the first 320 bp as the linker sequence and the last 430 bp as the reverse complement to the antisense fragment. This fragment was cloned into the expression vector using the *BsiWI* and *EcoRI* restriction sites at the 3' end of the *egfp:myd88_as* construct. The resulting plasmid DNA was purified using the Qiagen MidiPrep Kit, sequenced, and injected into *H. vulgaris* (AEP) embryos as previously described (Wittlieb *et al*, 2006). Embryos began to express the reporter gene 2–3 days after injection. Founder transgenic animals bearing the *egfp:myd88*-hairpin construct started to hatch 14 days after microinjection. One of them showed stable EGFP expression in a group of ectodermal as well as endodermal cells. The initial founder transgenic polyp was expanded further by clonal propagation. By selecting for eGFP-expression using an Olympus SZX16 stereomicroscope, mass cultures of both, polyps with no transgenic cells (MyD88-control) and polyps with full endodermal and ectodermal expression of eGFP (MyD88-knockdown), were generated. Successful down-regulation of *myd88* was verified by RT-PCR using primers targeting regions of the *myd88* gene that were not used in generating the hairpin construct.

5.4.2 Construct for downregulation of arminins

Hairpin mediated silencing of target genes in *Hydra* can be achieved as previously described for MyD88. For generation of *H. vulgaris* (AEP) transgenics, a cassette consisting of a 318 bp long antisense fragment of *arminin7965* and its corresponding sense sequence, separated by a spacer of 300 bp, was cloned in the LigAF1 vector 3' to *egfp*. The resulting vector was injected into *H. vulgaris* (AEP) embryos. Founder polyps showed stable eGFP expression in a group of endodermal cells and were expanded further by clonal propagation. By selecting for eGFP-expression, mass cultures of both, polyps with no transgenic cells (control) and polyps with full endodermal expression of eGFP (Arminin⁻) were generated.

5.4.3 Embryo- microinjection

Transgenic *H. vulgaris* (strain AEP) were generated at the University of Kiel Transgenic *Hydra* Facility (<http://www.unikiel.de/zoologie/bosch/transgenic.htm>) as described by Wittlieb *et al* (Wittlieb *et al*, 2006). A plasmid concentration of 1 µg/µl was used and 1 % Rhodamine B Isothiocyanate-Dextran R9379 were added as tracer. The solution was injected into *Hydra* embryos within the 2 to 4 cell developmental stage.

5.5 *Hydra* infection experiments

5.5.1 Infection with *Fusarium sp.*

The pathogenic fungi *Fusarium sp.* was cultured on R2A agar plates. A piece of hyphae containing agar was transferred into a falcon tube, containing 50 ml liquid R2A medium. The tube was sealed and incubated at RT for 48h. Fungal spores were retrieved from the supernatant and transferred into 1.5 ml reaction tubes. After centrifugation with 20,000 x g for 5 minutes, the pellet was resuspended in $\frac{1}{10}$ of the original volume using sterile Hydra-Medium. For fungal infection, groups of five *Hydra* polyps were placed in a volume of 480 µl sterile Hydra-Medium using 1.5 ml tubes. 20 µl of spore-solution were added to each tube and fungal growth was monitored seven days post infection by the outgrowth of hyphae.

5.5.2 Infection with *Pseudomonas aeruginosa* (PA14)

Pseudomonas aeruginosa strain PA14 was cultured in LB-medium for 16 hours at 37 °C. 50 ml culture was centrifuged for 10 minutes at 1380 x g. The resulting pellet was resuspended in 50 ml sterile Hydra-medium. This resulted in an optical density (OD₆₀₀) of 0.93, which was diluted to an OD₆₀₀ of 0.1 with sterile Hydra-medium. Single MyD88-knockdown- and – control polyps (n=25 each) were transferred in single wells of 24-well plates and incubated in 1 ml of the PA14-solution. CFU/ml were counted by plating 100 µl of a 1/10000 dilution of OD₆₀₀= 0.1. Mean resulting cell count was 1.8*10⁸ cells/ml. Plates were sealed and stored at 20 °C. Polyps were screened daily and scored by following criteria shown in **Figure 2.18**.

5.6 DNA Extraction and Sequencing of 16S rRNA Genes

For total DNA extraction, single polyps were subjected to the DNeasy Blood & Tissue Kit (Qiagen) after being washed 3 times with sterile filtered culture medium. Extraction was performed following the manufacturer's protocol, except that DNA was eluted in 50 μ l. For sequencing of *H. viridissima* associated bacteria, endosymbiotic algae (*Chlorella sp.*) were depleted mechanically. Therefore, polyps were placed in 180 μ l Buffer ATL (DNeasy Blood & Tissue Kit). The lid of the reaction tube was penetrated with a 0.6 x 60 mm injection needle and polyps were homogenized by drawing up an attached 10 ml syringe. The homogenous green suspension was centrifuged at 350 x g for 2 minutes and the supernatant was subjected to DNA extraction using the DNeasy Blood & Tissue Kit following manufacturer's instructions. For sequencing of the bacterial 16S rRNA genes, the variable regions 1 and 2 (V1V2) were amplified using the universal forward primer V2_B_Pyro_27F (5'-CTATGCGCCTTGCCAGCCCGCTCAGTCAGAGTTTGATCCTGGCTCAG-3') which consists of the 454 FLX Amplicon primer B (underlined), a two base linker (italics) and the universal 16S primer 27F (regular) and the barcoded reverse primer V2_A_338R (5'-CGTATCGCCTCCCTCGCGCCATCAGNNNNNNNNNNCATGCTGCCTCCCGTAGGAGT-3') which contains the 454 FLX Amplicon primer A (underlined), a sample specific 10-mer barcode (N's), a two base linker (italics) and the universal 16S primer 338R (regular). 25 μ l PCR reactions were performed using the Phusion® Hot-Start II DNA polymerase (Finnzymes, Espoo, Finland) following the manufacturer's instructions. PCR conditions consisted of an initial denaturation step (98 °C, 30 sec) followed by 30 cycles of denaturation (98 °C, 9 sec), annealing (55 °C, 30 sec) and elongation (72 °C, 20 sec). PCR was terminated by a final elongation of 72 °C for 10 min. All reactions were performed in duplicates, which were combined after PCR. PCR products were extracted from agarose-gels with the Qiagen MinElute Gel Extraction Kit and quantified with the Quant-iT™ dsDNA BR Assay Kit on a NanoDrop 3300 Fluorometer according to manufacturer's instructions. Equimolar amounts of purified PCR product were pooled and further purified using Ampure Beads (Agencourt). A sample of each library was run on an Agilent Bioanalyzer prior to emulsion PCR and sequencing as recommended by Roche. Amplicon libraries were subsequently sequenced on a 454 GS-FLX using Titanium sequencing chemistry.

5.6.1 16S rRNA 454 analysis

16S rRNA amplicon sequence analysis was conducted using the Qiime 1.3.0 package (Caporaso *et al.*, 2010). Using the sequence fasta-file, a quality file and a mapping file which assigned the 10 nt barcodes to the corresponding sample as input, the sequences were analyzed using the following parameters: length between 300 and 400 bp, no ambiguous bases and no mismatch to the primer sequence. Chimeric sequences were identified and removed using Chimera Slayer (Haas *et al.*). Sequences were normalized to the number of reads obtained for the lowest represented sample in a given analysis, grouped into operational taxonomic units (OTUs) at a $\geq 97\%$ sequence identity threshold (if not otherwise stated) and classified by RDP classifier. Alpha diversity was estimated using the Chao1 metric implemented in Qiime. Beta diversity was assessed using the weighted unifracs and Pearson distances (1000 replicates). 454 data are deposited at MG-RAST (see Appendix).

5.7 Mathematical Modeling

The mathematical basis of the model is the replicator-mutator equation, which describes the dynamics of different types in a competitive environment based on pairwise interactions. In this case, a colonization rate reintroducing bacterial types corresponds to mutations. The number of types was assumed to be fixed. The rate of change of a type's relative abundance is proportional to its fitness relative to the fitness averaged across all types. Competition means that a type that performs better than average increases in relative abundance. If it performs worse, it will decrease in relative abundance. The fitness of each type is either constant or depends on interactions with other types (frequency dependent fitness). It was also sought to maintain a minimum diversity irrespective of the performance in competition, which is modeled by a colonization rate: For each type, the relative abundance increases at the expense of an equally distributed decrease of all other types.

The bacterial types were labeled with i ($i = 1, \dots, n$). A type's relative abundance is denoted by x_i , its change over time (as a derivative with respect to time) is \dot{x}_i . All relative abundances sum up to one. The fitness of a type is denoted f_i . Fitness can be constant or frequency dependent. The average fitness across all bacterial types is $\bar{f} = x_1 f_1 + x_2 f_2 + \dots + x_n f_n$. Due to colonization, the rate at which the abundance of a type increases at the expense of other types is $\lambda/(n-1)$, multiplied with the average fitness of all other types, $\bar{f}'_i = \bar{f} - x_i f_i$. The

colonization rate can be time dependent, $\lambda(t)$, and corresponds to a mutation rate. The dynamics are governed by the following equation:

$$\dot{x}_i = x_i(f_i - \bar{f}) + \lambda(t) \left(\frac{\bar{f}_i^r}{n-1} - x_i f_i \right)$$

The first term describes change due to the difference to the average performance of the bacterial community. The second term describes random gain from, and loss to all other types proportional to the rate of colonization. The fitness of each type can either be a constant, $f_i = w_i$, or frequency dependent $f_i = a_{i1}x_1 + a_{i2}x_2 + a_{i3}x_3 + a_{i4}x_4$, where a_{ik} is the parameter for species i interacting with species k . For our numerical example in **Figure 2.11 C**, constant selection, $\{w_1, w_2, w_3, w_4\} = \{0.1, 0.4, 1.0, 0.6\}$ was used.

In **Figure 2.11 D, E**, frequency dependent selection, the following parameters were used:

$$\begin{pmatrix} a_{11} & a_{12} & a_{13} & a_{14} \\ a_{21} & a_{22} & a_{23} & a_{24} \\ a_{31} & a_{32} & a_{33} & a_{34} \\ a_{41} & a_{42} & a_{43} & a_{44} \end{pmatrix} = \begin{pmatrix} 0.20 & 0.85 & 0.95 & 0.05 \\ 0.05 & 0.90 & 0.35 & 0.80 \\ 0.35 & 0.10 & 0.10 & 0.75 \\ 0.55 & 0.35 & 0.35 & 0.35 \end{pmatrix}$$

In **Figure 2.11 C, D** the colonization rate was constant, $\lambda = 0.02$, in **Figure 2.11 E** it was time dependent according to $\lambda(t) = 0.02e^{-t/20}$. Note that the parameter choices are for illustration only, it does not represent a fit to the *Hydra* system.

5.8 Custom made *Hydra vulgaris* (AEP) microarray

The microarray is based on a full transcriptome of *Hydra vulgaris* (AEP) sequenced by 454 technology (Hemrich *et al*, 2012). The final assembly contained 49070 contigs resulting in 31192 peptide predictions. For the microarray design (Agilent Technologies) all contigs with a peptide prediction were used. Additionally, contigs without a peptide prediction that were larger than 260 bp were integrated. This results in a microarray platform having 45220 oligos of 60 nucleotides in length, resembling 37063 unique contigs.

5.8.1 RNA isolation and microarray gene expression experiments

Total RNA was isolated from 15 polyps using the TRIZOL plus protocol (Invitrogen). Three MyD88-control- and four biological replicates each of MyD88-knockdown and MyD88-

control-germfree animals were conducted. Quality was checked by 260/280 and 260/230 ratios and visualization of rRNA bands by agarose-gel electrophoresis. 400 ng of total RNA per sample were labeled with Cy3 using the one-color Quick Amp Labeling Kit protocol (Agilent). Labeled cDNAs were hybridized to custom made Agilent *Hydra* (AEP) Gene Expression Microarray slides (4×44k) for 17 hours at 65 °C and washed according to the Agilent protocol. Hybridized microarray slides were scanned using an Agilent High-Resolution Microarray Scanner.

5.8.2 Microarray data extraction, filtering and analysis

Raw microarray image files were processed and quality checked by Agilent's Feature Extraction 10.7 Image Analysis Software. Background subtracted signal intensity values that contain correction for multiplicative surface trends (gProcessedSignal) generated by the Feature Extraction Software were used for further data analysis. Using GeneSpring microarray data analysis software, probes were filtered that were flagged as non-uniform or as population outlier. For all samples, the average signal intensity values were calculated over the three (MyD88-control) or four (MyD88-knockdown and MyD88-control-germfree) biological replicates. Statistical analysis was conducted by ANOVA with SNK post-hoc test and FDR correction for multiple comparisons. After setting a threshold of ≥ 1.5 fold change compared to the control, resulting significant ($p \leq 0.05$) differentially expressed contigs were analyzed using the blast2go batchblast (Conesa *et al*, 2005) with blastx ($\leq E^{-6}$) and domain prediction by InterProScan (Zdobnov and Apweiler, 2001) and grouped into self chosen categories. Microarray data are deposited at Gene Expression Omnibus (GEO) with the accession number GSE32383.

5.9 SP600125 JNK inhibitor treatment

For the treatment with SP600125 (A.G. Scientific), polyps (25 each) were incubated at a density of 1 polyp per milliliter in SP600125 diluted in 5% DMSO/hydra medium for 30 minutes on ice. Following 3 short washes in 0.1 % DMSO/Hydra-medium, animals were transferred to SP600125 diluted in 0.1 % DMSO/Hydra-medium in the dark for 24 hours at 18 °C (Philipp *et al*, 2009). RNA was extracted using the TRIZOL plus protocol (Invitrogen).

5.10 Phylogenetic Analysis

For the calculation of the arminin tree a nucleotide alignment of the coding sequences were used. The nucleotide alignment was build with the TranslatorX (Abascal *et al*, 2010) program which aligns protein-coding nucleotide sequences based on their corresponding amino acid translations. As outgroup, the arminin-like peptides of the four different species were selected. Bayesian posterior probabilities were calculated using MrBayes version 3.1.2 (Huelsenbeck and Ronquist, 2001). A total of 3 million generations were calculated using the general time reversible model and four chains with a burn-in of 25% and the invgamma rate variation. The tree was visualized using Mega 5 (Tamura *et al*, 2011).

5.11 Peptide extraction from *Hydra* tissue

For peptide extraction, approximately 1000 control- or Arminin⁻-polyps were homogenated in 100 ml of 1 M HCl, 5 % (v/v) formic acid, 1 % (v/v) trifluoro acetic acid (TFA) and 1 % (w/v) NaCl at 4 °C over night as previously described (Augustin *et al*, 2009b). After centrifugation at 30,000 g for 1 hour, the supernatants were applied to tC18 6cc (500 mg) SepPak® Vac cartridges (Milford) for solid phase extraction. Bound material was eluted with 84 % acetonitrile in 0.1 % TFA (v/v). The eluates were lyophilized and redissolved in 0.01 % TFA (v/v). The protein concentration of the resulting elutions was determined using the Micro BCA™ Protein Assay Kit (Pierce) according to manufacturer's instructions.

5.11.1 Test for antimicrobial activity of *Hydra* tissue extracts

For radial diffusion assay (RDA), *e. coli* (DH5 α) cells were seeded on R2A Agar forming an uniform layer of cells. 50 μ g of extracted proteins from tissue of control- or Arminin⁻-polyps were pipetted on circular filter plates placed on the agar. After incubation at 37°C for 16 hours, bacterial growth inhibition zones were clearly visible.

Minimal inhibitory concentration assay (MIC) was performed using 96-well microtiter plates. The plates were pre-coated with sterile-filtered 0.1 % BSA for at least 30 minutes. BSA was removed and the wells were filled with a twofold dilution series of the extracted peptides, starting with 50 μ g/ml in 90 μ l 10 mM sodiumphosphate buffer (NaP, pH 7.4) supplemented with 10 % LB-media. Finally, each well was inoculated with 100 CFU of *E. coli* DH5 α , reaching a final volume of 100 μ l solution per well. The microtiter plates were incubated

overnight at 37 °C in a moisture chamber and MIC was determined by the absence of a bacterial cell pellet. Experiments were carried out with three technical replicates for each biological replicate.

6 References

- Abascal F, Zardoya R, Telford MJ. (2010). TranslatorX: multiple alignment of nucleotide sequences guided by amino acid translations. *Nucleic Acids Res* 38: W7-13.
- Akhouayri I, Turc C, Royet J *et al.* (2011). Toll-8/Tollo negatively regulates antimicrobial response in the *Drosophila* respiratory epithelium. *PLoS Pathog* 7: e1002319.
- Akira S, Uematsu S, Takeuchi O. (2006). Pathogen recognition and innate immunity. *Cell* 124: 783-801.
- Albiol Matanic VC, Castilla V. (2004). Antiviral activity of antimicrobial cationic peptides against Junin virus and herpes simplex virus. *Int J Antimicrob Agents* 23: 382-389.
- Anderson KV, Jurgens G, Nusslein-Volhard C. (1985). Establishment of dorsal-ventral polarity in the *Drosophila* embryo: genetic studies on the role of the Toll gene product. *Cell* 42: 779-789.
- Augustin R, Anton-Erxleben F, Jungnickel S *et al.* (2009a). Activity of the novel peptide arminin against multiresistant human pathogens shows the considerable potential of phylogenetically ancient organisms as drug sources. *Antimicrob Agents Chemother* 53: 5245-5250.
- Augustin R, Siebert S, Bosch TC. (2009b). Identification of a kazal-type serine protease inhibitor with potent anti-staphylococcal activity as part of Hydra's innate immune system. *Dev Comp Immunol* 33: 830-837.
- Augustin R, Fraune S, Bosch TC. (2010). How Hydra senses and destroys microbes. *Semin Immunol* 22: 54-58.
- Backhed F, Ding H, Wang T *et al.* (2004). The gut microbiota as an environmental factor that regulates fat storage. *Proc Natl Acad Sci U S A* 101: 15718-15723.
- Bates JM, Mittge E, Kuhlman J *et al.* (2006). Distinct signals from the microbiota promote different aspects of zebrafish gut differentiation. *Dev Biol* 297: 374-386.
- Bates JM, Akerlund J, Mittge E *et al.* (2007). Intestinal alkaline phosphatase detoxifies lipopolysaccharide and prevents inflammation in zebrafish in response to the gut microbiota. *Cell Host Microbe* 2: 371-382.
- Bennett BL, Sasaki DT, Murray BW *et al.* (2001). SP600125, an anthrapyrazolone inhibitor of Jun N-terminal kinase. *Proc Natl Acad Sci U S A* 98: 13681-13686.
- Bevins CL, Salzman NH. (2011a). The potter's wheel: the host's role in sculpting its microbiota. *Cell Mol Life Sci* 68: 3675-3685.
- Bevins CL, Salzman NH. (2011b). Paneth cells, antimicrobial peptides and maintenance of intestinal homeostasis. *Nat Rev Microbiol* 9: 356-368.
- Bosch T, David C. (1987). Stem cells of *Hydra magnipapillata* can differentiate into somatic cells and germ line cells. *Dev Biol* 121: 182-191.
- Bosch TC, David CN. (1984). Growth regulation in *Hydra*: relationship between epithelial cell cycle length and growth rate. *Dev Biol* 104: 161-171.
- Bosch TC, Krylow SM, Bode HR *et al.* (1988). Thermotolerance and synthesis of heat shock proteins: these responses are present in *Hydra attenuata* but absent in *Hydra oligactis*. *Proc Natl Acad Sci U S A* 85: 7927-7931.
- Bosch TC. (2007a). Why polyps regenerate and we don't: towards a cellular and molecular framework for *Hydra* regeneration. *Dev Biol* 303: 421-433.
- Bosch TC. (2007b). Symmetry breaking in stem cells of the basal metazoan *Hydra*. *Prog Mol Subcell Biol* 45: 61-78.

- Bosch TC, Augustin R, Anton-Erxleben F *et al.* (2009). Uncovering the evolutionary history of innate immunity: the simple metazoan Hydra uses epithelial cells for host defence. *Dev Comp Immunol* 33: 559-569.
- Bosch TC. (2012). What hydra has to say about the role and origin of symbiotic interactions. *Biol Bull* 223: 78-84.
- Brogden KA. (2005). Antimicrobial peptides: pore formers or metabolic inhibitors in bacteria? *Nat Rev Microbiol* 3: 238-250.
- Brucker RM, Harris RN, Schwantes CR *et al.* (2008). Amphibian chemical defense: antifungal metabolites of the microsymbiont *Janthinobacterium lividum* on the salamander *Plethodon cinereus*. *J Chem Ecol* 34: 1422-1429.
- Brucker RM, Bordenstein SR. (2011). The roles of host evolutionary relationships (genus: *Nasonia*) and development in structuring microbial communities. *Evolution* 66: 349-362.
- Caldera EJ, Poulsen M, Suen G *et al.* (2009). Insect symbioses: a case study of past, present, and future fungus-growing ant research. *Environ Entomol* 38: 78-92.
- Caporaso JG, Kuczynski J, Stombaugh J *et al.* (2010). QIIME allows analysis of high-throughput community sequencing data. *Nat Methods* 7: 335-336.
- Cario E, Podolsky DK. (2005). Intestinal epithelial TOLLerance versus inTOLLerance of commensals. *Mol Immunol* 42: 887-893.
- Catz SD, Johnson JL. (2001). Transcriptional regulation of *bcl-2* by nuclear factor kappa B and its significance in prostate cancer. *Oncogene* 20: 7342-7351.
- Chapman JA, Kirkness EF, Simakov O *et al.* (2010). The dynamic genome of Hydra. *Nature* 464: 592-596.
- Chow J, Lee SM, Shen Y *et al.* (2010). Host-bacterial symbiosis in health and disease. *Adv Immunol* 107: 243-274.
- Cilieborg MS, Boye M, Sangild PT. (2012). Bacterial colonization and gut development in preterm neonates. *Early Hum Dev* 88 Suppl 1: S41-49.
- Conesa A, Gotz S, Garcia-Gomez JM *et al.* (2005). Blast2GO: a universal tool for annotation, visualization and analysis in functional genomics research. *Bioinformatics* 21: 3674-3676.
- Damman CJ, Miller SI, Surawicz CM *et al.* (2012). The microbiome and inflammatory bowel disease: is there a therapeutic role for fecal microbiota transplantation? *Am J Gastroenterol* 107: 1452-1459.
- David C, Murphy S. (1977). Characterization of interstitial stem cells in hydra by cloning. *Dev Biol* 58: 372-383.
- David CN, Campbell RD. (1972). Cell cycle kinetics and development of *Hydra attenuata*. I. Epithelial cells. *J Cell Sci* 11: 557-568.
- De Lucca AJ, Walsh TJ. (1999). Antifungal peptides: novel therapeutic compounds against emerging pathogens. *Antimicrob Agents Chemother* 43: 1-11.
- Dean R, Van Kan JA, Pretorius ZA *et al.* (2012). The Top 10 fungal pathogens in molecular plant pathology. *Mol Plant Pathol* 13: 414-430.
- Dicksved J, Halfvarson J, Rosenquist M *et al.* (2008). Molecular analysis of the gut microbiota of identical twins with Crohn's disease. *Isme J* 2: 716-727.
- Dobber R, Hertogh-Huijbregts A, Rozing J *et al.* (1992). The involvement of the intestinal microflora in the expansion of CD4+ T cells with a naive phenotype in the periphery. *Dev Immunol* 2: 141-150.
- Douglas AE, Minto LB, Wilkinson TL. (2001). Quantifying nutrient production by the microbial symbionts in an aphid. *J Exp Biol* 204: 349-358.

- Dubel S, Hoffmeister SA, Schaller HC. (1987). Differentiation pathways of ectodermal epithelial cells in hydra. *Differentiation* 35: 181-189.
- Fire A, Xu S, Montgomery MK *et al.* (1998). Potent and specific genetic interference by double-stranded RNA in *Caenorhabditis elegans*. *Nature* 391: 806-811.
- Frank DN, St Amand AL, Feldman RA *et al.* (2007). Molecular-phylogenetic characterization of microbial community imbalances in human inflammatory bowel diseases. *Proc Natl Acad Sci U S A* 104: 13780-13785.
- Franzenburg S, Fraune S, Künzel S *et al.* (2012). MyD88-deficient Hydra reveal an ancient function of TLR signaling in sensing bacterial colonizers. *Proc Natl Acad Sci U S A* doi:10.1073/pnas.1213110109
- Franzenburg S, Fraune S, Altrock PM *et al.* (2013). Bacterial colonization of Hydra hatchlings follows a robust temporal pattern. *ISME J*.
- Fraune S, Bosch TC. (2007). Long-term maintenance of species-specific bacterial microbiota in the basal metazoan Hydra. *Proc Natl Acad Sci U S A* 104: 13146-13151.
- Fraune S, Abe Y, Bosch TC. (2009a). Disturbing epithelial homeostasis in the metazoan Hydra leads to drastic changes in associated microbiota. *Environ Microbiol* 11: 2361-2369.
- Fraune S, Augustin R, Bosch TC. (2009b). Exploring Host-Microbe Interactions in Hydra. *Microbe* 4: 457-462.
- Fraune S, Augustin R, Anton-Erxleben F *et al.* (2010). In an early branching metazoan, bacterial colonization of the embryo is controlled by maternal antimicrobial peptides. *Proc Natl Acad Sci U S A* 107: 18067-18072.
- Fraune S, Augustin R, Bosch TC. (2011). Embryo protection in contemporary immunology: Why bacteria matter. *Communicative & Integrative Biology* 4: 369 - 372.
- French N, Pettersson S. (2000). Microbe-host interactions in the alimentary tract: the gateway to understanding inflammatory bowel disease. *Gut* 47: 162-163.
- Gauthier ME, Du Pasquier L, Degnan BM. (2010). The genome of the sponge *Amphimedon queenslandica* provides new perspectives into the origin of Toll-like and interleukin 1 receptor pathways. *Evol Dev* 12: 519-533.
- Gilbert SF, Epel D (2009). *Ecological developmental biology: integrating epigenetics, medicine and evolution*. Palgrave Macmillan: Sunderland (USA).
- Gonzalez A, Stombaugh J, Lozupone C *et al.* (2011). The mind-body-microbial continuum. *Dialogues Clin Neurosci* 13: 55-62.
- Grehan MJ, Borody TJ, Leis SM *et al.* (2010). Durable alteration of the colonic microbiota by the administration of donor fecal flora. *J Clin Gastroenterol* 44: 551-561.
- Grens A, Shimizu H, Hoffmeister SA *et al.* (1999). The novel signal peptides, pedibin and Hym-346, lower positional value thereby enhancing foot formation in hydra. *Development* 126: 517-524.
- Haas BJ, Gevers D, Earl AM *et al.* (2011). Chimeric 16S rRNA sequence formation and detection in Sanger and 454-pyrosequenced PCR amplicons. *Genome Res* 21: 494-504.
- Halfon MS, Keshishian H. (1998). The Toll pathway is required in the epidermis for muscle development in the *Drosophila* embryo. *Dev Biol* 199: 164-174.
- Hemmrich G, Anokhin B, Zacharias H *et al.* (2007). Molecular phylogenetics in Hydra, a classical model in evolutionary developmental biology. *Mol Phylogenet Evol* 44: 281-290.
- Hemmrich G, Khalturin K, Boehm AM *et al.* (2012). Molecular signatures of the three stem cell lineages in Hydra and the emergence of stem cell function at the base of multicellularity. *Mol Biol Evol*.

-
- Hofbauer J, Sigmund K (1998). *Evolutionary Games and Population Dynamics*. Cambridge University Press: Cambridge.
- Hongoh Y, Deevong P, Inoue T *et al.* (2005). Intra- and interspecific comparisons of bacterial diversity and community structure support coevolution of gut microbiota and termite host. *Appl Environ Microbiol* 71: 6590-6599.
- Hooper LV, Gordon JI. (2001). Glycans as legislators of host-microbial interactions: spanning the spectrum from symbiosis to pathogenicity. *Glycobiology* 11: 1R-10R.
- Hsu DK, Hammes SR, Kuwabara I *et al.* (1996). Human T lymphotropic virus-I infection of human T lymphocytes induces expression of the beta-galactoside-binding lectin, galectin-3. *Am J Pathol* 148: 1661-1670.
- Huelsenbeck JP, Ronquist F. (2001). MRBAYES: Bayesian inference of phylogenetic trees. *Bioinformatics* 17: 754-755.
- Iraoqui JE, Urbach JM, Ausubel FM. (2010). Evolution of host innate defence: insights from *Caenorhabditis elegans* and primitive invertebrates. *Nat Rev Immunol* 10: 47-58.
- Jenssen H, Hamill P, Hancock RE. (2006). Peptide antimicrobial agents. *Clin Microbiol Rev* 19: 491-511.
- Johnson GL, Lapadat R. (2002). Mitogen-activated protein kinase pathways mediated by ERK, JNK, and p38 protein kinases. *Science* 298: 1911-1912.
- Kambris Z, Hoffmann JA, Imler JL *et al.* (2002). Tissue and stage-specific expression of the Tolls in *Drosophila* embryos. *Gene Expr Patterns* 2: 311-317.
- Kasahara S, Bosch TC. (2003). Enhanced antibacterial activity in *Hydra* polyps lacking nerve cells. *Dev Comp Immunol* 27: 79-85.
- Kau AL, Ahern PP, Griffin NW *et al.* (2011). Human nutrition, the gut microbiome and the immune system. *Nature* 474: 327-336.
- Kelly D, King T, Aminov R. (2007). Importance of microbial colonization of the gut in early life to the development of immunity. *Mutat Res* 622: 58-69.
- Kennerdell JR, Carthew RW. (2000). Heritable gene silencing in *Drosophila* using double-stranded RNA. *Nat Biotechnol* 18: 896-898.
- Khalturin K, Hemmrich G, Fraune S *et al.* (2009). More than just orphans: are taxonomically-restricted genes important in evolution? *Trends Genet* 25: 404-413.
- Kim DH, Ausubel FM. (2005). Evolutionary perspectives on innate immunity from the study of *Caenorhabditis elegans*. *Curr Opin Immunol* 17: 4-10.
- King N, Westbrook MJ, Young SL *et al.* (2008). The genome of the choanoflagellate *Monosiga brevicollis* and the origin of metazoans. *Nature* 451: 783-788.
- Koenig JE, Spor A, Scalfone N *et al.* (2011). Succession of microbial consortia in the developing infant gut microbiome. *Proc Natl Acad Sci U S A* 108 Suppl 1: 4578-4585.
- Lange C, Hemmrich G, Klostermeier UC *et al.* (2011). Defining the origins of the NOD-like receptor system at the base of animal evolution. *Mol Biol Evol*.
- Lazzaro BP. (2008). Natural selection on the *Drosophila* antimicrobial immune system. *Curr Opin Microbiol* 11: 284-289.
- Lemaitre B, Nicolas E, Michaut L *et al.* (1996). The dorsoventral regulatory gene cassette *spatzle/Toll/cactus* controls the potent antifungal response in *Drosophila* adults. *Cell* 86: 973-983.

-
- Lenhoff HM, Brown RD. (1970). Mass culture of hydra: an improved method and its application to other aquatic invertebrates. *Lab Anim* 4: 139-154.
- Ley RE, Peterson DA, Gordon JI. (2006a). Ecological and evolutionary forces shaping microbial diversity in the human intestine. *Cell* 124: 837-848.
- Ley RE, Turnbaugh PJ, Klein S *et al.* (2006b). Microbial ecology: human gut microbes associated with obesity. *Nature* 444: 1022-1023.
- Ley RE, Hamady M, Lozupone C *et al.* (2008a). Evolution of mammals and their gut microbes. *Science* 320: 1647-1651.
- Ley RE, Lozupone CA, Hamady M *et al.* (2008b). Worlds within worlds: evolution of the vertebrate gut microbiota. *Nat Rev Microbiol* 6: 776-788.
- Login FH, Balmand S, Vallier A *et al.* (2011). Antimicrobial peptides keep insect endosymbionts under control. *Science* 334: 362-365.
- Lozupone CA, Stombaugh JI, Gordon JI *et al.* (2012). Diversity, stability and resilience of the human gut microbiota. *Nature* 489: 220-230.
- Lupton JR. (2004). Microbial degradation products influence colon cancer risk: the butyrate controversy. *J Nutr* 134: 479-482.
- Mao-Jones J, Ritchie KB, Jones LE *et al.* (2010). How microbial community composition regulates coral disease development. *PLoS Biol* 8: e1000345.
- Martin VJ, Littlefield CL, Archer WE *et al.* (1997). Embryogenesis in *Hydra*. *Biol Bull* 192: 345-363.
- Matsuzaki K, Sugishita K, Fujii N *et al.* (1995). Molecular basis for membrane selectivity of an antimicrobial peptide, magainin 2. *Biochemistry* 34: 3423-3429.
- Matsuzaki K. (1999). Why and how are peptide-lipid interactions utilized for self-defense? Magainins and tachyplesins as archetypes. *Biochim Biophys Acta* 1462: 1-10.
- Mazmanian SK, Liu CH, Tzianabos AO *et al.* (2005). An immunomodulatory molecule of symbiotic bacteria directs maturation of the host immune system. *Cell* 122: 107-118.
- McKenzie VJ, Bowers RM, Fierer N *et al.* (2011). Co-habiting amphibian species harbor unique skin bacterial communities in wild populations. *Isme J* 6: 588-596.
- McManus MT, Sharp PA. (2002). Gene silencing in mammals by small interfering RNAs. *Nat Rev Genet* 3: 737-747.
- Meijer BJ, Dieleman LA. (2011). Probiotics in the treatment of human inflammatory bowel diseases: update 2011. *J Clin Gastroenterol* 45 Suppl: S139-144.
- Miller DJ, Hemmrich G, Ball EE *et al.* (2007). The innate immune repertoire in cnidaria--ancestral complexity and stochastic gene loss. *Genome Biol* 8: R59.
- Moran AP, Gupta A, Joshi L. (2011). Sweet-talk: role of host glycosylation in bacterial pathogenesis of the gastrointestinal tract. *Gut* 60: 1412-1425.
- Mowat AM. (2009). Does TLR2 regulate intestinal inflammation? *Eur J Immunol* 40: 318-320.
- Murray JD (2002). *Mathematical Biology: I. An Introduction*. Springer: Berlin.
- Nagalingam NA, Lynch SV. (2012). Role of the microbiota in inflammatory bowel diseases. *Inflamm Bowel Dis* 18: 968-984.

- Nakamoto M, Moy RH, Xu J *et al.* (2012). Virus recognition by Toll-7 activates antiviral autophagy in *Drosophila*. *Immunity* 36: 658-667.
- Nyholm SV, McFall-Ngai MJ. (2004). The winnowing: establishing the squid-vibrio symbiosis. *Nat Rev Microbiol* 2: 632-642.
- Ochman H, Worobey M, Kuo CH *et al.* (2010). Evolutionary relationships of wild hominids recapitulated by gut microbial communities. *PLoS Biol* 8: e1000546.
- Oh DC, Poulsen M, Currie CR *et al.* (2009). Dentigerumycin: a bacterial mediator of an ant-fungus symbiosis. *Nat Chem Biol* 5: 391-393.
- Olszak T, An D, Zeissig S *et al.* (2012). Microbial exposure during early life has persistent effects on natural killer T cell function. *Science* 336: 489-493.
- Ott SJ, Musfeldt M, Wenderoth DF *et al.* (2004). Reduction in diversity of the colonic mucosa associated bacterial microflora in patients with active inflammatory bowel disease. *Gut* 53: 685-693.
- Otte JM, Cario E, Podolsky DK. (2004). Mechanisms of cross hyporesponsiveness to Toll-like receptor bacterial ligands in intestinal epithelial cells. *Gastroenterology* 126: 1054-1070.
- Palmer C, Bik EM, DiGiulio DB *et al.* (2007). Development of the human infant intestinal microbiota. *PLoS Biol* 5: e177.
- Pasare C, Medzhitov R. (2005). Toll-like receptors: linking innate and adaptive immunity. *Adv Exp Med Biol* 560: 11-18.
- Philipp I, Aufschnaiter R, Ozbek S *et al.* (2009). Wnt/beta-catenin and noncanonical Wnt signaling interact in tissue evagination in the simple eumetazoan *Hydra*. *Proc Natl Acad Sci U S A* 106: 4290-4295.
- Pujol N, Link EM, Liu LX *et al.* (2001). A reverse genetic analysis of components of the Toll signaling pathway in *Caenorhabditis elegans*. *Curr Biol* 11: 809-821.
- Putnam NH, Srivastava M, Hellsten U *et al.* (2007). Sea anemone genome reveals ancestral eumetazoan gene repertoire and genomic organization. *Science* 317: 86-94.
- Rahme LG, Stevens EJ, Wolfort SF *et al.* (1995). Common virulence factors for bacterial pathogenicity in plants and animals. *Science* 268: 1899-1902.
- Rahme LG, Ausubel FM, Cao H *et al.* (2000). Plants and animals share functionally common bacterial virulence factors. *Proc Natl Acad Sci U S A* 97: 8815-8821.
- Rakoff-Nahoum S, Paglino J, Eslami-Varzaneh F *et al.* (2004). Recognition of commensal microflora by toll-like receptors is required for intestinal homeostasis. *Cell* 118: 229-241.
- Rawls JF, Samuel BS, Gordon JI. (2004). Gnotobiotic zebrafish reveal evolutionarily conserved responses to the gut microbiota. *Proc Natl Acad Sci U S A* 101: 4596-4601.
- Rawls JF, Mahowald MA, Ley RE *et al.* (2006). Reciprocal gut microbiota transplants from zebrafish and mice to germ-free recipients reveal host habitat selection. *Cell* 127: 423-433.
- Reshef L, Koren O, Loya Y *et al.* (2006). The coral probiotic hypothesis. *Environ Microbiol* 8: 2068-2073.
- Rosenberg E, Sharon G, Zilber-Rosenberg I. (2009). The hologenome theory of evolution contains Lamarckian aspects within a Darwinian framework. *Environ Microbiol* 11: 2959-2962.
- Rosetto M, Engstrom Y, Baldari CT *et al.* (1995). Signals from the IL-1 receptor homolog, Toll, can activate an immune response in a *Drosophila* hemocyte cell line. *Biochem Biophys Res Commun* 209: 111-116.
- Round JL, Lee SM, Li J *et al.* (2011). The Toll-like receptor 2 pathway establishes colonization by a commensal of the human microbiota. *Science* 332: 974-977.

- Ryu JH, Nam KB, Oh CT *et al.* (2004). The homeobox gene *Caudal* regulates constitutive local expression of antimicrobial peptide genes in *Drosophila* epithelia. *Mol Cell Biol* 24: 172-185.
- Sackton TB, Lazzaro BP, Schlenke TA *et al.* (2007). Dynamic evolution of the innate immune system in *Drosophila*. *Nat Genet* 39: 1461-1468.
- Salzman NH, Hung K, Haribhai D *et al.* (2009). Enteric defensins are essential regulators of intestinal microbial ecology. *Nat Immunol* 11: 76-83.
- Salzman NH, Hung K, Haribhai D *et al.* (2010). Enteric defensins are essential regulators of intestinal microbial ecology. *Nat Immunol* 11: 76-83.
- Sandstrom J, Telang A, Moran NA. (2000). Nutritional enhancement of host plants by aphids - a comparison of three aphid species on grasses. *J Insect Physiol* 46: 33-40.
- Sanger F, Nicklen S, Coulson AR. (1977). DNA sequencing with chain-terminating inhibitors. *Proc Natl Acad Sci U S A* 74: 5463-5467.
- Sartor RB. (2004). Therapeutic manipulation of the enteric microflora in inflammatory bowel diseases: antibiotics, probiotics, and prebiotics. *Gastroenterology* 126: 1620-1633.
- Scheffe JH, Lehmann KE, Buschmann IR *et al.* (2006). Quantitative real-time RT-PCR data analysis: current concepts and the novel "gene expression's CT difference" formula. *J Mol Med (Berl)* 84: 901-910.
- Schramm A, Davidson SK, Dodsworth JA *et al.* (2003). Acidovorax-like symbionts in the nephridia of earthworms. *Environ Microbiol* 5: 804-809.
- Scott PM. (2012). Recent research on fumonisins: a review. *Food Addit Contam Part A Chem Anal Control Expo Risk Assess* 29: 242-248.
- Sharon G, Segal D, Ringo JM *et al.* (2010). Commensal bacteria play a role in mating preference of *Drosophila melanogaster*. *Proc Natl Acad Sci U S A* 107: 20051-20056.
- Shin SC, Kim SH, You H *et al.* (2011). *Drosophila* microbiome modulates host developmental and metabolic homeostasis via insulin signaling. *Science* 334: 670-674.
- Skerratt LF, Berger L, Speare R *et al.* (2007). Spread of Chytridiomycosis Has Caused the Rapid Global Decline and Extinction of Frogs. *EcoHealth* 4: 125-134.
- Stagni A, Lucchi ML. (1969). Is fresh water *Hydra vulgaris attenuata* a spirochaetales' reservoir host? *Experientia* 25: 662-663.
- Stecher B, Hardt WD. (2008). The role of microbiota in infectious disease. *Trends Microbiol* 16: 107-114.
- Takeda K, Kaisho T, Akira S. (2003). Toll-like receptors. *Annu Rev Immunol* 21: 335-376.
- Tamura K, Peterson D, Peterson N *et al.* (2011). MEGA5: molecular evolutionary genetics analysis using maximum likelihood, evolutionary distance, and maximum parsimony methods. *Mol Biol Evol* 28: 2731-2739.
- Tannock GW, Munro K, Harmsen HJ *et al.* (2000). Analysis of the fecal microflora of human subjects consuming a probiotic product containing *Lactobacillus rhamnosus* DR20. *Appl Environ Microbiol* 66: 2578-2588.
- Tardent P. (1995). The cnidarian cnidocyte, a high-tech cellular weaponry. *Bioassays*: 351-362.
- Tennessen JA. (2005). Molecular evolution of animal antimicrobial peptides: widespread moderate positive selection. *J Evol Biol* 18: 1387-1394.
- Tsuchida T, Koga R, Fukatsu T. (2004). Host plant specialization governed by facultative symbiont. *Science* 303: 1989.

- Ueno Y, Ishii K, Sakai K *et al.* (1972). Toxicological approaches to the metabolites of Fusaria. IV. Microbial survey on "bean-hulls poisoning of horses" with the isolation of toxic trichothecenes, neosolaniol and T-2 toxin of *Fusarium solani* M-1-1. *Jpn J Exp Med* 42: 187-203.
- Vaishnav S, Behrendt CL, Ismail AS *et al.* (2008). Paneth cells directly sense gut commensals and maintain homeostasis at the intestinal host-microbial interface. *Proc Natl Acad Sci U S A* 105: 20858-20863.
- Vandewalle A. (2008). Toll-like receptors and renal bacterial infections. *Chang Gung Med J* 31: 525-537.
- Walter J, Ley R. (2011). The human gut microbiome: ecology and recent evolutionary changes. *Annu Rev Microbiol* 65: 411-429.
- Wang J, Tao Y, Reim I *et al.* (2005). Expression, regulation, and requirement of the toll transmembrane protein during dorsal vessel formation in *Drosophila melanogaster*. *Mol Cell Biol* 25: 4200-4210.
- Weisburg WG, Barns SM, Pelletier DA *et al.* (1991). 16S ribosomal DNA amplification for phylogenetic study. *J Bacteriol* 173: 697-703.
- Wen L, Ley RE, Volchkov PY *et al.* (2008). Innate immunity and intestinal microbiota in the development of Type 1 diabetes. *Nature* 455: 1109-1113.
- Wiens M, Korzhev M, Perovic-Ottstadt S *et al.* (2007). Toll-like receptors are part of the innate immune defense system of sponges (demospongiae: Porifera). *Mol Biol Evol* 24: 792-804.
- Wittlieb J, Khalturin K, Lohmann JU *et al.* (2006). Transgenic Hydra allow in vivo tracking of individual stem cells during morphogenesis. *Proc Natl Acad Sci U S A* 103: 6208-6211.
- Wong CN, Ng P, Douglas AE. (2011). Low-diversity bacterial community in the gut of the fruitfly *Drosophila melanogaster*. *Environ Microbiol* 13: 1889-1900.
- Woodhams DC, Vredenburg VT, Stice MJ *et al.* (2007). Symbiotic bacteria contributed to innate immune defenses of the threatened mountain yellow-legged frog, *Rana mucosa*. *Biol Conserv* 138: 390-398.
- Xi Z, Ramirez JL, Dimopoulos G. (2008). The *Aedes aegypti* toll pathway controls dengue virus infection. *PLoS Pathog* 4: e1000098.
- Xu J, Bjursell MK, Himrod J *et al.* (2003). A genomic view of the human-*Bacteroides thetaiotaomicron* symbiosis. *Science* 299: 2074-2076.
- Zamore PD. (2002). Ancient pathways programmed by small RNAs. *Science* 296: 1265-1269.
- Zaslloff M. (2002). Antimicrobial peptides of multicellular organisms. *Nature* 415: 389-395.
- Zdobnov EM, Apweiler R. (2001). InterProScan--an integration platform for the signature-recognition methods in InterPro. *Bioinformatics* 17: 847-848.

7 List of Publications

Parts of the present thesis have been published previously:

Franzenburg S[°], S Fraune[°], S Künzel, JF Baines, T Domazet-Lošo, TCG Bosch (2012)
MyD88 deficient *Hydra* reveal ancient function of TLR-signaling in sensing bacterial colonizers.
Proc. Natl. Acad. Sci. USA 109: 19374-19379 (°Authors contributed equally)

Franzenburg S[°], S, Fraune[°], P. M. Altrock, S. Künzel, J. F. Baines, A. Traulsen, T. C. G. Bosch (2012) Bacterial colonization of *Hydra* hatchlings follows a robust, temporal pattern.
ISME Journal, in press (°Authors contributed equally)

Augustin R, Fraune S, Franzenburg S, Bosch TCG (2012)
Where simplicity meets complexity: hydra, a model for host-microbe interactions.
Adv Exp Med Biol. 2012;710:71-81. Review.

8 Acknowledgements

Zunächst danke ich Prof. Thomas Bosch für seine intensive Betreuung, für das Vertrauen und die Wertschätzung, die er mir in den vergangenen drei Jahren entgegen gebracht hat. Ich bin dankbar für die inspirierenden, motivierenden und manchmal auch kritischen wissenschaftlichen Diskussionen im Rahmen dieser Zusammenarbeit.

Mein besonderer Dank gilt Dr. Sebastian Fraune für seine wissenschaftliche Betreuung und seine Freundschaft. Wissenschaftliche als auch persönliche Gespräche mit ihm haben mich stets voran gebracht, gestützt und motiviert. Danke.

Ich danke Dr. Sven Künzel und Prof. John F. Baines, ohne die Untersuchungen der Hydra-assoziierten Bakterien mittels 454-Technologie nicht möglich gewesen wären. Dr. Tomislav Domazet-Loso gilt mein Dank für die Hilfe bei der Auswertung der Microarray-Ergebnisse. Ebenfalls danken möchte ich meinen Kooperationspartnern Dr. Philipp Altrock und Dr. Arne Traulsen für ihre Expertise in der mathematischen Modellierung bakterieller Kolonisierungsprozesse.

Ein ganz herzlicher Dank gebührt Doris Willoweit-Ohl für ihre exzellente technische Hilfe und Fröhlichkeit und Jörg Wittlieb für die Transfektion von Hydra-Polypen. Bei Christa Kuzel möchte ich mich für die Unterstützung in allen bürokratischen Angelegenheiten herzlich bedanken. Im Rahmen dieser Doktorarbeit betreute ich die Master-Arbeit von Jonas Walter, dem ich hiermit für die Zusammenarbeit am Arminin-Projekt danken möchte.

Weiterhin bedanke ich mich herzlich bei allen Mitgliedern der Arbeitsgruppe für die freundschaftliche Atmosphäre und die wissenschaftlichen Diskussionen. Besonders erwähnen möchte ich hierbei meine Labor-Nachbarin Cleo Pietschke und meine Büro-Kollegen Javier Lopez und Anna-Marei Böhm. Meinem Kollegen Juris Grasis danke ich für das Korrekturlesen.

Der größte Dank allerdings gilt meinen Eltern Hanna und Horst und meiner Freundin Jeanette, ohne deren Liebe und Rückhalt diese Arbeit nicht möglich gewesen wäre.

9 Appendices

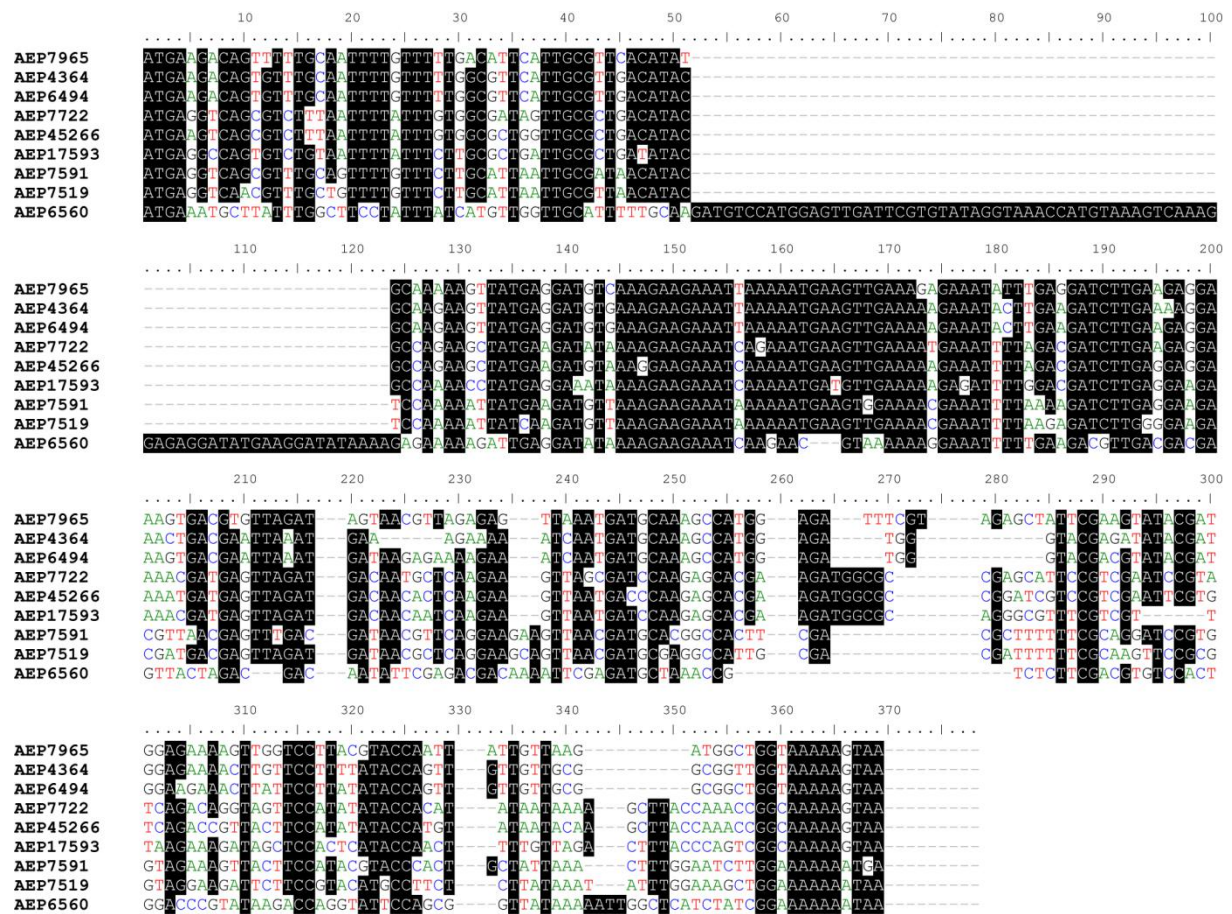


Figure 9.1: Alignment of *H. vulgaris* (AEP) arminins.

Clustel W Alignment of the coding sequence of *H. vulgaris* (AEP) arminins. Amino acids with $\geq 75\%$ identity in all paralogs are shaded black. Note the relatively conserved region between base 130 and 200.

The attached DVD contains the following data:

1. 454 sequencing data of *Hydra* microbiota studies
2. Microarray data (MyD88 and germfree)
3. Construct maps of MyD88-Hairpin and Arminin-Hairpin
4. 16S rRNA sequences of cultured bacteria
5. List of barcoded 454 amplicon primer
6. Multi-species arminin alignment

Additionally, 454 data of the *Hydra* microbiota establishment and MyD88-deficient *Hydra* are deposited at MG-RAST under the following IDs:

Experiment	MG-RAST ID	URL
Hydra Microbiota Establishment	1706	http://metagenomics.anl.gov/linkin.cgi?project=1706
MyD88 deficient Hydra	1719	http://metagenomics.anl.gov/linkin.cgi?project=1719

Raw microarray data for MyD88-deficient and germfree *Hydra* are deposited at NCBI's Gene Expression Omnibus (GEO) with the accession number GSE32383 (<http://www.ncbi.nlm.nih.gov/geo/query/acc.cgi?acc=GSE32383>).

10 Erklärung

Hiermit erkläre ich, dass ich die vorliegende Dissertation nach den Regeln guter wissenschaftlicher Praxis eigenständig verfasst und keine anderen als die angegebenen Hilfsmittel und Quellen benutzt habe. Dabei habe ich keine Hilfe, außer der wissenschaftlichen Beratung durch meinen Doktorvater Prof. Dr. Dr. h.c. Thomas C. G. Bosch in Anspruch genommen. Des Weiteren erkläre ich, dass ich noch keinen Promotionsversuch unternommen habe. Teile dieser Arbeit wurden bereits zur Publikation eingereicht.

Kiel, den 21. Januar 2013

Sören Franzenburg